INVESTIGATION ON VARIOUS ASPECTS OF MIMO RADAR

DEBASISH DEB

INVESTIGATION ON VARIOUS ASPECTS OF MIMO RADAR

A

Thesis Submitted

in Partial Fulfilment of the Requirements

for the Degree of

DOCTOR OF PHILOSOPHY

By

DEBASISH DEB

Department of Electronics and Electrical Engineering

Indian Institute of Technology Guwahati

Guwahati - 781 039, INDIA.

February, 2017

TH-1898_08610214

Certificate

This is to certify that the thesis entitled "**Investigation on various aspects of MIMO radar**", submitted by **DEBASISH DEB** (08610214), a research scholar in the *Department of Electronics & Electrical Engineering, Indian Institute of Technology Guwahati*, for the award of the degree of **Doctor of Philosophy**, has been carried out by him under our joint supervision and guidance. The thesis has fulfilled all requirements as per the regulations of the institute and in our opinion has reached the standard needed for submission. The results embodied in this thesis have not been submitted to any other University or Institute for the award of any degree or diploma.

Dated:
Guwahati

Prof. R. Bhattacharjee
Dept. of Electronics & Electrical Engg.
Indian Institute of Technology Guwahati
Guwahati - 781039, Assam, India.

Dr. A Vengadarajan
Scientist G
Defence R&D Organisation
Bangalore 560093

TH-1898_08610214

To my wife, my son Divyansh and my mother

TH-1898_08610214

Acknowledgements

I would like to express my sincere gratitude to my supervisors, Prof. Ratnajit Bhattacharjee and Dr A Vengadarajan, for their helpful discussions, support and encouragement throughout the course for this work. Their vision and passion for research influenced my attitude for research work and spurred my creativity. I would particularly like to thank for all their help in patiently and carefully correcting all my manuscripts.

I would like to thank my doctoral committee members Prof. A K Gogoi, Prof. Rohit Sinha and Dr. Tony Jacob for sparing their precious time to evaluate the progress of my work. Their suggestions have been valuable. I would also like to thank other faculty members for their kind help during my academic studies.

I had a great time with my many friends at IIT Guwahati. I thank them for their support and encouragement.

Specially, I wish to express my deep appreciation to my wife for her unconditional support, love and understanding all these moments. I thank my son Divyansh for keeping me energetic and reducing my worries. Again, I am grateful to my mother and sisters, whose love and encouragement made this research possible.

I am thankful to Defence Research and Development Organisation for granting me the permission and facilitating to carry out my research amidst all the official work.

I am thankful to IIT Guwahati for providing the opportunity to undertake my PhD research. Finally, I would like to thank the Almighty God for bestowing me this opportunity and showering his blessings on me to come out successful against all odds.

(DEBASISH DEB)

TH-1898_08610214

Abstract

Multiple input multiple output (MIMO) radar uses multiple antennas at input and output. It processes the signals from these multiple antennas jointly to yield target detection and information on other parameters of the target. It contrasts itself from traditional radar wherein single antenna is used for transmission of signal and reception of the same. Though there are bistatic and multistatic radar configurations studied in literature but MIMO as a unified stream of research in the field of radar has emerged only recently. There are multiple configurations of MIMO radar based on the arrangement of antennas and the processing performed. Thus, under the gamut of MIMO, various configurations are studied. Depending on the application area of MIMO radar, the configuration and the processing scheme changes. The current research work aims at investigating various aspects of MIMO radar. This thesis provides the work carried out on the same. We have carried out work on virtual array for planar antenna and performance comparison of different configurations of collocated MIMO radar. The effectiveness of the proposed configuration of the same is compared with monostatic uniform linear array (ULA). A metric to ascertain the goodness of antenna configuration from the perspective of virtual array is also proposed. We have investigated enhanced range resolution based on stepped frequency across transmit subapertures. The ambiguity function for the proposed technique and the doppler tolerance is also brought out. We have proposed design of a primitive scheduler for MIMO which takes advantages of transmit subarraying in accomplishing multiple tasks simultaneously. This has obtained superior results when the load on the radar is high for tracking of targets. Waveform design is an important aspect which requires detailed study. We proposed design of orthogonal waveforms based on hyperbolic frequency hopping sequence. Some aspects of distributed MIMO have already been studied under the gamut of multistatic radar in literature. We have proposed a configuration of MIMO radar under distributed class wherein the transmitters will be capable of monopulse. This class of distributed MIMO radar has definite advantages which are brought out in detail in this thesis.

TH-1898_08610214

Contents

TH-1898_08610214

TH-1898_08610214

TH-1898_08610214

List of Figures

TH-1898_08610214

TH-1898_08610214

TH-1898_08610214

List of Tables

TH-1898_08610214

Acronyms

MIMO	Multiple-input multiple-output
RCS	Radar Cross Section
RIAS	Synthetic Impulse and Aperture Radar (In english)
SIAR	Synthetic Impulse and Aperture Radar
SNR	Signal to Noise Ratio
SLL	Side Lobe Level
FM	Frequency Modulation
DF	Direction Finding
SIMO	Single Input Multiple Output
SA-MIMO	Sub Apertured Multiple Input Multiple Output
PAG	Power Aperture Gain
HF-OTH	High Frequency - Over The Horizon
TS-MIMO	Transmit Subapertured Multiple Input Multiple Output
ToT	Time on Target
ULA	Uniform Linear Array
SISO	Single Input Single Output
GPS	Global Positioning System
CW	Continuous Wave
IDFT	Inverse Discrete Fourier Transform
IFFT	Inverse Fast Fourier Transform
PRT	Pulse Repetition Time
FH	Frequency Hopping
LOS	Line of Sight
PAPR	Peak to Average Power Ratio

TH-1898_08610214

MSRS	Multi Site Radar Systems
PRF	Pulse Repetition Frequency
CSR	Cooperative Signal Reception
RF	Radio Frequency
1 PPS	1 Pulse Per Second
LFM	Linear Frequency Modulation

TH-1898_08610214

Mathematical symbols

λ	Wavelength of operation
c	Velocity of light
$A_M(\theta)$	Combined array manifold
η	Goodness of virtual array
h_t	Target altitude in km
h_A	Antenna altitude in km
r_{Ti}	Range of a point from transmitter
r_{Ri}	Range of point from receiver
h_{jk}^{p}	Back scattering coefficient of p^{th} scatterer for j^{th} receiver and k^{th} transmitter
h_{jk}	Back scattering coefficient of target for j^{th} receiver and k^{th} transmitter
Δt_r	Timing synchronisation error in receiver
S_{Tt}	Timing signal in Transmitter
S_{Rt}	Timing signal in receiver
$S_k^{Q_i}$	Signal transmitted by the i^{th} quadrant of k^{th} transmitting antenna
S_k^T	Total signal (All quadrants) transmitted by k^{th} antenna
S_{jk}^R	Signal received by j^{th} antenna as contribution from k^{th} transmit antenna
$S_j^R(t)$	Signal received by j^{th} receiver as summation of contributions from all transmitters
X_{jk}^S	Sum channel signal
X_{jk}^{Az}	Azimuth channel signal
X_{jk}^{El}	Elevation channel signal
$dbys_{Az}$	Monopulse ratio for azimuth channel
$dbys_{El}$	Monopulse ratio for elevation channel
θ_{Az}	Look angle in azimuth direction
θ_{El}	Look angle in elevation direction

TH-1898_08610214

θ^c_{Az}	Corrected look angle in azimuth direction
θ^c_{El}	Corrected look angle in elevation direction
$\Delta\theta_{Az}$	Monopulse error angle in azimuth direction
$\Delta\theta_{El}$	Monopulse error angle in elevation direction
R_Σ	Range sum of target in bistatic scenario
R_t	Range of target from transmitter in bistatic scenario
R_r	Range of target from receiver in bistatic scenario
θ_t	Angle between baseline and the line connecting target and transmitter
(x_{jk}, y_{jk}, z_{jk})	Position of target with respect to k^{th} transmitter estimated in j^{th} receiver
(X, Y, Z)	Fused position of target
Δfd_i	Doppler filter width for i^{th} filter
$A_u(\tau)$	Auto correlation function at a delay τ
$A_{u_1,u_2}(\tau)$	Cross correlation function at a delay τ
$A_u(\tau, \omega)$	Auto ambiguity function at a delay τ and doppler frequency ω
$A_{u_1,u_2}(\tau, \omega)$	Cross ambiguity function at a delay τ and doppler doppler frequency ω

TH-1898_08610214

List of Publications

Conference Publications

1. Debasish Deb, R. Bhattacharjee and A. Vengadarajan, "An Efficient MIMO Configuration for Virtual Array Radar" *International Radar Symposium India-2011, Bangalore, Nov 30 - Dec 4, 2011, Bangalore*

2. Debasish Deb, R. Bhattacharjee and A. Vengadarajan, "MIMO Radar: Analysis of SNR, Beamwidth and Sidelobe Level"" *Antennas and Propagation (APCAP) Conf. Singapore Aug 27 - Aug 29, 2012*

3. Debasish Deb, R. Bhattacharjee and A. Vengadarajan, "High Range Resolution with stepped FM in subapertured MIMO" *IEEE Conference on Radar South Africa Oct 27 - Oct 30, 2015*

4. Debasish Deb, R. Bhattacharjee and A. Vengadarajan, "Resource manager for MIMO Radar" *IEEE Conference on Radar South Africa Oct 27 - Oct 30, 2015*

5. Debasish Deb, R. Bhattacharjee and A. Vengadarajan, "Design of orthogonal waveforms for MIMO radar with phase randomised frequency hopping (FH) sequence" *IEEE Conference on Electrical, Computer and Electronics Engineering, UPCON-2016 IIT-BHU Dec 9 - Dec 11, 2016*

Manuscript submitted to Journal

1. Debasish Deb, R. Bhattacharjee and A. Vengadarajan, "Distributed MIMO Radar with transmit monopulse" submitted to the Journal IET Radar, Sonar & Navigation

TH-1898_08610214

1

Introduction

भारतीय प्रौद्योगिकी संस्थान गुवाहाटी • Indian Institute of Technology Guwahati •

Contents

TH-1898_08610214

1.1 Introduction

In recent past, MIMO radar has received a lot of attention from researchers [1–5]. MIMO radar has parallels with MIMO wireless technology where in either the capacity is maximised or the probability of error is minimised [6]. In radar, MIMO is used for either combating RCS (radar cross section) fluctuation or it is used for obtaining better parameter identifiability, improved resolution or better interference rejection capability. MIMO radar is a generic framework and encompasses all configurations which have multiple antennas at transmit and receive. The configurations of them vary greatly based on the target function. Broadly, there are two different kinds of approaches for MIMO radars. First configuration increases spatial diversity. In this configuration, the transmitting antennas are deployed in such a way that they are far from each other when compared to the range of target from them. This ensures that for different transmitting paths the RCS are uncorrelated. Orthogonal waveforms are used across these transmitters to ensure that they carry independent information of the target [3]. This aids in better detectibility of targets. In second configuration, better spatial resolution is achieved by leveraging a larger virtual array. In this configuration, the transmit antennas are deployed very close to each other compared to the range of the target. The transmit and receive antennas can be collocated or separate. These are called coherent MIMO. In this configuration, the RCS seen by all the antennas are same. The phase difference produced by the transmit-receive path jointly forms a large virtual array. This virtual array is longer than the physical array and thus provides all the benefits of larger array albeit with restrictions on some parameters. [7]

1.2 Brief Survey of Relevant Literature

MIMO radar is comparatively a new field wherein there is a lot of research activity going on. As it is known that the term MIMO is taken from the field of communication. MIMO has been very effective in communications.

RIAS was the first MIMO radar with collocated antennas which used coded signals. In English RIAS is: Synthetic Impulse and Aperture Radar, SIAR. The first paper on RIAS was published in 1984 [8]. Sparse circular arrays are used as transmit and receive antennas. Mutually orthogonal signals are used in transmission. The orthogonal waveforms are shifted in frequency. All the signals get added at the target with phase shifts depending on the frequency of operation, target position, transmitter position and velocity of the target. These signals do not interfere with each other as

TH-1898_08610214

they are orthogonal. The antennas receive the scattered signals from target for all frequencies. The contribution of each transmit antenna is separated at receive and processed properly. In this configuration, it is claimed to have superfast scanning of surveillance sector. A great amount of emphasis was put on digital technology in the paper titled 'Ubiquitous MIMO Multifunction Digital Array Radar' published in *Asilomar Conf. Signals, Systems and Computers, 2003* [2]. It is imperative that use of digital technology enables adaptation of many of the parameters which the MIMO technology allows.

Use of multiple independent observations of radar target eases the detection of same at high SNR (Signal to noise ratio). The problem was initially addressed in Multisite radar [9]. Most of the concepts used in statistical MIMO are either studied in multisite radar or it is adapted from the field of communication. The concepts from the field of MIMO communication shall be judiciously weighed before applying to MIMO radar. The coherent MIMO or collocated MIMO as it is called has a lot of new things to offer. It allows increased angle resolution and reduced antenna sidelobes, increased target parameter identifiability, increased adaptation capability including adaptive transmit beamforming [1].

Waveform design is another area of MIMO radar which has received a lot of attention. Various studies are carried out for design of orthogonal waveforms, correlated waveforms with specified covariance structure. A survey of iterative and closed-form constant envelope and low PAPR (Peak to Average Power Ratio) correlated waveform design techniques is presented in [10] and in [11], a few candidate orthogonal waveforms are studied and performance comparison is brought out.

Study of ambiguity function is very important as it reveals a lot of information about the capabilities of the radar. In [12], mathematical properties of the MIMO radar ambiguity function are derived. These properties provide insights into the MIMO radar waveform design.

The benefits and pitfalls of MIMO radar needs to be analysed judiciously before its deployment. This aspect of is brought out very succinctly in [13].

1.3 Motivation

It is seen that the collocated MIMO has a lot of advantages over phased array radars but this comparison shall be made on the basis of many parameters. An all round comparison can enable a designer to decide which fits the application. The work on analysis of SNR, beamwidth and Side Lobe Level (SLL) of MIMO radar and comparison of the same was motivated by the above facts. It is

TH-1898_08610214

known that in MIMO radar, a large virtual array can be produced using a small physical array. The configuration of physical array which can produce a large virtual array is proposed in literature for linear array but the same is not studied for planar array. As there can be many configurations which may produce a large virtual array, it is ideal if a measure can be defined to ascertain the goodness of the configurations. Though collocated MIMO provides primarily the advantages brought out in earlier section, it is not limited to the same. The various applications where this can yield superior performance can be studied. Most of the studies of collocated MIMO radar are carried out for omni MIMO. From the standpoint of feasibility of compensation of SNR loss and practical realizability of omni MIMO for large array, subaperturing becomes a necessity. The transmit subaperturing can be again used in many different ways. The proposed work on resource manager for MIMO is motivated by use of transmit subaperturing in carrying out multiple tasks efficiently. The work reported in literature on stepped frequency across pulses inspired investigating stepped frequency across transmit subapertures for enhanced range resolution. Realisability of MIMO radar with orthogonal waveforms across transmit subapertures depend heavily on availability of large number of orthogonal waveforms. This motivates to investigate design of orthogonal waveforms. In addition to the collocated MIMO, distributed MIMO has a lot of potential, which is also investigated in this research work.

1.3.1 Gaps in Existing Literature

From the the survey of relevant literature, details of which are presented in the next chapter, it is observed that an all round comparison of collocated MIMO with phased array is not studied which will enable a designer to be aware of strong points of both the radars along with limitations and their physical realisability. The candidate configuration for planar array to produce large virtual array is not addressed adequately in the literature. Many of the concepts of communication are used in statistical MIMO without addressing the change of scenario when the concepts are applied to radar. Though there are many ways to harness the benefits of MIMO, the use of stepped frequency across transmit subapertures for enhanced range resolution is not studied in literature. Resource management in radar is a very crucial element, with enhanced degrees of freedom, the resource management in MIMO radar assumes elevated importance. The same is not studied adequately in the existing literature. There is limited study on distributed MIMO though there is a lot of study on multi site radar systems (MSRS).

TH-1898_08610214

1.3.2 Problem Statement of the Research

The objective of the research work is to carry out the analysis of different facets of MIMO. In this research work, it is intended to study different configurations of collocated MIMO radar. We plan to study the use of stepped frequency for subapertured MIMO to achieve high range resolution and also study the ambiguity function for the same. As MIMO radar gives higher degrees of freedom, it is also intended to study a primitive scheduler for MIMO radar based on transmit subaperturing. Design of orthogonal waveforms for MIMO radar is another area which will be investigated in detail. Distributed MIMO based on transmit monopulse will be studied and a scheme for fusion of the estimates from all distributed receivers will be proposed.

1.4 Thesis Contribution

The topic wise major contribution of the thesis is brought out below:

(i) Carried out analysis of different processing schemes of MIMO radar

  (a) Evaluation of SNR of MIMO radar and comparison with phased array radar

  (b) Evaluation of SLL of MIMO radar with/without phased repetition, with sparse transmit/receive array and its comparison with phased array

(ii) Proposed a configuration for sparse planar array to produce large virtual array

  (a) Proposed a metric to ascertain the efficiency of any sparse array for its capability to produce large virtual array

(iii) Developed a resource manager for MIMO radar. Demonstration of increase of benefit in using the resource manager for MIMO radar with increase in tracking load of radar

(iv) Proposed use of stepped frequency across transmit subapertures for obtaining enhanced range resolution

  (a) Evaluated the performance of the proposed technique for single target while in motion and stationary

  (b) Evaluated the performance of the proposed technique for multiple targets while in motion and stationary

TH-1898_08610214

(c) Evaluated the ambiguity function for the proposed technique and demonstration of its dependence on the range of the target

(v) Design of orthogonal waveforms based on frequency hopping sequence

(a) Modification of the waveform with phase randomisation to achieve superior performance

(b) Evaluation of the doppler tolerance of the waveform

(vi) Introduced the concept of distributed MIMO with transmit monopulse

(a) Compared monopulse in transmit and receive

(b) Evaluation of transmit monopulse using noise waveform

(c) Evaluation of performance improvement for multiple receivers

1.5 Brief Description of Different Chapters

First chapter brings out the brief survey of relevant literature followed by motivation for the research. It also brings out the gaps in existing literature followed by the problem statement of the research. Chapter 2 brings out the detailed literature survey and state of the art in the field of the current research. As this is a comparatively new field of research, it also brings out the various view points of researchers in terms of applicability of MIMO radar in field deployment. It also brings out the first such deployed system. The topic wise contribution is brought out in chapter 3 to chapter 7. Conclusion and scope of further work is brought out in chapter 8.

- In chapter 3, the different configurations of MIMO radar; its benefits and disadvantages are studied. It compares the various benefits enumerated by researchers of MIMO radar with phased array radar. It also brings out that the improvement in virtual array aperture for MIMO radar for a given monostatic arrangement is possible only in case of sparse array. It also proposes a planar array configuration to achieve large virtual array for MIMO radar. A metric is proposed to quantify the effectiveness of sparse transmit-receive array to produce a large virtual array. The evaluation of the proposed metric shows that both the sparse planar array proposed in this chapter and the sparse linear array studied in literature produce same value.

- A resource manager for MIMO radar is proposed in chapter 4. The proposed resource manager for MIMO radar utilises the additional degrees of freedom brought in by MIMO radar viz., selectively

TH-1898_08610214

using transmit subaperturing based on SNR requirement. It is shown that there is significant benefit in using MIMO radar for scheduling multiple tasks using transmit subapertures. The benefit is achievable only for special beams of radar viz., verification, track initiation, track maintenance. It is also seen from the study that for increase in load of special beams in radar, the benefit of MIMO with respect to phased array becomes more prominent.

- Chapter 5 brings out distributed MIMO radar using transmit monopulse. In this configuration, the transmitter is capable of transmitting orthogonal signals from its quadrants. The location of the target is calculated from the range-sum and angle estimate of the target. The angle of the target is estimated with respect to transmitter which is enabled by transmit monopulse. The location estimates from multiple receivers are fused in a fusion centre to yield more accurate estimate of the location of target. This configuration brings in a paradigm shift as the receiver can have broad beamwidth and can be very simple in design. This also avoids the problem of beam scan-on-scan, pulse chasing.

- In chapter 6, the use of stepped frequency across transmit subapertures for enhanced range resolution is proposed and detailed analysis is carried out. Stepped frequency across transmit subapertures has many benefits compared to stepped frequency across pulses. Major challenge in any radar is to mitigate clutter and the same is done using frequency domain processing along slow time. The use of stepped frequency across subapertures enables the doppler processing. Also, the method of using stepped frequency across subapertures provides partial mitigation of effect of target velocity on finer range resolution. As time span over which the stepped frequency processing is carried out is much smaller than that of stepped frequency across pulses; the impact of velocity on phase of the signal is minimal. In addition to these, we have also studied the ambiguity function of the proposed technique. It is concluded that the proposed technique provides a superior method for obtaining finer range resolution with an additional cost of beamforming at element level.

- Chapter 7 brings out the design of orthogonal waveforms based on frequency hopping sequence. Most of the MIMO radar concepts rely on transmission of orthogonal waveforms from its transmitters. There are existing methods to design orthogonal waveforms based on polyphase sequences and chirp rate diversity. The performance of the proposed technique is compared with

TH-1898_08610214

the existing design techniques. It is shown that the proposed method for generation of orthogonal waveforms yields superior results. Moreover, the proposed method allows to generate large number of orthogonal waveforms.

TH-1898_08610214

2

Literature Survey

Contents

TH-1898_08610214

2.1 Extended Literature Survey

In last chapter, a brief discussion on the topics already studied in existing literature is brought out. This chapter will bring out the survey of literature in detail. There are many important facets which are studied and investigated in the ongoing research activities. The existing body of literature spans the following areas.

- MIMO radar systems
- Different types of MIMO radar
- Detection criteria for different MIMO configurations in Gaussian and non-Gaussian heterogeneous clutter
- Adaptive processing
- Transmit subaperturing for MIMO radar with collocated antennas
- Signaling strategies for hybrid MIMO phased-array radar
- Performance of MIMO radar with angular diversity under Swerling scattering models
- Time reversal in MIMO radar
- Antenna placement for different criterion
- MIMO radar in microwave imaging

The paper titled 'MIMO Radar: An idea whose time has come' [5], has discussed many facets of MIMO radar. In this paper, the transmit array is considered to be widely-spaced ensuring returns are gathered from different aspects of the target which produces uncorrelated RCS. Conventional array is used in receive. Cramer-Rao bound of the mean square error in estimating the target direction is evaluated. It is seen that it leads to improvement in DF (Direction finding) accuracy. MIMO radar imaging, degrees of freedom and resolution is studied in [14]. The enhanced parameter identifiability is addressed in [15]. In [16], various performance issues are brought out.

The digital technology turns out to be very useful in realisation of MIMO radar. It enables excitation of each element with different waveforms. Also the outputs of all elements are required to be digitised before any signal processing can be applied. In [2], radar equipment specifications including

TH-1898_08610214

dynamic range, phase noise, system stability, isolation and spurs for MIMO radar are brought out. In this paper, it is brought out how the digital array radars can be used to optimally exploit radar time and energy, leading to simplified radar equipment design.

The waveform design in a adaptive radar plays a vital role. As MIMO has higher degrees of freedom, the same will enable the designer to use it for many different purposes. The design of waveform based on different criteria is studied in [17–19]. In [17], the problem of radar waveform design for target identification and classification is studied. Both the ordinary radar with a single transmitter and receiver and MIMO radar are considered. The scattering characteristics of a nonpoint target is modeled using random target impulse response. Design of waveforms with constraint on power have been investigated. Water filling algorithm is used for power allocation. In [18], signal synthesis and optimal receive filter design for MIMO radar is studied. Signals with good auto and cross-correlation properties having constant-modulus based on computationally attractive cyclic optimization is studied in this paper. The waveform was studied with emphasis on range compression. In phased array radar, the transmit antennas transmit coherent waveforms which is phase shifted to form a beam in a particular direction. In MIMO radar, the signal transmitted can be designed to achieve a desired criterion like ensuring that the signal when reflected back to receiver by targets become uncorrelated. This aspect is studied at length in [19]. It designs the transmit waveform to have a specified correlation structure. In [20] and [21] , the design of waveforms and the correlation between them is studied. Though a lot of study is carried for design of waveform based on a given covariance matrix, most of the practical radars depend on the transmission of orthogonal waveforms from each of its transmitter. The generation of orthogonal waveform based on polyphase coding is studied in [22] and [23]. The performance figures obtained was also reported for a given length of code. In a recent paper [24], the design of orthogonal waveforms based on chirp with frequency and chirp rate diversity was brought out. The idea behind this is that the starting frequency of chirp and the chirp rate is kept different for different waveforms. It had reported results for some designed waveforms. No specific guidelines have been provided for choosing those starting frequency and chirp rate. In [25], the orthogonal waveform based on ultrawideband impulse is discussed. In [26], the design of waveforms which is orthogonal at transmit and receive is brought out. The design is based on spread spectrum technique. The salient finding are (1) Signal designed meets nearly transmit and receive orthogonality (2) The length of the code decides the amount of interference suppression (3) There can be different ways of processing the

TH-1898_08610214

received signals (4) Biorthogonal codes can be used to reduce the bandwidth. In [27], the optimisation of the waveform is discussed for a random phase radar. A survey of iterative and closed-form constant envelope and low PAPR correlated waveform design techniques is studied in [10] and in [11], a few candidate orthogonal waveforms are studied and performance comparison are brought out.

The ambiguity function of radar is a very powerful tool. The ambiguity function for phased array is studied widely in literature. The ambiguity function of MIMO radar is studied in [28] and [12]. The range and Doppler resolutions can be characterized by the radar ambiguity function for traditional radar. It is a very important tool for analyzing and characterising radar signals. In [12], mathematical properties of the MIMO radar ambiguity function are derived. These properties provide deeper understanding into the MIMO radar waveform design. Though synthesis of waveform from ambiguity function is a difficult task and generally is not tried but this provides a tool to evaluate the designed waveform for its efficacy. The effects of array geometry and transmitted waveforms on resolution performance is studied using MIMO ambiguity functions in [28]. The performance is shown to be dependent on the space-time covariance function. This can be controlled using waveform diversity on transmit. Examples are used to demonstrate the resolution enhancement in MIMO technology. In [29], the ambiguity function for widely separated antennas is studied. It is also shown that the ambiguity function is dependent on the geometry. In [30], the optimisation of the ambiguity function with frequency hopping signal is studied. The geometry assumed in this was arbitrary.

For statistical MIMO, the biggest advantage comes from spatial diversity. In [31], statistical MIMO was formally introduced for the first time as claimed by the author. The fundamental difference between statistical MIMO and other configurations of MIMO radar lies in the fact that the former depends on the uncorrelated RCS (diversity) to improve performance. Generally, in other configurations, the performance enhancements are obtained by maximising coherent processing gain. To enhance coherent processing gain, the fundamental requirement is to transmit correlated waveforms from all transmit antennas. Complex radar targets comprise of many small scatterers; these produce a fluctuating RCS. A small variation in target aspect or change in frequency can produce uncorrelated RCS. It is shown that by separating the transmit-receive antenna so as to harvest the benefit of spatial diversity, possibilities of various new techniques for performance improvement opens up. Optimal detectors are developed in this paper and analysis for statistical MIMO is carried out. It is shown that for practical cases, the detection performance using non-coherent processing is superior

TH-1898_08610214

to coherent processing. Though many works are done in showing that statistical MIMO yield better results in combating scintillation of targets which is otherwise considered nuisance but the detailed study on target models to study performances available when real targets are under surveillance is not present. A detailed model for target back scatterer to facilitate a deeper understanding into the true potential of statistical MIMO is brought out in [32]. The principal motivation of the paper is to investigate the improvement possible in MIMO radar for real targets in surveillance. It also studied the conditions in which MIMO radars perform best or at least, better than a netted radar system. The target models introduced there was a step towards this aim. In the similar lines of statistical MIMO lies the distributed MIMO. In [33], the distributed MIMO was studied wherein the impetus was on tracking with monopulse receivers. The allocation of receive beams for tracking of multiple target in MIMO setup is studied in [34].

It is widely claimed that MIMO provides all advantages but there are concerns on the applicability of the same or at the least the applicability of MIMO radar shall be judiciously analysed. Towards this, a detailed analysis was brought out in [13]. It is outlined there that the comparison between the performance of MIMO radar and phased array are not done on level grounds. It was also brought out that a monostatic MIMO array radar does provide a better angle accuracy than its conventional monostatic equivalent, but it is only about 29 percent better and its resolution is the same. Alternately, a monostatic MIMO array radar can offer the advantage of the same accuracy as a conventional monostatic array radar with a smaller aperture size, one that 29 percent smaller. It also argued that this advantage comes at a huge computational cost. The author proposed that the same advantage can be achieved with doubling the power of phased array radar. It is brought out by the author that MIMO radar is best suitable for search but not for tracking. To obtain high coherent gain in tracking, the conventional processing shall be used as brought out by the author. When a large area is under surveillance by a radar, subaperture MIMO (SA-MIMO) may be used. This will ensure coverage of a larger volume without scanning the beam in transmit. For coverage of a smaller area, the subarrays can be accordingly chosen. The use of SA-MIMO also reduces throughput requirement on processing system. It was concluded in that paper that in recent future, MIMO radar will be useful in combining the existing radar equipments to achieve better power-aperture-gain (PAG). Though lot of new techniques and designs are studied by many researchers, there were occasional review of the aspects of MIMO radar which required attention so that they are not compared unfairly with their

TH-1898_08610214

phased array counterpart. Even from the realisability point of view, it is required that the flip side of MIMO technology or at the least the cost effectiveness is also studied. In [35], titled as 'MIMO Radar : snake oil or good idea', the various aspect of MIMO is looked into. It was aptly brought out by the author that MIMO communication is theoretically superior to conventional communication under certain conditions. It is also cost effective and realisable for real world applications. Though extension of MIMO communication to MIMO radar is natural but the underlying situation may be different, which is not clear. In this paper, the advantages provided by MIMO radar as claimed by many researchers was looked at from system engineering view point. It was opined that an overall investigation reveals that there are serious tradeoffs in MIMO vs. phased array radar. In the existing body of literature, many real world effects are not included. Many of the benefits may be possible to achieve using existing phased array radar. This paper evaluated many assertions made by researchers to ascertain the efficacy of this claims in real world scenarios. In the conclusion, it was asserted by the author that some of the comparison of MIMO radar with phased array did not use the later in a correct way to achieve good performance. In another paper published in 2014 [36], the applications where the potential benefits of MIMO radar become evident, were brought out. It was brought out that, MIMO radar may be effective in search radar because (1) space scanning and pulse chasing are not required thus a very profitable CSR (Cooperative signal reception) is realisable (2) the combination of non coherent processing at each receiver with joint signal processing at MSRS (Multi Site Radar System) can compensate for the loss of transmit gain in MIMO. It was also brought out that for high positional accuracy, N out of N criteria can be used. In [37], developments and breakthroughs in radars and phased array including MIMO radar is brought out. The author also expressed that MIMO radar might be a good fit for High Frequency Over the Horizon radar (HF OTH).

Though in limited extent, researchers also have made experimental set up for MIMO for communication and radar. In [38], the technical realization of the MIMO radar MIRA-CLE Ka (MIMO radar-configurable in Ka-band) is presented. It is a imaging radar which is highly portable. The deployment time is very short (couple of minutes). In the current stage of development as reported then, it is capable of processing one radar image per second. The frequency band of operation is Ka band. It has 16 elements each in transmit and receive. The dimension of the antenna front end is approximately 80 centimeters in width; only a bit larger than the real array.

TH-1898_08610214

Phased array radar provides agile beam and thus very much suited for multifunction applications. As this class of radar does multiple functions in a time sliced manner, it becomes highly dependent on how the multiple tasks are scheduled and the resource management is carried out. As MIMO radar has higher degrees of freedom, the resource management in MIMO radar assumes elevated importance. The resource management in phased array radar is widely studied in [39], [40] and [41]. In [40], the comparison of different scheduling algorithms for phased array radar is studied in detail. The resource manager for MIMO radar utilises the additional degrees of freedom viz., selectively using transmit subaperturing based on SNR requirement. There is no significant study carried out in literature for design of resource manager for MIMO radar though a very preliminary study was carried out in [42].

It is proposed in [7], to use subapertures to circumvent the problems of omni MIMO. The basic idea behind of this paper is to take the middle path, wherein the loss of SNR in omni MIMO is mitigated partially by having subapertures in transmit. Each of the subaperture will have a separate RF (Radio frequency) chain in transmit and capable of transmitting different waveforms (correlated, partially correlated or orthogonal). The resulting system is referred to as a TS-MIMO (Transmit Subapertured-MIMO) radar. Beam for each of the subapeture is separately steerable. This was also presented as a tunable system, as this can function as phased array when waveforms across all the subapertures are correlated or as omni MIMO with very large beamwidth having high degrees of freedom when the waveforms across transmit subapertures are orthogonal. These two forms the extreme points of the systems; any performance in between them can be obtained by changing the subaperture configuration. Though the subaperturing of transmit array is addressed in this but the methodology for carrying out the subaperturing is not brought out. The impact of subaperturing on degree of freedom is also not studied.

In conclusion, we can quote from the paper titled 'Radar 2020: The Future of Radar Systems' [43] that the following are the areas of radar which will receive impetus in coming days:

- Intelligent signal coding
- MIMO radar - multiple transmit and receive antennas
- Digital beamforming for a higher angular resolution with wide coverage
- Efficient systems of reduced size and cost
- Combination of radar-communication

TH-1898_08610214

3

Analysis of Different Configurations of MIMO Radar

भारतीय प्रौद्योगिकी संस्थान गुवाहाटी • Indian Institute of Technology Guwahati •

Contents

TH-1898_08610214

3.1 Introduction

MIMO radar comes in different configurations. The configuration can vary based on the placement of antennas, the waveforms transmitted, the processing involved. Broadly they can be classified as statistical MIMO radar and collocated or coherent MIMO radar.

3.2 Statistical and Collocated MIMO Radar

3.2.1 Statistical MIMO Radar

The MIMO radar concept exploits the independence between signals at the array elements unlike beamforming which presumes a high correlation between signals either transmitted or received by an array. Radar Cross Section (RCS) of a complex target varies with both transmitted frequency and target geometry. By widely separating transmit and receive antennas, MIMO radar systems observe a target simultaneously from different aspects resulting in spatial diversity, thus improving the detection performance. Also, by utilizing different frequencies, independent RCS of the target can be observed, thus resulting in frequency diversity. This type of MIMO radar wherein the benefit comes from the fact that the target RCS observed by the radar is statistically independent or partially correlated is called statistical MIMO. Statistical MIMO produces better results at higher SNR wherein Phased array radar produces better results at lower SNR. Hence, the benefits derived from MIMO radar may only be apparent above certain SNR for a given probability of detection and probability of false alarm. Studies have shown that by appropriately spacing the antennas, the uncorrelated target aspects can be seen from individual antenna simultaneously, thus resulting in spatial diversity which can be used in receive side and/or transmit side. The spacing requirement between antennas for such a system is given by [5].

$$d_t \geq \frac{\lambda R}{D} \tag{3.1}$$

where

λ = Wavelength of the carrier used

R = Range of the target

D = Size of the target

TH-1898_08610214

The diversity can also be obtained by transmitting different frequencies from different antennas. Although the behavior of real targets can be quite complex, the change in frequency and angle required to decorrelate a target or clutter can be obtained using the relation given in [44], [45].

$$\delta F = \frac{c}{2Lsin(\phi)} \tag{3.2}$$

where

δF = Frequency separation

c = Velocity of light

L = Size of the target

ϕ = Target aspect angle

3.2.2 Collocated MIMO Radar

In this configuration, the antennas are closely spaced. This configuration of MIMO radar provides better parameter identifiability, enhancement of resolution and interference/jamming suppression. Virtual array concept is utilised to analyse the performance of this configuration of MIMO. Most of the adaptive array techniques can be applied to the virtual array concepts. The virtual array is formed at the output of the receiver after performing the MIMO processing which has got bank of matched filters to separate the signal from different transmitters.

3.2.2.1 Omni MIMO Radar

In MIMO radar, the transmit antennas use orthogonal, partially correlated or fully correlated waveforms. By omni MIMO, it is referred to a system where each antenna element is treated separately and is excited by a separate waveform which could be either any of the above. It is so called because the underlying unit of antenna is a single element which is theoretically taken as omni directional. The application of omni MIMO is limited owing to the SNR loss in the system when the transmit beam is formed after receive. In case of large array, it is practically infeasible to have waveform generator circuitry at element level. Owing to these reasons, the applicability of omni MIMO is limited. Most of the basic concepts of MIMO radar can be explained using omni MIMO which can be later extended to subapertured MIMO as defined later.

TH-1898_08610214

3.2.2.2 Subapertured MIMO Radar

In subapertured MIMO, the transmit aperture is divided into small subapertures which are excited by a separate waveform generation module. In this case, the degree of freedom comes down as the element level excitations are not possible. For large array, this methodology leads to realisability of the system. Also subapertured MIMO does not suffer from SNR loss as severely as omni MIMO as brought out in subsequent sections.

3.3 Analysis

As mentioned, MIMO radar provides significant improvements in many system parameters depending on the configuration or processing schemes used. As most of modern radars are multimode, it operates in many different modes just by change of processing schemes or configuration. This chapter analyses different possible antenna configurations and processing schemes which could be employed to achieve either a narrower beam using virtual array concept or the same beamwidth as that of phased array radar with high degree of freedom and instantaneous scanning of the whole search volume as mentioned in [2].

Though virtual array can be used to achieve higher spatial resolution, the same is done at the cost of reduction of the SNR because of transmit beamforming after receive and degradation in SLL which is shown in [16]. Any windowing technique to obtain better SLL broadens the beamwidth, thus reducing the advantage provided by virtual array. This technique of obtaining narrower beam may probably find applications for smaller apertures and in a scenario where peak SLL is not much of a concern. If a narrower beam has to be obtained without having these stringent restrictions then a sparse array at transmit and receive is possibly the best option to reap the benefit of virtual array. The use of sparse array for obtaining large virtual array has been discussed in [16].

In another configuration [2], it is claimed that the scanning of the whole search volume can be done by not requiring to physically scan the search volume. Such advantage is obtained essentially because of transmit beam that will be formed after receive. While forming the beam after MIMO processing, there are repetitions of the phase terms which may or may not be removed. For configuration in [2], the phase repetitions are not removed to ensure that there is no degradation of SLL but the SNR degradation still remains high.

It is proposed in literature that this reduction in gain may be compensated with increase in Time-

TH-1898_08610214

on-Target (ToT) [16], but it may not be possible for large arrays. It is brought out in this study that the compensation using a higher ToT as suggested in [16] is practical only for very slow moving target or array with very small number of elements.

It is shown in here that the beamwidth improvement for fully filled transmit-receive array comes with a large penalty in SNR and SLL. It is also shown that the improvement in beamwidth without any degradation in peak SLL becomes only evident for sparse transmit-receive array though the degradation in SNR still remains a point of concern. It brings out that the total compensation of SNR degradation is not possible with just increase in ToT.

3.3.1 System Configuration

Let us consider a uniform linear array (ULA) with N antenna elements. As mentioned in [1], if each of the element transmits a orthogonal waveform and each receiver employs a matched filter to extract the waveform transmitted by each transmitter, then the aperture of the resultant configuration will be of length $2N-1$, resulting in a longer virtual array. Let us consider the inter-element distance as d on λ scale and the array manifold in the direction of θ be denoted by $\mathbf{a}(\theta)$

$$\mathbf{a}(\theta) = \left[1 \; e^{j2\pi dsin(\theta)} \; e^{j2\pi 2dsin(\theta)} ... \; e^{j2\pi(N-1)dsin(\theta)}\right]^T \tag{3.3}$$

The combined array manifold after MIMO processing will be given by

$$a_M(\theta) = \mathbf{a}(\theta)\mathbf{a}(\theta)^{\mathbf{T}} \tag{3.4}$$

$$\mathbf{A_M}(\theta) = \begin{bmatrix} 1 & \cdots & e^{j2\pi(N-1)dsin(\theta)} \\ e^{j2\pi dsin(\theta)} & \cdots & e^{j2\pi Ndsin(\theta)} \\ \vdots & \ddots & \vdots \\ e^{j2\pi(N-1)dsin(\theta)} & \cdots & e^{j2\pi(2N-2)dsin(\theta)} \end{bmatrix} \tag{3.5}$$

As seen from eq. 3.5 manifold for MIMO has phase repetitions. To obtain a narrow beam, these phase repetitions has to be removed. If these phase repetitions are not removed, it will provide the same performance as that of phased array radar without any sidelobe degradation except the reduction in SNR.

In subsequent sections, we will analyse two configurations at length, a) MIMO with phase repetitions b) MIMO without phase repetitions. Both of these configurations assume that the array used

TH-1898_08610214

Table 3.1: The phase repetition for 4 element ULA

Tx/Rx	Rx_1	Rx_2	Rx_3	Rx_4
Tx_1	ϕ	2ϕ	3ϕ	4ϕ
Tx_2	2ϕ	3ϕ	4ϕ	5ϕ
Tx_3	3ϕ	4ϕ	5ϕ	6ϕ
Tx_4	4ϕ	5ϕ	6ϕ	7ϕ

Table 3.2: The weighting to be applied at the output of MIMO processing

Tx/Rx	Rx_1	Rx_2	Rx_3	Rx_4
Tx_1	1	1/2	1/3	1/4
Tx_2	1/2	1/3	1/4	1/3
Tx_3	1/3	1/4	1/3	1/2
Tx_4	1/4	1/3	1/2	1

at transmit-receive is fully filled.

3.3.2 Analysis of Different Configurations

Let us denote the output for the i^{th} transmitter and j^{th} receiver as s_{ij}. The output of MIMO processing for N element transmit-receive array is given by:

$$\mathbf{S} = \begin{bmatrix} s_{11} & s_{12} & \cdots & s_{1N} \\ s_{21} & s_{22} & \cdots & s_{2N} \\ \vdots & \vdots & \ddots & \vdots \\ s_{N1} & s_{N2} & \cdots & s_{NN} \end{bmatrix} \tag{3.6}$$

In first configuration, (i.e., MIMO with phase repetitions) the transmit beam after receive may be formed at the output of each receiver after matched filtering. This beamforming will reduce the matrix given by eq. 3.6 to a vector with a length equal to the number of receive elements. The receive beam then can be formed using this vector. This provides the same beamwidth and sidelobe as that of phased array radar.

In second configuration, MIMO without phase repetitions, the matrix given by eq. 3.6 is weighted by a weighting matrix to nullify the repetitions of phases in the manifold. Let us consider an array with 4 elements. The phase terms for the transmit receive pair is given by table 3.1. To remove these phase repetitions, the received matrix is weighted by the weights shown in table 3.2. This ensures the removal of phase repetitions and synthesis of a narrower beam.

TH-1898_08610214

Now, let us look at the beamwidth and the SLL of both the configurations.

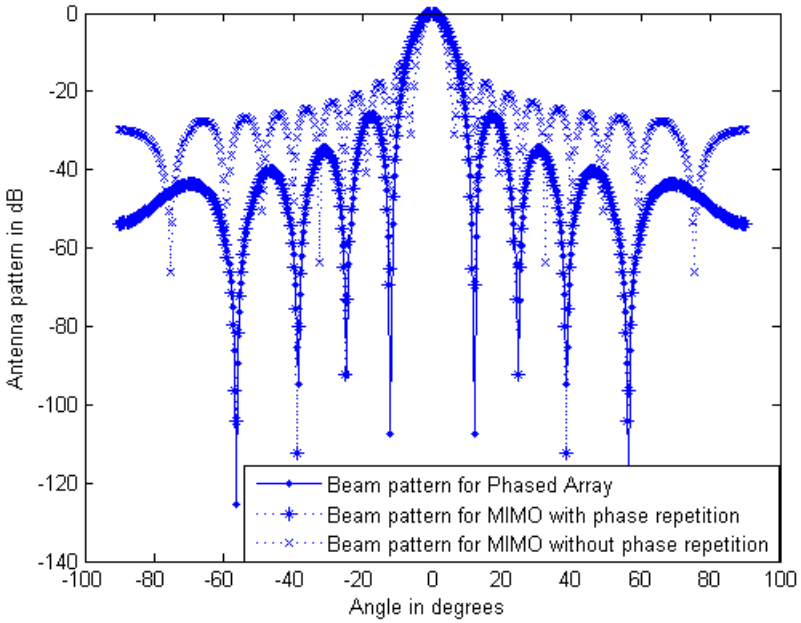

Figure 3.1: Antenna pattern for Phased Array and MIMO for N=16

The 3dB beamwidth, 1^{st} Null beamwidth and peak SLL for these two configurations are tabulated with phased array as the reference in table 3.3. The same table also includes results for a Taylor window of array dimension applied to second configuration. It is worth mentioning here that in MIMO the beams are formed only after receive, there is no beamforming in transmit as all the transmit antennas are isotropic. In phased array, the beams are formed in transmit and receive separately, hence it is prudent to compare the two way phased array performance parameters with that of MIMO radar.

As seen from table 3.3, the beamwidth and SLL for phased array and that of first configuration is exactly the same. But for second configuration, the beamwidth is narrower than that of phased array but the SLL is poorer by 13.2dB. It is seen that if Taylor window is used to achieve the same peak SLL for second configuration as that of phased array, the improvement in beamwidth declines as expected and the advantage of virtual array starts diminishing. Considering the fact that a sparse array at transmit receive produces large virtual array, it is expected that the same SLL with significantly narrower beam can be obtained if a sparse array is used at transmit-receive. Simulation was carried out to verify the same and the details are described next.

The method of construction of sparse array at transmit-receive for monostatic configuration given

TH-1898_08610214

Table 3.3: Various parameters for 4 element ULA

Parameters	Phased Array	MIMO with PR	MIMO w/o PR	MIMO w/o PR and taylor window
3dB θ_{BW}	7.6^o	7.6^o	5.5^o	6.6^o
Null-Null θ_{BW}	24^o	24^o	12.4^o	17.2^o
Peak SLL (dB)	26.4	26.4	13.2	26.7

in [16] is used here to achieve a long virtual aperture. For an array with 16 elements in transmit-receive in this configuration achieves a virtual array of length 79. Following the notation in [16], for an array with 16 elements, $N = 16$, $k = 10$, $m = 3$ and the maximum length l of contiguous non-zero region of MIMO virtual array is given by

$$l = 2k(m + 1) - 1 \tag{3.7}$$

which yields the length of virtual array as 79. The antenna pattern for this virtual array with windowing to produce same peak SLL as that of phased array having uniform weighting is shown in fig. 3.2 along with the beam pattern for phased array with 16 elements.

As seen from the fig. 3.2, the 3dB beamwidth at the output of MIMO processing for the sparse real array is 3.75^o as against 7.5^o for phased array for the same peak SLL, thus providing considerably large improvement in beamwidth.

Let us now turn attention to the SNR performance of N element array for these configurations as SNR is another important system parameter which affects the detectability to a considerable extent.

The SNR at the output of receiver after beamforming for phased array antenna with N elements is given by

$$SNR|_{PA} = 10log(N/\sigma^2) \tag{3.8}$$

where σ^2 is noise power. Phased array has got additional transmit gain of $10log(N)$.

The SNR at the output of MIMO processing with the phase repetitions is also given by the eq. 3.8 but it does not have the transmit gain. The SNR at the output of MIMO processing after removal of

TH-1898_08610214

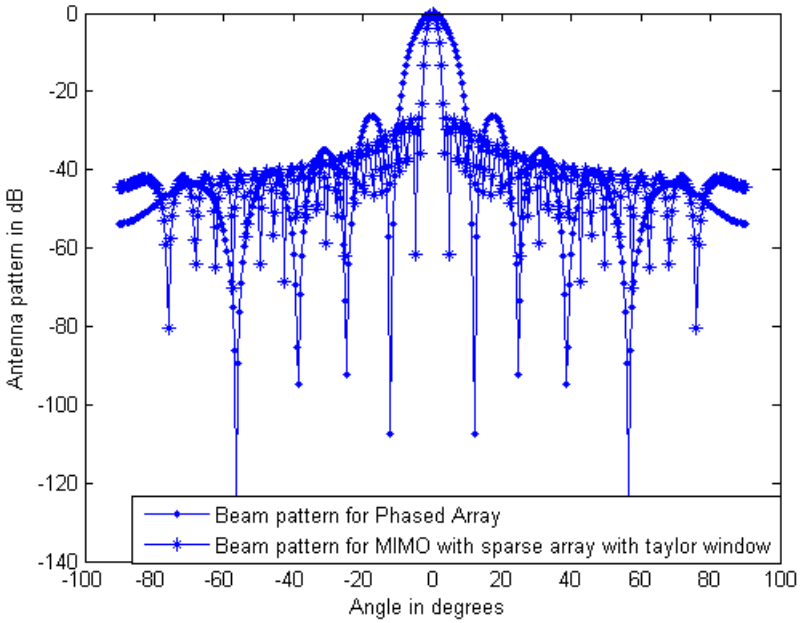

Figure 3.2: Antenna pattern for Phased Array and MIMO with sparse Array for N=16

phase repetitions is derived (given in Appendix) and given by eq. 3.9.

$$SNR|_{MIMOWOPR} \approx 10log\left(\frac{(2N-1)^2}{2Nln(N-1)+1}\right) \tag{3.9}$$

Though there is no closed form expression for SNR for sparse array used in [16], the SNR for this case is also evaluated using simulation. The SNR for all four cases are shown in fig. 3.3. It is very clear from the fig. 3.3, there is a degradation of SNR of almost the same order for all configurations when compared to that of phased array.

The reduction in SNR as a result of MIMO processing (with or without phase repetitions removal; fully filled or sparse array at transmit-receive) may be compensated in slow moving target detection by increase of ToT as suggested in [16]. But while increasing the ToT, it has to be ensured that the area search rate are kept same as that of phased array [16] and the range migration does not occur. The former being essential to ensure the fairness of comparison but the later is an absolute necessity to ensure system performance.

Though slow moving target enables increase in ToT but for longer array, the compensation becomes difficult as the target starts migrating from one range to the other. Fig. 3.4 gives the maximum gain that can be compensated by increase of integration time over a nominal integration time of 15msec

TH-1898_08610214

for different target velocities considering a range resolution of 30m. The nominal integration time of 15msec and a range resolution of 30m are system parameters which may vary from radar to radar. These are used here to only form a basis of the study performed here. The maximum ToT is calculated based on the fact that for maximum velocity of interest, the target shall not move by more than half the range resolution. Thus maximum ToT is given by

$$ToT|_{max} = \frac{\Delta r}{2v} \tag{3.10}$$

where

$$\Delta r = \text{Range resolution}$$

$$v = \text{Velocity of target}$$

From fig. 3.3, it is seen that MIMO has degradation of approximately 27dB for an antenna with 350 elements and from fig. 3.4, it can be seen that only 16dB can compensated with increase in ToT for a target of velocity 25m/s. The target velocity of 25 m/s and number of element as 350 are representative values and only show that with higher velocity of target and larger size of the array the compensation will become increasingly difficult.

From this it is very clear that for a large array, the complete compensation of the gain is not possible with increase in ToT for MIMO. As suggested in [7], partial compensation of SNR degradation can be carried out using transmit subaperturing, but transmit subaperturing can be done only for MIMO with phase repetitions, as removal of phase repetitions is not possible with transmit subaperturing.

3.4 Virtual Array in MIMO Radar

When the transmitters in MIMO radars transmit orthogonal signals, the transmit and receive beamforming happens after receive. The phase centres in transmit and receive together give rise to combined phase centers after MIMO processing. It can be easily seen that the phase centres spans a larger length/area when MIMO configuration is used. The effective aperture which this configuration produces is called virtual array. For critically sampled monostatic configuration with N elements in transmit and receive produces a virtual array of size $2N - 1$.

TH-1898_08610214

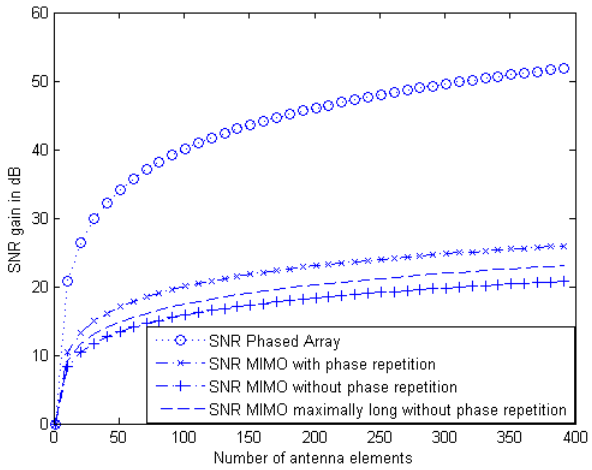

Figure 3.3: SNR at the output of beamformer for different configurations of radar

3.4.1 Virtual Array for ULA

In monostatic configurations, let us assume that the phase centers are at $\{X_T\} \equiv \{Y_T\}$, which are common to transmitters and receivers. This will give rise to the phase centres of MIMO virtual array at $\{X_T + Y_T\}$ which spans a larger aperture. Sparse real array are constructed in such a way that it produces very long virtual array.

In literature [16], the construction of sparse ULA is proposed to produce large virtual array. This is brought out here for its comparison with the sparse planar array proposed in this thesis. The construction is shown in fig. 3.5. In this '1' represents presence of physical antenna and '0' represents absence of the same. The parameter in the overbrace denotes the repetition index of a particular pattern and the parameter in the underbrace denotes number of contiguous presence of physical elements or absence of the same. Here, the number of repetitions denoted by m of the sequence $0 \ldots 0\ 1$ and $1\ 0 \ldots 0$; the number of contiguous physical elements, k, are free parameters that is optimised to produce large virtual array. The total number of physical antenna elements N is given by :

$$N = k + 2m \tag{3.11}$$

The length of total contiguous virtual array is given by:

TH-1898_08610214

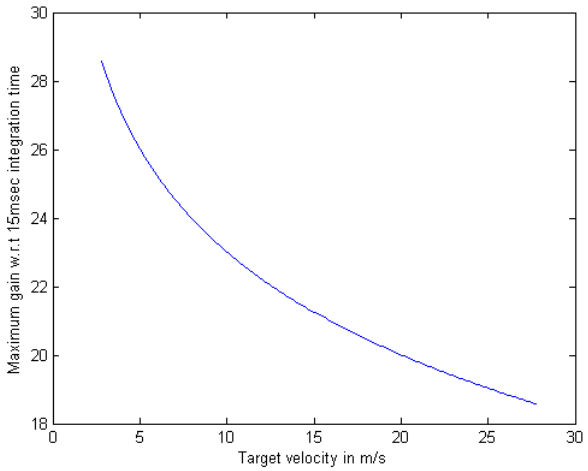

Figure 3.4: Maximum gain compensation with integration time w.r.t. 15msec

$$\overbrace{1\underbrace{0\ldots0}_{k-1}}^{1}\ \overbrace{1\underbrace{0\ldots0}_{k-1}}^{2}\ \ldots 1\overbrace{\underbrace{0\ \ldots0}_{k-1}}^{m}\ \underbrace{1\ 1\ \ldots1}_{k}\overbrace{\underbrace{0\ \ldots0}_{k-1}}^{1}\ 1\overbrace{\underbrace{0\ \ldots\ 0}_{k-1}}^{2}\ 1;\ldots\overbrace{\underbrace{0\ \ldots0}_{k-1}}^{m}\ 1$$

Figure 3.5: Construction of sparse ULA for large virtual array

$$l = 2k(m+1) - 1 \tag{3.12}$$

The value of m is given by

$$m \equiv \left\lfloor \frac{N-1}{4} \right\rfloor \tag{3.13}$$

where

$\lfloor \ldots \rfloor$ indicates floor operation

With this, the sparse ULA can be constructed to produce a large virtual array.

3.4.2 Virtual Array for Planar Antenna

Let us consider four-element uniformly filled array with half wavelength separation is used by both the transmitter and the receiver. This real antenna array can be represented using the notation '1 1 1 1', where each entry corresponds to the number of antennas at a particular location on the $\lambda/2$ linear grid. Using this array, the corresponding MIMO virtual array, which is constructed by calculating the

TH-1898_08610214

convolution of the real array antenna positions [7], is given by '1 2 3 4 3 2 1'. There are two important points to note here namely, the MIMO array aperture is much larger, with length $2n-1$; and many of the virtual antenna locations are overrepresented. Overrepresented points are basically equivalent to a scenario as if multiple antenna elements are present at that point.

It may be noted here that in order to have representation at each point on the virtual array, even a sparse real array is sufficient. As an example, by using the following sparse array '1 1 0 1 1' for the transmitter and receiver, a virtual MIMO array can be constructed with array configuration as '1 2 1 2 4 2 1 2 1'. Further, as seen from the previous example, a four element real array in the sparse form can give a virtual array of length nine where as a traditional four element array can give a virtual array of length seven.

We can similarly analyze the MIMO configurations for planar array. For example, let us consider the arrangement of antenna elements as shown in fig. 3.6, here the grid where antenna elements are placed is two dimensional $\lambda/2$ grid.

$$\begin{matrix} 1 & 1 & 1 \\ 1 & 1 & 1 \end{matrix}$$

Figure 3.6: Arrangement of antenna elements

Performing 2-dimensional convolution we get the MIMO virtual aperture as shown in fig. 3.7

$$\begin{matrix} 1 & 2 & 3 & 2 & 1 \\ 2 & 4 & 6 & 4 & 2 \\ 1 & 2 & 3 & 2 & 1 \end{matrix}$$

Figure 3.7: Equivalent arrangement of antenna elements after MIMO processing

Our main aim is to optimize the transmit/receive array such that the MIMO virtual array has a very large nonzero contiguous region. Ideally, we would like to obtain a very large virtual array with none of the elements being overrepresented i.e., with all elements equal to unity. In the case of collocated antennas with identical transmit and receive positions, this is very difficult to achieve.

TH-1898_08610214

3.4.3 Proposed Planar MIMO Array Configuration

In this section, we propose a configuration of planar array. It is an arrangement of the antenna elements in the two dimensional grid of $\lambda/2$ in the form of a square ring of dimensions NxN, where '4(N-1)' is the number of transmit/receive antennas. Fig. 3.8 shows the arrangement for twelve element transmit-receive array, i.e., of dimension $4X4$.

$$\begin{matrix} 1 & 1 & 1 & 1 \\ 1 & 0 & 0 & 1 \\ 1 & 0 & 0 & 1 \\ 1 & 1 & 1 & 1 \end{matrix}$$

Figure 3.8: Arrangement of antenna elements for square ring array

The entry '1' represents the presence of antenna element and '0' otherwise. The MIMO virtual array for the above square ring array is shown in fig. 3.9:

$$\begin{matrix} 1 & 2 & 3 & 4 & 3 & 2 & 1 \\ 2 & 2 & 2 & 4 & 2 & 2 & 2 \\ 3 & 2 & 2 & 6 & 2 & 2 & 3 \\ 4 & 4 & 6 & 12 & 6 & 4 & 4 \\ 3 & 2 & 2 & 6 & 2 & 2 & 3 \\ 2 & 2 & 2 & 4 & 2 & 2 & 2 \\ 1 & 2 & 3 & 4 & 3 & 2 & 1 \end{matrix}$$

Figure 3.9: Equivalent arrangement of antenna elements after MIMO processing for square ring array

It can be noted that all elements are non-zero, which shows that the square ring of dimension $4X4$ has has produced a MIMO virtual array with contiguous antenna elements at the MIMO receiver. Other dimensions e.g., $3X3$ and $5X5$ are also checked if it produces contiguous MIMO virtual array and it was found that it indeed does so. This motivated us to examine if this configuration produces contiguous MIMO virtual array for all values of 'N'. We have evaluated the MIMO virtual aperture for fairly large value of 'N' to see if the above condition is satisfied. We have evaluated for very high value of 'N' upto around 10,000. This is also intuitive to see that the MIMO virtual array will be contiguous as while evaluating the convolution, the square rings will intersect at least at one point to produce an entry of '1', thus making it contiguous. An intuitive explanation is also provided in

TH-1898_08610214

the following paragraph. But it is clear that a few antenna positions are overrepresented. The best configuration with bistatic arrangement will produce a virtual array with all entries as '1', indicating that no position is overrepresented. In this connection, a new measure is proposed to quantify the efficiency of any proposed array configuration. The proposed measure (η) finds out the mean value of the matrix representing virtual array which depicts the extent of representation of a particular position. As it is understood, in ideal case, each position in the virtual will be represented by '1', hence the measure for best configuration will be '1'. Now, we calculate the mean of the elements of the matrix representing MIMO virtual array for the proposed configuration to examine if we are close to achieving the ideal result, i.e., '1'. For the proposed arrangement we plotted in fig. 3.10, N vs. the value of the mean for each case and it was found that the curve was asymptotic and approached a value of 4 for the maximum value of N for which simulation was carried out. This shows that this configuration has a good scalability as number of N goes high. A measure of '4' shows that MIMO virtual aperture is smaller than the maximum possible virtual aperture by a factor of four. It is also prudent to check the value of this proposed measure for sparse array configuration proposed in literature for ULA. Fig. 3.11 show the measure for same. It is seen from this figure that the value of the measure asymptotically touches '4' for ULA also. Thus it can be claimed that the planar array proposed by us have the same efficacy for producing virtual array as that of sparse ULA as proposed in literature.

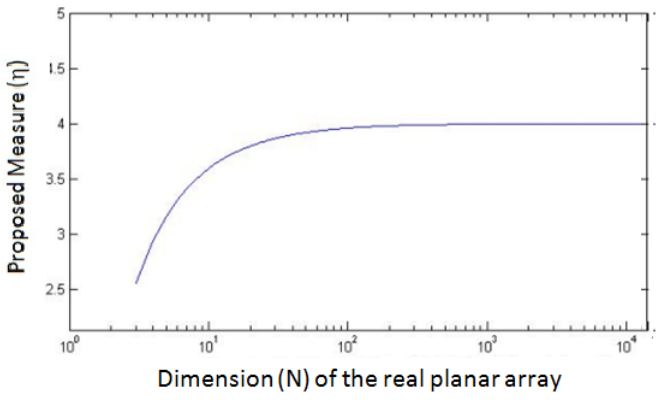

Figure 3.10: Plot of proposed measure for virtual array vs dimension of planar real array

The reason for the ring like planar array producing a fully filled virtual array is explained here.

TH-1898_08610214

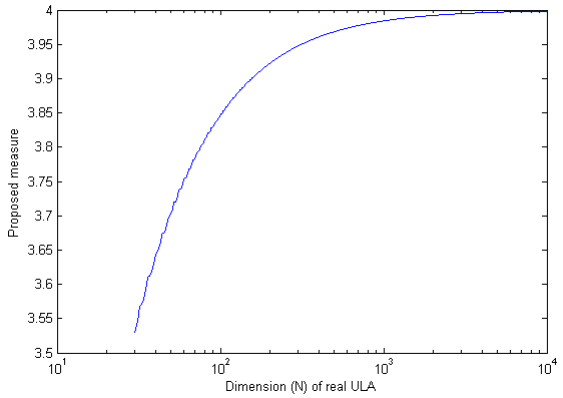

Figure 3.11: Plot of proposed measure for virtual array vs dimension of ULA real array

			1	1	1	1
			1	0	0	1
			1	0	0	1
1	1	1	{11}	1	1	1
1	0	0	1			
1	0	0	1			
1	1	1	1			

Figure 3.12: Overlap of transmit and receive array at least at one point

		1	1	1	1
		1	0	0	1
1	1	{11}	{10}	0	1
1	0	{01}	{11}	1	1
1	0	0	1		
1	1	1	1		

Figure 3.13: Overlap of transmit and receive array at multiple points

TH-1898_08610214

The virtual array is formed by convolution of the transmit and receive array where each array is represented by a '1' indicating the presence and '0' indicating absence of antenna element. In case of a ring like structure of the array, the two arrays will have overlap at least at one position at the extreme end and more than one positions at all other shifts while evaluating convolution for different shifts. The bracketed entries in the fig. 3.12 and fig. 3.13 show the places where transmit-receive pair has both entry as '1'.

As it is seen that there can be no transmit receive pair element without at least one overlap where both transmit and receive positions are represented by '1'. This ensures that the virtual array will be fully filled array. If there are more positions having transmit receive pair represented by '1', then that position is said to be overrepresented. Though this is not a proof for the ring like structure of planar array producing fully filled virtual array, it gives a reasonable explanation for the same. It can also be seen that there might be planar array with other structure producing lower value of η indicating better efficiency of the array.

3.4.4 Conclusion

The capability of MIMO radar to produce long virtual array or to scan whole search volume without requiring to physically scan the volume suffers from degradation of SNR and/or SLL. It may be concluded from the above studies that the advantage of omni MIMO radar for fully filled transmit-receive array is limited. For sparse array at transmit-receive, the enhancement in the beamwidth for same peak SLL as that of phased array becomes evident and justifies the cost of the system realisation. But the SNR degradation which can only be compensated to a very minimal level by integration gain as shown in this study remains as a point of concern for all the configurations. With increase in array size the problem becomes intractable and can not be compensated by increase in ToT. The advantages of omni MIMO radar comes with a severe tradeoff in SNR and/or SLL which has to be weighed before this can be deployed to achieve performance improvement for system parameters. However, this can be alleviated to a significant extent by subapertured MIMO. In this chapter, a sparse planar array is also proposed. It can be seen that the proposed sparse planar array produces a large virtual array compared to fully filled planar array. The evaluation of the proposed metric shows that both the sparse planar array proposed in this chapter and the sparse linear array studied in literature produces same value. The proposed metric will serve to evaluate any other sparse planar structure for its efficacy in producing large virtual array.

TH-1898_08610214

4

Resource Manager for MIMO Radar

Contents

TH-1898_08610214

4.1 Introduction

The multi-function radar is equivalent to a suite of radars, employed for some applications. To fulfill its purpose, it performs several different functions which previously would have been undertaken by many different, dedicated radars. The exact functions that are undertaken may depend upon the specific application for which the radar is deployed but the essence that it does multiple functions remains of paramount importance when we look at design or evaluation of a resource manager for such a system [41].

At simplest level, a multi-function radar consists of the following:

(i) Antenna: Antenna is a subsystem of radar capable of forming beam in any direction within the field of view of the radar almost instantly. The number of antennas can be one or many or may be a single antenna capable of subarraying and/or capable of transmitting orthogonal and/or correlated and/or partially correlated waveform.

(ii) Signal processor: With advent of high number crunching capability, a lot more than what was possible earlier can be done these days, thus providing more flexibility to exploit the above points.

(iii) Radar controller or radar computer: This coordinates all the activities that needs to taken up in real-time.

(iv) Waveform generator: This can have a database of waveforms and generates the optimum waveform based on the task at hand.

It is essential to emphasize that the essence of carrying out multi-function has a huge bearing on optimally utilising the resources which includes time, bandwidth, power and antenna aperture. It was brought out by David K Barton [46] that the managing radar time is second most important factor after choice of frequency.

The various functionalities that radars carry out are enumerated below with brief explanations:

- **Search**: In this functionality, the radar carries out the surveillance of the area with a specific probability of detection and probability of false alarm. As the detections emerging out of this function are used for TWS (Track while scan), a specific positional accuracy also has to be

TH-1898_08610214

met. To optimise the time, the total volume may be divided into many different sectors with predefined revisit time.

- **Verification**: This functionality is used for verifying if the detection is actually arising out of a real target or it is a false alarm. Many a times the waveform may be optimised based on the detection parameters and the lookback time is kept short. The lookback may also be done with different Pulse Repetition Frequency (PRF) in case of medium PRF radar to resolve ambiguity. The verification is done only if the target is not associated with any existing target. This ensures that the resources are not unnecessarily wasted.

- **Track initiation**: This function ensures a track with some acceptable level of accuracy is established as quickly as possible. In case of traditional radar, this would have taken a long time. For this purpose, the radar issues multiple beams one after another so that track with sufficient quality can be established. Post this, the track is handed over to track maintenance function. This function is also called track init.

- **Track maintenance**: In this case, the target track is maintained by the way of associating the detection which belongs to the target under track and filtering the position based on that. The track can be maintained based on the detections coming from search or from special beam which are scheduled for the specific target. As dedicated tracking is closed loop, the optimum waveform may be used for illuminating the target.

Depending on the application area of MIMO radar, the configuration and the processing scheme changes. MIMO radar can provide improvements in many system parameters depending on the configuration of deployed system. Scheduling is important sub problem of radar resource management because of the strong correlation between how tasks should be performed, as well as the time available to carry them out and their timeliness [40]. Here, we bring out the additional degree of freedom that is available to the resource manager of MIMO radar and propose a resource manager for MIMO radar and show how this improves the performance.

4.2 Scheduler for Phased Array Radar

The main job of radar as brought out earlier could be broadly classified into surveillance and tracking. All modern radars do multiple tasks simultaneously. It encounters detections from potential

TH-1898_08610214

Table 4.1: Priority of different beams

Priority	Beam type
1 (Lowest)	Surveillance
2	Track update
3	Initiation
4	Verification
5 (Highest)	Maintenance

new targets along with detections from existing targets and this decides whether the radar shall schedule verification, initiation, track update or track maintenance beam. These different types of beams demand different level of priority [40]. The same is brought out in table 4.1. For these different beam requests, different queues are maintained. Depending on the type of beam requests arising in real-time, different queues are updated. The resource manager handles the radar resources and schedules the beam in real-time. The architecture of the resource manager for phased array is brought out in [41] from which the proposed resource manager is evolved. Referring to fig. 4.1, surveillance manager is a module which provides the scheduler with a small list of surveillance requests that are close to its execution time along with waveform to be used. Track manager is another module which keeps list of beams to be scheduled for updation of the track or for track initiation or maintenance or verification. These requests are associated with a predicted range, SNR demanded, doppler resolution required and look direction.

There are different schedulers for phased array radar, viz., Oman et al type scheduler, Butler scheduler algorithm [40]. The resource manager for MIMO radar is evolved from the later.

4.3 MIMO Radar Configuration

The configuration of the MIMO radar system under study assumes collocated transmit and receive antenna with subaperturing in transmit [7]. It is assumed to have multiple subapertures at transmit and single aperture at receive. The transmit subapertures could be used as separate transmit antennas or a single antenna based on the waveforms used across them. Orthogonal or coherent waveforms across transmit subapertures will make the antenna appear as multiple antennas or single phased array antenna respectively. At receiver, the signal received has combined contributions from all transmit subapertures. The received signal is passed through matched filters to separate the contributions from subapertures when orthogonal waveforms are used. For coherent waveforms across transmit subaper-

TH-1898_08610214

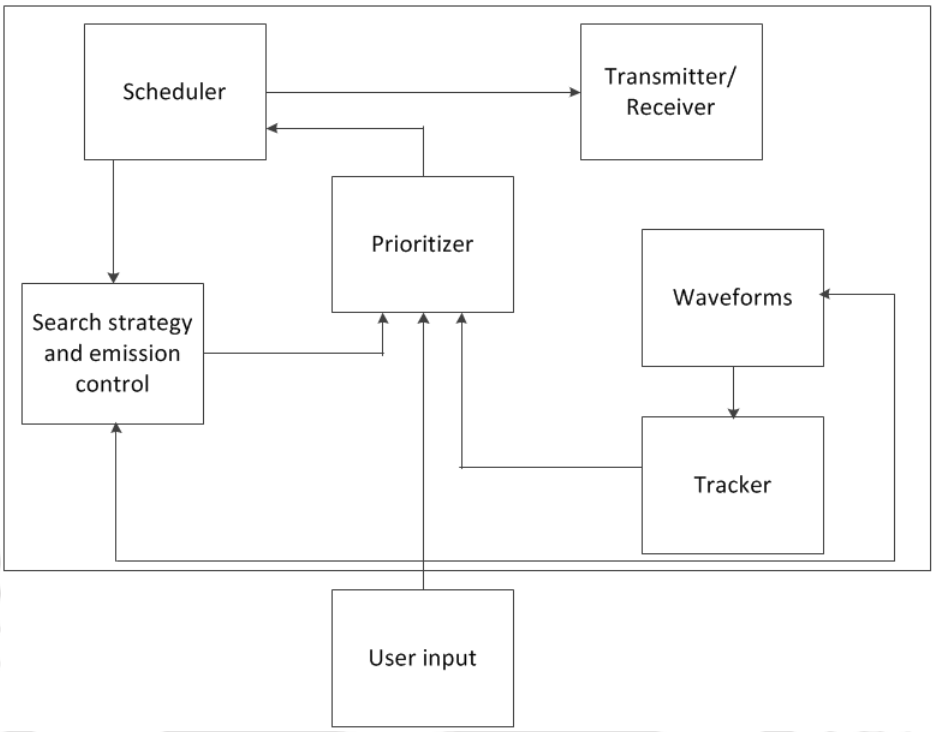

Figure 4.1: Architecture of the resource manager

tures, the system essentially becomes a phased array. Following this, normal detection processing as that of phased array is carried out. Thus, the number of independent channels available for scheduling different types of beams depend on number of orthogonal waveforms used in transmission. The configuration of the MIMO radar is brought out in fig. 4.2. It is worth mentioning here that these independent channels available at the transmit can have the beam pointing in different directions. As the beam is formed digitally at receiver, equal number of beams can be formed corresponding to the number of transmit beams using the full receive aperture. This ensures that the accuracy and resolution do not suffer as full receive aperture is used for all beams. As different transmit subapertures could be used independently, the same could be exploited to carry out multiple task simultaneously unlike phased array radar where multiple tasks are executed in a time sliced manner.

With this configuration, MIMO becomes helpful as described below.

In surveillance, the maximum range of the radar is same at all look angles in general and in this mode the radar looks for new potential targets, hence there is no a priori information for it to adapt to. In verification and initiation the approximate range of the detection is known. In tracking function, a priori information about the range of the target, approximate RCS is also known. This can be used

TH-1898_08610214

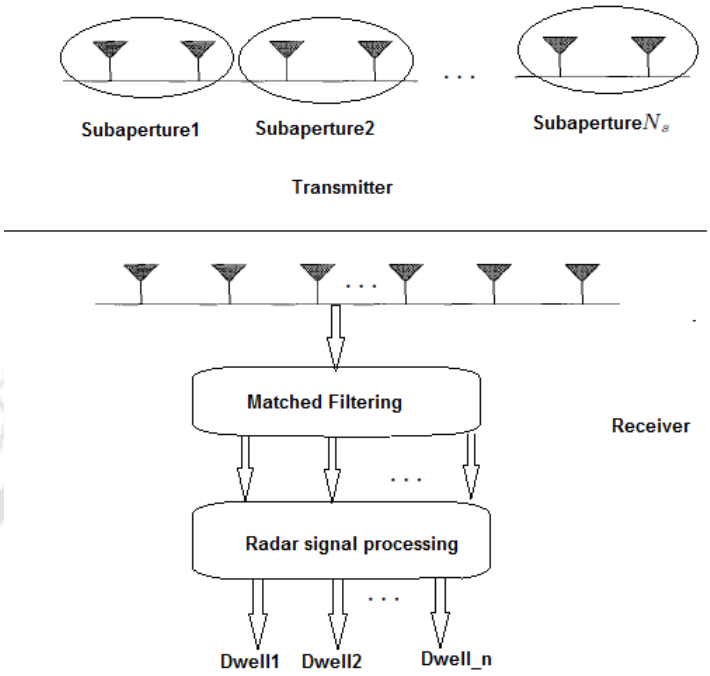

Figure 4.2: MIMO radar configuration with transmit subapertures

to decide the number of transmit subapertures that is required to be used. In a phased array, as the whole aperture is used even when the SNR required does not warrant the use of such a big aperture, this leads to the waste of radar resources. Though in many cases the ToT is adjusted based on the SNR requirement but use of minimum ToT which is required to be used for achieving doppler resolution along with fill pulses if any leads to higher wastage of resource in case transmit subaperturing is not used. The transmit subaperturing is enabled by MIMO radar. As the resolution is dictated by the receive beam characteristics, the variation of transmit subapertures based on target parameters does not effect target resolution. The accuracy of the various target parameters depends on SNR, receive beamwidth and range resolution. Fig. 4.3 shows two dimensions of radar resources viz., aperture and time. This is visualised as a block, a portion of the block or whole could be used by radar beam or dwell while achieving certain performance. This block is divided in one direction as subapertures and other direction as time slots. If the required SNR mandates the full aperture to be used, the same is used for a single dwell. In many cases, where a priori knowledge of target indicates that the total aperture is not required; a part of it can be used for the said job and rest of the aperture can be used

TH-1898_08610214

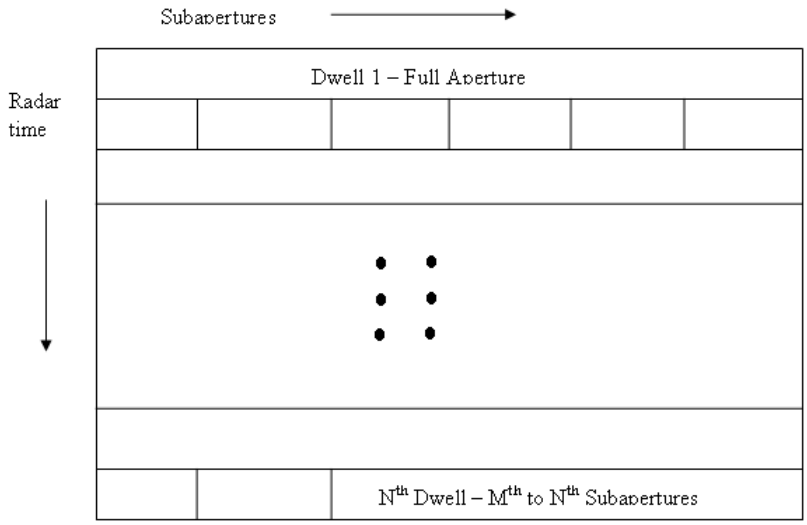

Figure 4.3: Radar resource block

for another. As shown in fig. 4.3, in the first time slot the full aperture is used for 1^{st} dwell and in last time slot, N^{th} dwell uses M^{th} to N^{th} subapertures. Thus, in second and last time slots multiple beams/dwells could be scheduled leading to better utilisation of resources.

4.4 Scheduler for MIMO Radar

The proposed resource manager for MIMO radar works on blocks of radar resource requirement. The algorithm schedules radar beams from a group of beam requests within a fixed time interval called scheduling interval. As the surveillance requests do not have any a priori information of the targets and cannot take advantage of transmit subapertures, they yield the same performance as that of phased array radar. Because of this reason, they are not studied here for comparison. Only verification, initiation and track beam requests are considered for resource allocation. Once the block of requests is formed, the resource manager works on this for scheduling of beams. The beam scheduling is dictated by maximisation of utilisation of radar resources and not based on priority but it ensures that the high priority requests always receive radar resources. If the resources are not sufficient in a given scheduling interval, then the beam requests are postponed for next scheduling interval based on priority i.e., low priority requests are postponed for next scheduling interval.

The algorithm for the resource manager is brought out in following paragraphs:

TH-1898_08610214

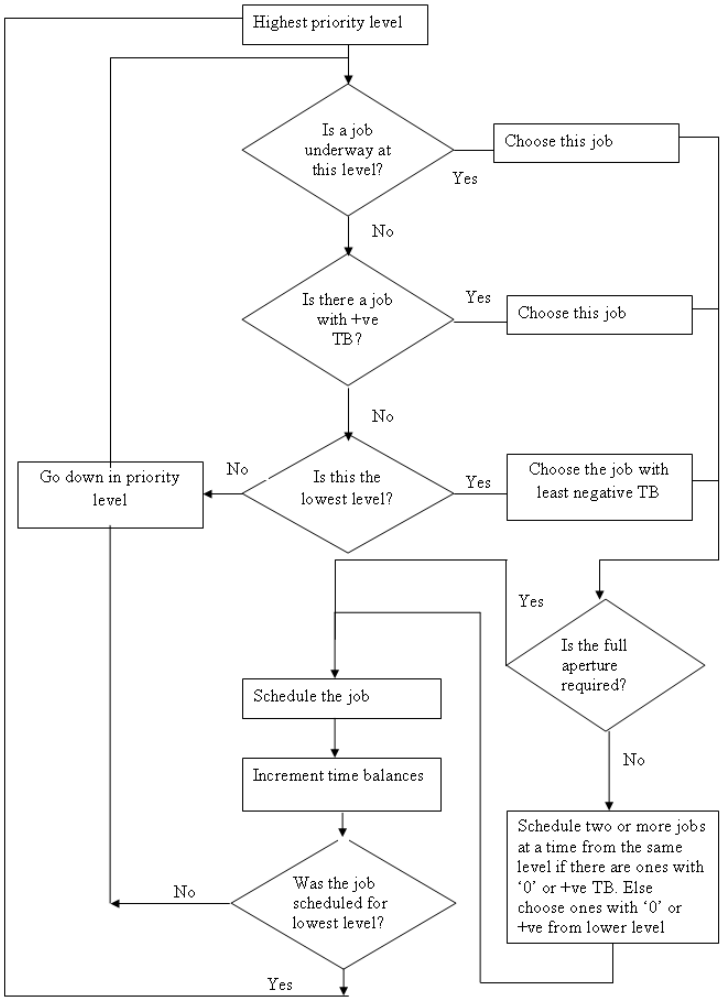

Figure 4.4: Algorithm for scheduler for MIMO

Step 1: Decide the scheduling interval for running the resource management algorithm. And initialise the starting time with '0'.

Step 2: Point to different queues one by one for picking up radar jobs requested to be scheduled within this scheduling time interval.

Step 3: Calculate the ToT required from the view point of SNR requirement (which is dictated by the a priori knowledge of range, RCS, look angle) for all the job extracted in step 2.

Step 4: Calculate the ToT required from the view point of doppler resolution and round trip delay of farthest target leading to number of fill pulses for all the requests as extracted in Step 2.

TH-1898_08610214

Step 5: The job for which the ToT requirement as calculated in step 3 is more than or equal to that calculated in step 4; use the full aperture and schedule the beam. For each beam scheduled, the radar time resource consumed is calculated to keep an watch on the availability of resources.

Step 6: The job for which the ToT calculated in Step 3 is less than that of Step 4, we need to schedule the beam with partial transmit aperture and ToT equal to the one calculated in Step 4.

Step 7: As partial transmit aperture is used for the job, keep scheduling more requests with remaining transmit aperture until it gets exhausted.

Step 8: Repeat step 7, until all the job gets scheduled. If all the radar time resource gets consumed before completing scheduling of all the requests, then remove jobs one by one from the lowest priority queue for this scheduling interval and go to step 2 and repeat the whole process until the resources are just enough to schedule the requests.

The step 8 ensures that all the high priority jobs are scheduled and is not deprived of resources because of low priority jobs. Postponement of the low priority jobs for next scheduling interval will alleviate the problem only if the excess load on radar resource is momentary. If there is sustained overload on the radar, a radar load management scheme will need to be worked out based on strategic and operational requirement.

4.5 Simulation and Results

The following points are assumed while carrying out the simulation:

1. The total frame time is divided into time for surveillance and dedicated beams. As no a priori information is used in surveillance, the use of MIMO will not yield any benefit. Hence resource utilisation is studied for track, initiation, verification beams only.
2. A minimum ToT is must even if the SNR requirement can be met with a lesser ToT so as to provided adequate doppler resolution.
3. New targets are assumed to be uniformly distributed along range.
4. The velocities of the targets are uniformly distributed in an interval.

Different queues are maintained for different beam requests. The track beam requests get generated at a rate based on the update rate required. It is assumed that different tracks have different update rates requirement varying between lowest and highest value as shown in table 4.2. Though the update rates depend on the target dynamics, for this simulation without impacting the outcome of the study,

TH-1898_08610214

Table 4.2: Various simulation parameters - Resource Manager

Parameters	Values
No. of targets in track	20
Update Time	Variable between 1 to 2.25sec
No. of verification	2 per sec (Avg)
No. of init beams	6 per successful verification
Range	300 to 50km
ToT	Variable between 15 to 5msec
Scheduling interval	250msec

this is assumed to be distributed uniformly between maximum and minimum value. The verification requests get generated at a average rate of two requests per second. It is also assumed that 10 percent of verification beam yields positive detections and for those verified detections, the init beam requests are generated. The simulation parameters are brought out in table 4.2.

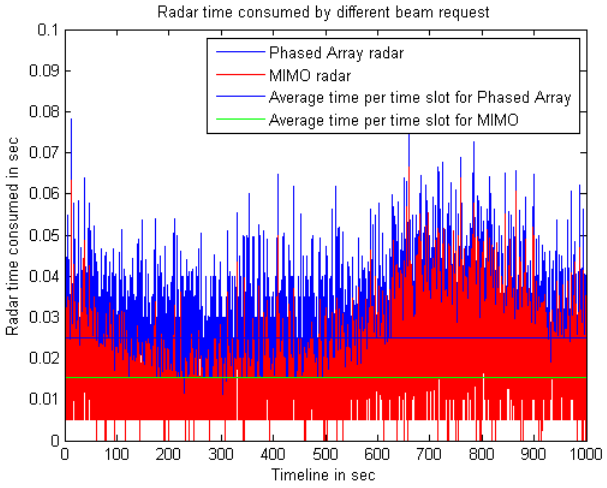

Figure 4.5: Radar resource consumption

Fig. 4.5 shows the radar time consumed by scheduling different beams at different scheduling interval by phased array and MIMO radar. Here, x-axis is the timeline and y axis the radar time consumed for scheduling all the beam requests. The radar time consumed for scheduling is evaluated for every scheduling period. In the simulation, the scheduling period is taken as 250msec. Thus, the time consumed can not exceed 250msec as all the beam requests are to be scheduled within this time. As it is seen that, the time consumed is much below 250msec, this is because of the fact that rest of the time is used for scheduling surveillance beam requests. It can also be seen that the radar time

TH-1898_08610214

consumed by the different beam request for MIMO radar is less than that by phased array radar. This ensures that more time will be available for MIMO radar to schedule surveillance beams. The concept of transmit subaperturing in MIMO was proposed in [7] for mitigating gain reduction but the same can be exploited for different purposes like the one used here. It is also seen that the average time consumed by MIMO radar for scheduling beams are less than phased array by almost 40 percent for the current simulation settings. The resource manager can incorporate many finer aspects for it to be used in real radar, but this brings out the fundamental advantages obtained in MIMO radar with transmit subaperturing.

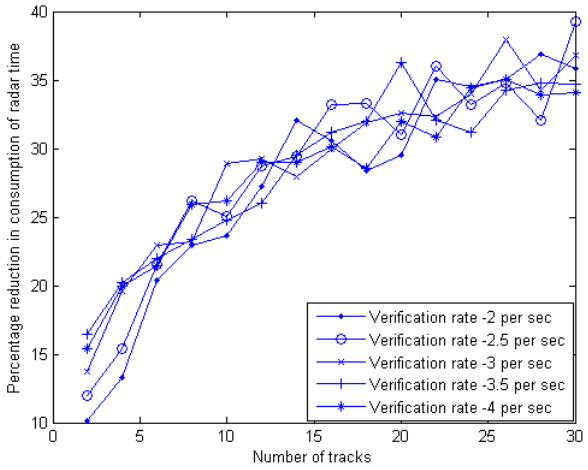

Figure 4.6: MIMO radar resource consumption reduction compared to phased array for different loads

Fig. 4.6 depicts the reduction in consumption of radar time for differing loads of radar. In the radar, the maximum load for special beams (e.g., track, init, verification) comes from track. It can be seen from the figure that as track load increases, the reduction in radar resource consumption by MIMO radar compared to that of phased array radar becomes more prominent. This is owing to the fact that as the load for special beam increases, the opportunity for utilizing the flexibility provided by MIMO radar also increases thus yielding higher efficiency. It can be seen that the impact of variation in the load of verification beam is not visible; this is because of the reason that the verification load is much less compared to the load of track beams. In this simulation it is assumed that for each successful verification, six track initiation beams are scheduled. Thus, it can be concluded that for higher load of special beams, the flexibility of MIMO radar yields superior performance.

TH-1898_08610214

4.6 Conclusion

The proposed resource manager for MIMO radar utilises the additional degrees of freedom brought in by MIMO radar viz., selectively using transmit subaperturing based on SNR requirement. It shows in principle that by utilising the steps outlined, the radar resources could be utilised in a better manner. The detailed design of resource manager for MIMO radar can address many additional issues viz., timeliness, overload management. The studies reported here only outlined a basic scheduler. Further works can be in direction of optimally using the radar resource based in maximum flexibility in transmit subaperture formation in real-time. One more parameter which can be addressed in tightly coupling the resource manager is exploring the possibility of forming a transmit beam whose beam width can be made a function of the target under tracking so that there is a very high probability that the target falls within the 3dB beamwidth. Though the same can be achieved using subarrays but use of correlated waveforms between them ensures the availability of continuum of beamwidth. Moreover, here the update time was chosen in a rather very simplistic manner without any due consideration given to target dynamics, a more detailed way of ascertaining the update time may be incorporated to predict the performance improvement in specific way.

TH-1898_08610214

5

Distributed MIMO Radars with Transmit Monopulse

Contents

TH-1898_08610214

5.1 Introduction

Distributed sensing has many benefits. Radar network of late has received a lot of attention as it can outperform conventional monostatic and bistatic configuration. Various aspects of distributed radar have been studied in literature. The basic aspect of moving target detection in distributed MIMO is studied in [47]. Finer issues like registration errors between different sensors are addressed in [48]. The distributed radar derive its benefit from the fact that (a) the transmitters and receivers are not collocated and (b) the receivers receives return from different aspects of target. Almost all the benefits listed in following sections can be categorized into these two categories. However, configurations studied in literature considered the basic construction of transmitter and receiver as that of traditional monostatic radar. In the configuration of distributed MIMO proposed in this thesis, the basic construction of transmitter is modified while keeping the basic essence of distributed MIMO same as studied in literature. Particularly, in strategic deployment, it may be noted that transmitter being a costly resource; the same needs to be protected, whereas the receivers can be made simpler and low cost so that they can be deployed much nearer to the adversaries' boundary line. The vulnerability of the receivers because of its nearness to the boundary line is offset by the simplicity of the design. This too has the parallel to any communication paradigm wherein the base station can be complex whereas the receivers are kept simpler. The use of distributed MIMO radar with a well protected transmitter for surveillance area can be very attractive. The transmitter in this configuration is proposed to have the capability of monopulse so that it can measure the angle accurately. The MIMO processing with monopulse in the transmit along with the range sum estimate is used for ascertaining the location of the target. These estimates from multiple receivers are fed to fusion centre which fuses the data to produce a more reliable estimate of the location of the target.

5.2 System Configuration

The configuration of the system is shown in fig. 5.1. The basic configuration is inspired by [33] and is adapted from the same paper. There are multiple transmit and receive antennas. Each transmit-receive pair estimates the location of the target. The waveforms used across transmitters are orthogonal. Moreover, each transmitters have four quadrants e.g., Quadrant-1, Quadrant-2, Quadrant-3, Quadrant-4. Each of these quadrant transmits a orthogonal signal. Let the signal be denoted by $S_k^{Q_i}(t)$ for Q_i^{th} quadrant of k^{th} transmitter. Thus, if there are K transmitters, we need $4K$ orthogonal

TH-1898_08610214

signals. The waveforms used for this can be noise waveforms, frequency hopping sequence or any other orthogonal waveform. A target in the field of view of the transmitter is illuminated by it and the receiver having the target in its field of view receives the signal from it. The signal received by j^{th} receiver as a contribution from k^{th} transmitter is denoted as $S_{jk}^{R}(t)$.

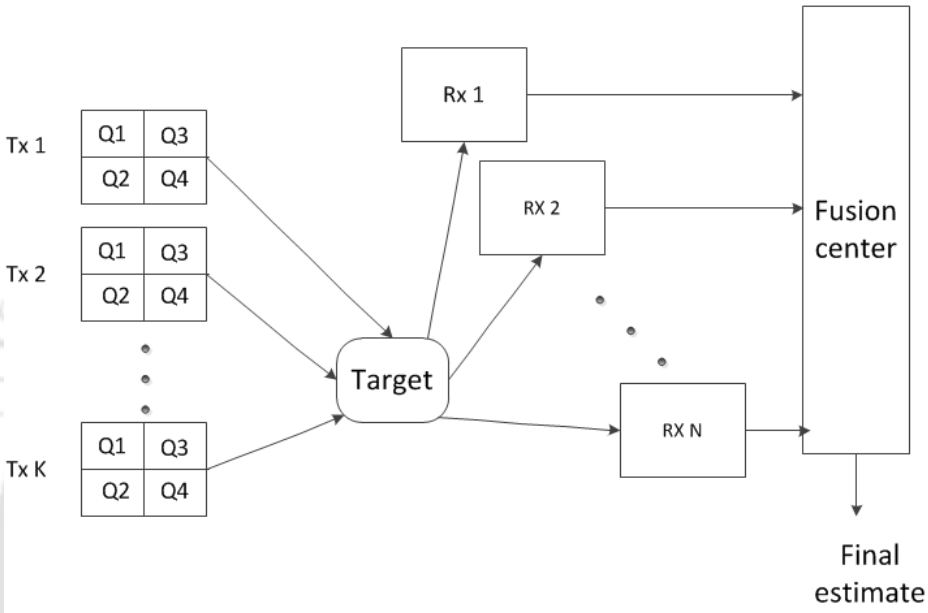

Figure 5.1: Configuration of the proposed distributed MIMO system

This signal has contribution of all four quadrants of k^{th} antenna. The signal received by j^{th} antenna is summation of the signals from all the transmit antennas and denoted by $S_{j}^{R}(t)$.

$$S_{j}^{R}(t) = \sum_{k=1}^{K} S_{jk}^{R}(t) \tag{5.1}$$

In receiver, the range sum and the transmit angle is estimated. With this, the location estimate is ascertained in each transmit-receive pair. The resultant measurement of the target location is sent to fusion center for fusing.

5.3 Advantage of the Proposed System

In addition to the advantages of multisite radar system [9], the proposed configuration provides a new paradigm wherein the search strategy becomes simpler as the receive antenna need not be directional. It also provides for protected transmitters and distributed receivers. The advantages of multisite radar which are also available in this configuration are brought out below:

TH-1898_08610214

- Reduced vulnerability of the system : As the transmitters and receivers are separate, the transmitter can be well guarded and well inside the boundary and away from adversaries. The receivers can be in the forward areas with higher vulnerability but owing to the lower cost of receiver the same may be acceptable.

- Low cost receivers : In case of traditional bistatic radar, the angle information from receivers and the round trip delay estimates are used to produce the location estimates. Here, using MIMO technique, the monopulse angle at transmitter is estimated in the receiver along with the round trip delay. These allow the receiver to be non directive and hence can be a low cost solution, allowing it to be exposed to higher vulnerability.

- Less vulnerability to countermeasure : In MIMO radar, when the receiver is much separated from the transmitter; it will fall out of the retrodirected antennas main beam thus reducing the effect of countermeasure.

- Higher probability of detection for stealth target: Conventional SISO system has collocated transmit and receive antenna. The detection of the target relies on backscattering from the target. The ongoing effort to have stealth aircraft system reduce the backscattering but generally the forward scattering does not get affected much. This can be leveraged to enhance the detectability. This is done using bistatic or distributed MIMO radar. Moreover, the scattered energy in all other direction which otherwise would have got wasted is utilised to boost detection.

- Enhanced RCS: It is brought out in literature [9] that in the effort to reduce monostatic RCS; the specular reflections are purposely been directed away from the monostatic radar direction. When the radar receivers are distributed randomly in the space, there is a finite possibility that the they will receive these specular reflective component as well thus enhancing the probability of detection.

- Doppler diversity : As the targets are seen from different aspects, the possibility of targets velocity component to be zero in direction of all the receivers are minimal unless the target's velocity itself is very low or flying in a plane perpendicularly to these transmit-receive pairs. This provides a great advantage in detecting targets which otherwise may fall in clutter notches.

TH-1898_08610214

5.4 Coverage

The coverage provided by the distributed MIMO can be seen as the union of the coverages provided by the pairwise bistatic configuration. If binary integration is carried out at the detection level, then the given area shall be covered by at least minimum number of transmit-receive pair. Bistatic coverage, like monostatic radar coverage, is determined by both sensitivity and propagation. Bistatic radar sensitivity is set by the contour of constant $\frac{S}{N}$ and the oval of Cassini. Transmitter and receiver altitudes shall ensure that the target is within the LOS (Line of sight) of both the sites. Targets in the area common to both circles have a LOS to transmitter and receiver simultaneously. For a 4/3 earth model, the radius of the LOS circle , in kilometers, is approximated by [49]

$$r_R = 130(\sqrt{h_t} + \sqrt{h_A}) \tag{5.2}$$

where

h_t = Target altitude in km

h_A = Antenna altitude in km

If the receiver establishes synchronization via direct path link, then an adequate LOS is required between transmitter and receiver.

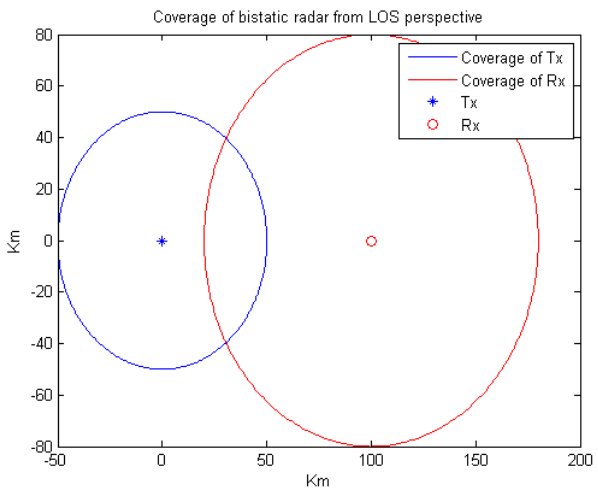

Figure 5.2: Coverage of a bistatic system based on LOS

In addition to the LOS, the coverage is dictated by the SNR. In the proposed configuration, there

TH-1898_08610214

will be multiple directional transmitters capable of transmitting orthogonal signals. It is known from literature that the coverage provided by bistatic radar can be depicted as Cassini's oval as shown in fig. 5.3. The figure is only representative. Thus the overall coverage will be decided by the area where LOS is there from both transmitter, receiver and falls within the oval of Cassini.

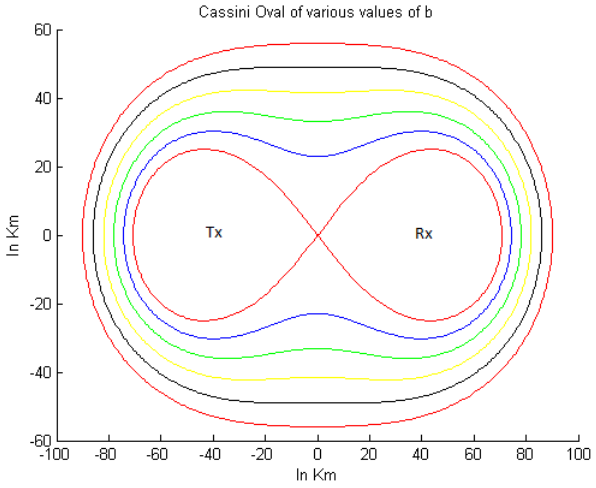

Figure 5.3: Coverage of a bistatic system - Oval of Cassini

Oval of Cassini is the locus of points from which the product of distances of two points are constant. These two points are where transmitter and receiver are kept. Alternately, the oval of Cassini's is the contour of constant SNR on bistatic plane. This assumption of constant SNR is valid only when the RCS of target remain constant for all aspects which is generally not true. But this provides the coverage based on the assumption of constant RCS. When many transmitters and receivers are deployed, the coverage obtained by the whole system is given by the overlap of all these Cassini's oval. Though this figure shows the coverage of a single pair of transmitter and receiver, the actual coverage requires synchronization in the scanning of transmitter and receiver if both are directional. If one of them is non-directional the synchronization between them is not required for scanning. Each transmit antenna covers the space from $-\theta_{Az}$ to θ_{Az} by scanning. As the transmitters are distributed and the phase centres are displaced, they cover a separate volume which may or may not have overlap.

For both transmit and receive directional antenna, the synchronisation in scanning can be obtained as follows:

Let the range of a point P_i from the transmitter is r_{Ti} and from receiver the range is r_{Ri}. Then the total time for the signal to travel from transmitter to receiver via the target τ_i is given by

TH-1898_08610214

$$\tau_i = \frac{(r_{Ti} + r_{Ri})}{c} \tag{5.3}$$

where c is velocity of light.

Let at time $t = 0$ the transmitter starts the transmission than at time $t = \tau_i$ the receiver shall be looking at point P_i. When there are multiple directional transmitters; this method cannot be used as the receiver needs to look at many different points at same point of time. In those cases; interleaving of transmitters can be done.

For omnidirectional receivers, as the synchronised scanning is not required, hence multiple receivers can simultaneously do the surveillance while all transmitters remain active all the time.

5.5 RCS of Target for Distributed MIMO

Let there be M transmit antennas and N receive antennas. The target is modeled as having Q scatterers with complex scattering coefficients. The approach of modeling complex target as collection of many scatterers are well studied in literature [5]. It is assumed that the scatterers and the antennas lie on a same plane. The model for the same is depicted in fig. 5.4. Let τ_{Tk}^{q} be the propagation time from k^{th} transmitter to q^{th} scatterer and τ_{Rl}^{p} be the propagation time for l^{th} receiver from p^{th} scatterer. Let $S_k^T(t)$ be the total signal (from all quadrants) transmitted by the k^{th} transmitter.

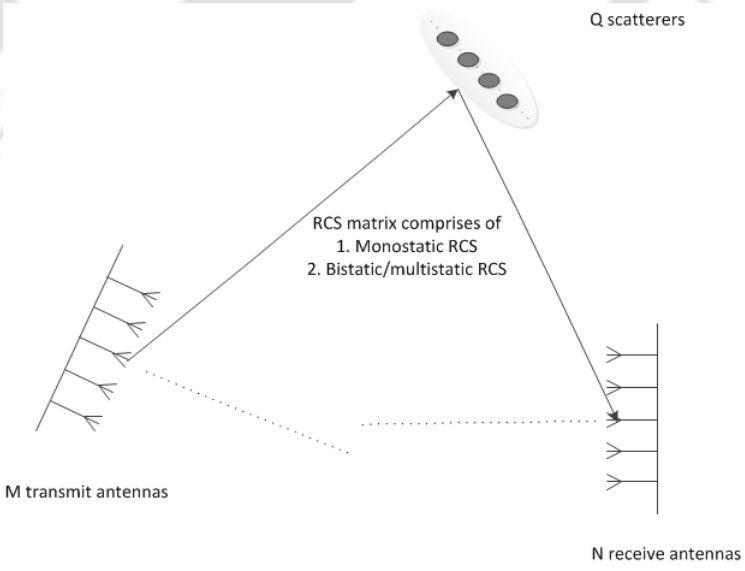

Figure 5.4: Target model for RCS estimation

TH-1898_08610214

$$S_k^T(t) = S_k^{Q_1}(t) + S_k^{Q_2}(t) + S_k^{Q_3}(t) + S_k^{Q_4}(t) \tag{5.4}$$

Let the signal received by j^{th} receiver as contribution from k^{th} transmitter from p^{th} scatterer be

$$y_{jk}^p(t) = h_{jk}^p S_k^T(t - \tau_{Tk}^p - \tau_{Rj}^p) \tag{5.5}$$

where h_{jk}^p is the back scattering coefficient from the p^{th} scatterer for j^{th} receiver and k^{th} transmitter.

Contribution from all scatterer is

$$y_{jk}(t) = \sum_{p=1}^{p=Q} h_{jk}^p S_k(t - \tau_{Rk}^p - \tau_{Rk}^p) \tag{5.6}$$

For narrowband signal, the delay can be approximated as phase difference.
Thus, the scattering coefficient for a transmitter-receiver pair can be written as

$$h_{jk} = \sum_{p=1}^{p=Q} h_{jk}^p e^{j\phi_p} \tag{5.7}$$

where $e^{j\phi_p}$ is uniformly distributed between 0 to 2π.

The term h_{jk} can be organised in a matrix of dimension $M \times N$. In case of monostatic netted radar M and N are same and the diagonal elements are monostatic RCS; wherein the off-diagonal elements are bistatic/multistatic RCS. The diagonal elements represent backscattering wherein the off-diagonal elements represent forward scattering. There are many benefits which can be derived if the bistatic/multistatic RCS can be used in a system. But, there is no probabilistic model to ascertain the performance benefit objectively rather than subjectively.

5.6 Synchronisation

The synchronisation between transmitters and receivers is very crucial for coherent or noncoherent processing. In case of coherent processing the phase information between all transmitters and receivers are mandatory to be known for combining it coherently in addition to time synchronisation. In non-coherent processing, the synchronisation between carrier of receivers is ignored. But, the synchronisation between transmitter and receiver pairs are must for clutter cancellation. But, in all cases, timing synchronisation between transmitters and receivers is must for delay measurement (Range sum

TH-1898_08610214

measurement).

Irrespective of the processing configuration, it is required that the sampling clocks in transmitter and receiver are aligned.

Let $S_{Tt}(t)$ be the timing signal for transmitter and Δt_r be the error in the timing signal of the receiver. Then

$$S_{Tt}(t) = rect\left(\frac{t}{T}\right) \tag{5.8}$$

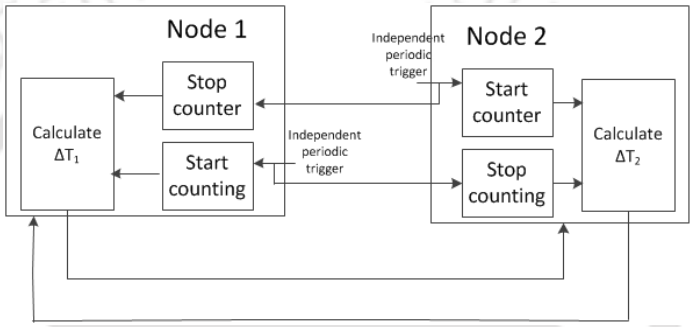

Figure 5.5: Synchronisation setup for timing signal between two nodes

$$S_{Rt}(t) = rect\left(\frac{t - \Delta t_r}{T}\right) \tag{5.9}$$

The value of Δt_r effects the range measurement accuracy.

In cases where joint processing is done before detection, it is must to ascertain the effect of inaccuracies in time synchronisation on probability of detection. In distributed detection, the timing inaccuracy will effect the accuracy of range measurement of the target.

Let $S_k^T(t)$ be the signal transmitted by the k^{th} transmitter and $S_{ik}(t)$ be the signal received by i^{th} antenna.

$$S_{ik}(t) = h_{ik} S_k^T(t - \tau_{Tk} - \tau_{Ri}) \tag{5.10}$$

where h_{ik} is the scattering coefficient.

With narrowband assumption these delay of $\tau_{Tk} + \tau_{Ri}$ can be approximated as phase change.

Let ϕ_{Tk} be the phase change because of the range from k^{th} transmitter to target and ϕ_{Ri} be the phase change because of range from target to i^{th} receiver then

$$\phi_{Tk} = 2\pi f_c \tau_{Tk} \tag{5.11}$$

TH-1898_08610214

$$\phi_{Ri} = 2\pi f_c \tau_{Ri} \tag{5.12}$$

where f_c is carrier frequency

The total phase difference ϕ_{total} is given by:

$$\phi_{total} = \phi_{Tk} + \phi_{Ri} \tag{5.13}$$

If there is a lack of synchronisation between transmitter and receiver then these equations will get modified as follows:

$$\phi_{total} = 2\pi f_c(\tau_{Tk} + \tau_{Ri}) + 2\pi f_c \Delta t_r \tag{5.14}$$

The second term is the additional phase which comes because of the lack of synchronization between the transmitters and receivers.

If in addition to the timing synchronisation error, there is also carrier synchronisation error; there will be one more additional term which will depend on the frequency error.

The timing synchronisation and the carrier synchronisation is carried out at a regular interval. The lack of synchronisation in carrier induces a extra phase shift between signal processed by receivers like the lack of timing synchronization produces. But in addition to that, it also produces additional doppler because of carrier offset.

The synchronisation can be achieved in two steps. The first step is to use very high stability oscillator. The carrier frequency is derived from this. The timing signal is also derived from that which in turn can be synchronised with 1pps (Pulse per second) signal of GPS (Global positioning system). Second step is to synchronise them at regular intervals. The synchronisation method can follow the process brought out in [50]. The scheme is shown in fig. 5.5. In this method of synchronisation, a local time counter gets started at transmitter and receiver on a predefined trigger signal and the same is also transmitted to each other. This transmitted trigger signal stops the counter on its reception which is already started as respective nodes. The time difference between transmitter and receiver is roughly $T_1 - T_2 \approx \frac{1}{2}(\Delta T_1 - \Delta T_2)$. ΔT_1 denotes the measured time difference in transmitter and ΔT_2 is the time difference in receiver. This time difference needs to be exchanged in order to calculate the error in timing signals. In case, where only timing synchronisation is done, the second step can be skipped which will make the system much simpler.

TH-1898_08610214

5.7 Transmit Monopulse

The monopulse in MIMO radar is studied in [51]. Mono-pulse is used for refining the angular estimates. The performance of monopulse technique is brought out at length in [52]. The angle measurement of a target with respect to receive antenna can be done in the receiver using the look angle of the beam or using any of the super resolution technique. In case where the angle measurement of the target is done using the look angle of the beam, the accuracy suffers to a great extent, as obtaining a very narrow beamwidth requires large antenna. Thus, in those cases monopulse technique is used. The term monopulse has its meaning in the fact that the refined angle measurement can be done using a single pulse measurement. Generally, monopulse measurement is done at the receiver to refine the estimate of angle of arrival of return from target to receiver. The angle of the target is required to be estimated after its detection. But possibility of having monopulse in transmitter looks attractive as this can bring some paradigm shift in the configuration of radar. The benefit of monopulse at transmit can be having simpler receivers. By transmit monopulse, we mean to estimate the angle of target with respect to the transmitter, though the measurement can be done only in receiver. It can be contrasted here that though the measurement of angle of the target with respect to the antenna (transmit or receive) is done at receiver; but depending on whether it is measured with respect to transmit antenna or receive antenna, it is called transmit or receive monopulse. Depending on whether the monopulse measurement follows transmit or receive monopulse method, it decides the requirement of narrower beam in transmit or receive. Transmit monopulse is essentially attractive if there are multiple receivers and their design needs to be simpler. It does not require calibration of different channels of receiver. Moreover, this can be treated as another technique whose application can be weighed based on the deployment scenarios. In this section, we intend to study the transmit monopulse technique and its imposition on system requirements.

In the proposed transmit monopulse based distributed MIMO, the transmitters are directional wherein the receivers are either omni directional or having broad beamwidth. Each receiver carries out the signal processing as shown in fig. 5.6.

Let the signal received by j^{th} receiver for k^{th} transmitter be given by $S^R_{jk}(t)$.

It was already brought out that the transmitter has four quadrants and each of them transmits orthogonal signal. Let the signal for i^{th} quadrant from k^{th} transmitter be given by $S^{Q_i}_k(t)$. The signal received by j^{th} receiver as contribution from k^{th} transmitter is given by

TH-1898_08610214

$$S_{jk}^{R}(t) = h_{jk}(S_{k}^{Q_1}(t) + S_{k}^{Q_2}(t) + S_{k}^{Q_3}(t) + S_{k}^{Q_4}(t)) \tag{5.15}$$

In the receiver, the signal is passed through matched filter to extract the contribution of each quadrant of a particular transmitter; with all the signals from four quadrants extracted; sum and difference beam is formed for estimating the monopulse angle in the transmit. The processing carried out is depicted in fig. 5.6. The process of forming sum and difference beams follow the process of phased array radar except that it is formed for transmitter in this case. Let the extracted signal for i^{th} quadrant of k^{th} transmitter extracted in j^{th} receiver be denoted by $X_{jk}^{Q_i}(t)$.

Then the sum, azimuth and elevation beam is formed as follows:

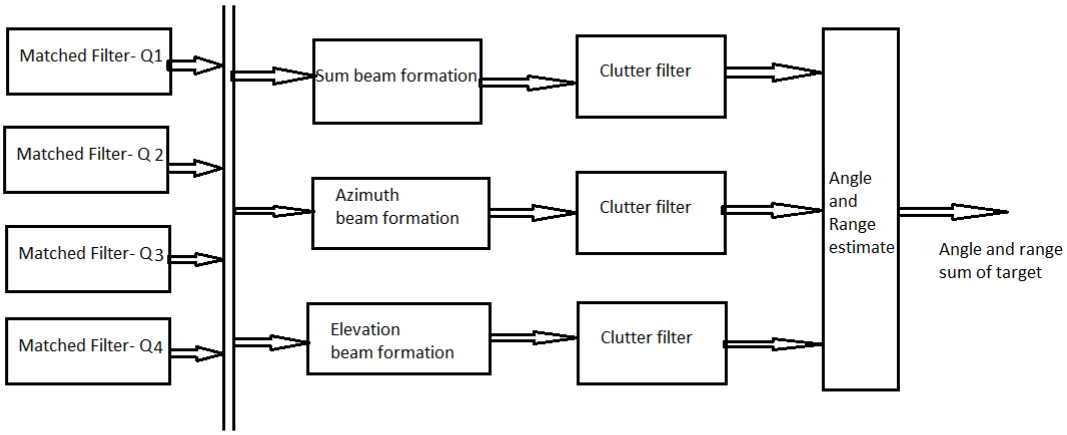

Figure 5.6: Processing for transmit monopulse

$$X_{jk}^{S}(t) = X_{jk}^{Q_1}(t) + X_{jk}^{Q_2}(t) + X_{jk}^{Q_3}(t) + X_{jk}^{Q_4}(t); \tag{5.16}$$

$$X_{jk}^{Az}(t) = X_{jk}^{Q_1}(t) + X_{jk}^{Q_2}(t) - X_{jk}^{Q_3}(t) - X_{jk}^{Q_4}(t); \tag{5.17}$$

$$X_{jk}^{El}(t) = X_{jk}^{Q_1}(t) + X_{jk}^{Q_3}(t) - X_{jk}^{Q_2}(t) - X_{jk}^{Q_4}(t); \tag{5.18}$$

where

TH-1898_08610214

$X_{jk}^{S}(t)$ denotes sum channel output

$X_{jk}^{Az}(t)$ denotes azimuth channel output

$X_{jk}^{El}(t)$ denotes elevation channel output

Let

$$X_{jk}^{S^1Az}(t) \equiv X_{jk}^{Q_1}(t) + X_{jk}^{Q_2}(t) \tag{5.19}$$

$$X_{jk}^{S^2Az}(t) = X_{jk}^{Q_3}(t) + X_{jk}^{Q_4}(t) \tag{5.20}$$

$$X_{jk}^{S^1El}(t) = X_{jk}^{Q_1}(t) + X_{jk}^{Q_3}(t) \tag{5.21}$$

$$X_{jk}^{S^2El}(t) = X_{jk}^{Q_2}(t) + X_{jk}^{Q_4}(t) \tag{5.22}$$

Then

$$X_{jk}^{S}(t) = X_{jk}^{S^1Az}(t) + X_{jk}^{S^2Az}(t) \tag{5.23}$$

$$X_{jk}^{S}(t) = X_{jk}^{S^1El}(t) + X_{jk}^{S^2El}(t) \tag{5.24}$$

$$X_{jk}^{Az}(t) = X_{jk}^{S^1Az}(t) - X_{jk}^{S^2Az}(t) \tag{5.25}$$

$$X_{jk}^{El}(t) = X_{jk}^{S^1El}(t) - X_{jk}^{S^2El}(t) \tag{5.26}$$

From these, the monopulse ratio is obtained as follows:

$$dbys_{Az} = \frac{X_{jk}^{Az}(t)}{X_{jk}^{S}(t)} \tag{5.27}$$

$$dbys_{El} = \frac{X_{jk}^{El}(t)}{X_{jk}^{S}(t)} \tag{5.28}$$

The beam formed by all quadrants look at the same direction but their phase centres are displaced by an amount depending on the quadrants. Thus, the following expression can be written

$$dbys_{Az} = \frac{A_1 e^{(j\phi_1)} - A_1 e^{(j\phi_1 + j\frac{2\pi d_{Az} sin\theta_{Az}}{\lambda})}}{A_1 e^{(j\phi_1)} + A_1 e^{(j\phi_1 + j\frac{2\pi d_{Az} sin\theta_{Az}}{\lambda})}} \tag{5.29}$$

TH-1898_08610214

$$dbys_{El} = \frac{A_2 e^{(j\phi_2)} - A_2 e^{(j\phi_2 + j\frac{2\pi d_{El} sin\theta_{El}}{\lambda})}}{A_2 e^{(j\phi_2)} + A_2 e^{(j\phi_2 + j\frac{2\pi d_{El} sin\theta_{El}}{\lambda})}} \tag{5.30}$$

where d_{Az} and d_{El} is the distance between phase centres of the quadrants in azimuth and elevation direction respectively. θ_{Az} and θ_{El} is the angle of target in azimuth and elevation direction respectively. A_1 and A_2 are arbitrary multiplication factor. ϕ_1 and ϕ_2 are arbitrary phase. λ is the wavelength of the carrier.

Eq. 5.29 and eq. 5.30 reduces to

$$dbys_{Az} = jtan(\frac{\pi d_{Az} sin\theta_{Az}}{\lambda}) \tag{5.31}$$

$$dbys_{El} = jtan(\frac{\pi d_{El} sin\theta_{El}}{\lambda}) \tag{5.32}$$

These two ratios are also called as 'dbys' ratio for azimuth and elevation. A lookup table can be generated so that given the 'dbys' ratio; the offset angle of target from the look angle ($\theta_{Az}\theta_{El}$) can be estimated.

5.8 Location Estimate

Target position can be estimated following the technique used for bistatic radar with required modification to incorporate transmit monopulse. There are studies carried out for obtaining closed form expression for localisation in distributed MIMO radar [53]. We intend to use the standard methods for location estimates which is used in bistatic radar. Following are four different methods [49]:

(i) Technique 1:

Target position is estimated with respect to the receiver. The look angle in receiver can be directly measured. Techniques for improving the measurement of look angle can be used. This measurement along with the range sum measurement can yield the target position.

(ii) Technique 2:

The transmit beam pointing angle can also be used. Unless the transmitter and the receiver are collocated, the accuracy of the angle measurement is sacrificed. Thus, the accuracy of location estimate suffers.

TH-1898_08610214

(iii) Technique 3:

The receiver estimates the difference in the propagation times of return from target from different transmitters. This along with the AOA at receiver can estimate the location of the target. This requires the detections to be associated with the actual target to ascertain the difference in propagation times.

(iv) Technique 4:

This technique is called theta-theta. In this technique, the location is estimated by knowing the look angle in transmit and receive along with the baseline. Here also the inaccuracies of transmit look angle have penalty in the location estimate.

The proposed method for estimating the location of target is based on technique 2 but does not suffer from penalty brought out there as the angle estimated in transmit is refined using monopulse. The reasons for choosing technique 2 are (a) Unlike in technique 1, the proposed method does not require any specified accuracy for the lookangle in receive, thus allows receive antenna to have wide beamwidth (b) technique 3 requires multiple transmit antennas, but the proposed method works for single transmitter case also (c) technique 4 requires accurate lookangle in both transmitter and receiver, which we want to avoid to have the receiver antenna with wide beamwidth. The transmit monopulse angle from the look direction in azimuth and elevation plane is obtained as brought out in earlier section and the corrected angle is obtained as below:

$$\theta^c_{Az} = \theta_{Az} + \Delta\theta_{Az} \tag{5.33}$$

$$\theta^c_{El} = \theta_{El} + \Delta\theta_{El} \tag{5.34}$$

Let us look at the bistatic triangle as shown in fig. 5.7 formed by the target, transmitter and receiver. From this, the range from transmitter R_t and range from receiver R_r can be computed as follows;

$$R_r = \frac{R_\Sigma^2 + L^2 - 2R_\Sigma L cos(\theta_t)}{2(R_\Sigma - L cos\theta_t)} \tag{5.35}$$

TH-1898_08610214

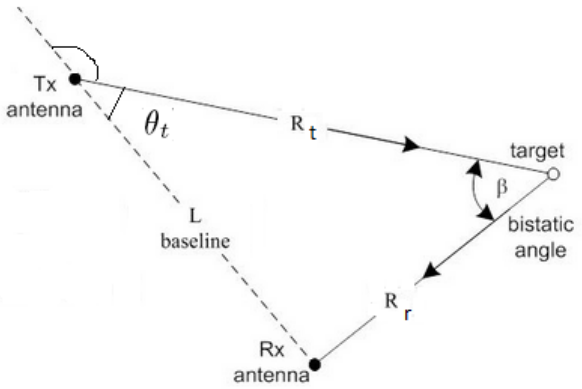

Figure 5.7: Bistatic Angle

$$R_t = R_\Sigma - R_r \tag{5.36}$$

where

R_r = Range of target from receiver

R_t = Range of target from transmitter

R_Σ = Total distance (From transmitter to receiver via target)

L = Baseline as shown in figure

θ_t = Angle between baseline and the line connecting transmitter and target

With R_r, R_t, θ^c_{Az} and θ^c_{El}, the position of the target with respect to transmitter can be ascertained. As the position of the receiver and the target with respect to the transmitter is known; the angle between baseline and the line connecting transmitter and target can be easily found out. We denote the position of the target with respect to k^{th} transmitter and measured at j^{th} receiver by (x_{jk}, y_{jk}, z_{jk}).

5.9 Scanning of Beams and Timing in Transmitter and Receiver

The scanning in bistatic radar is required to be different than the monostatic radar. In monostatic radar, the transmitter scans the area and the receiver also looks at the same direction at the same time. In case of distributed MIMO with single transmitter, all the receivers needs to look at a given object in space at a given time when this is illuminated by the transmitter. This means that when the transmitter and receiver are at two different place only the intersection of their beams will illuminate

TH-1898_08610214

the target and energy will be received by the receiver. This is known as beam scan on scan in bistatic radar literature. This results in huge loss of energy when the receive beamwidth is narrow. This can be alleviated by having multiple beams in receiver or using pulse chasing. Fig. 5.8 shows the pulse chasing technique. In this technique, the single receive beam rapidly scans the volume covered by the transmit antenna. As brought out in [49], the scan rate of receive antenna can go as high as 0.1 degree per μsec. To achieve such high speed of beam scanning, it mandates the use of phased array.

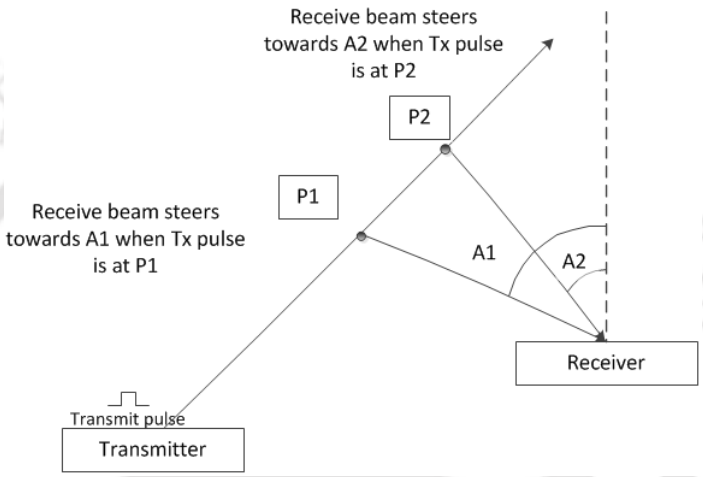

Figure 5.8: Pulse chasing technique

In the proposed distributed MIMO using the transmit monopulse, there is no requirement on angular accuracy of the receive antenna and the same can have wide beamwidth thus reducing the cost drastically. In the proposed technique, it is only required to know the look angle of the transmitter for the purpose of estimating the location of the target by measurement of the monopulse angle at transmit and the range sum delay. If the receiver beamwidth is sufficiently wide, then it may be required to only step it very slowly with a granularity of beamwidth. This will alleviate the problem of beam scan on scan, pulse chasing and multiple receive beam to a great extent. It is proposed to have the timing generation in transmitter to follow a predefined pattern so that the same need not be communicated to the receiver and the direction of transmit beam can be calculated based on the time elapsed from specific trigger which is used for generation of timing. We propose to use the 1pps signal from GPS receiver as trigger for generation of timing signal.

TH-1898_08610214

5.10 Fusion of Measurements

Let the position estimate from each transmit-receive pair be (x_{jk}, y_{jk}, z_{jk}). These estimates are with respect the location of the respective transmitter. Before carrying out fusion, these need to be transformed to a single origin. Let $(x^{'}_{jk}, y^{'}_{jk}, z^{'}_{jk})$ be the transformed location estimates of the a target with same point as origin of the coordinate system (may be location of the first transmitter).

In general, the fusion of the information can follow any of these below mentioned three architecture [54].

- Direct fusion of the sensor data
- Representation of the sensor data with feature vectors with subsequent fusion of the feature vectors
- Processing of each sensor to achieve high level inferences or decisions, which are subsequently combined

These are pictorially depicted in fig. 5.9.

The first methodology is highly studied in literature [54] and our main aim is to show that in principle the accuracy of the estimate improves using the proposed configuration. We propose to use the first method for the purpose of combining the data. Once all the measurements are obtained the same is associated to a prospective target. All the associated measurements are fused subsequently. The fused estimate of the target location will be given by:

$$X = \sum_{\forall(i,j)} w_{jk} x^{'}_{jk} \tag{5.37}$$

$$Y = \sum_{\forall(i,j)} w_{jk} y^{'}_{jk} \tag{5.38}$$

$$Z = \sum_{\forall(i,j)} w_{jk} z^{'}_{jk} \tag{5.39}$$

where $w_{jk} = \frac{SNR_{jk}}{\sum SNR_{jk}}$. SNR_{jk} is the signal to noise ratio associated with the target detection for (k, j) transmit-receive pair.

TH-1898_08610214

These fused estimate will provide a superior estimate of the target location.

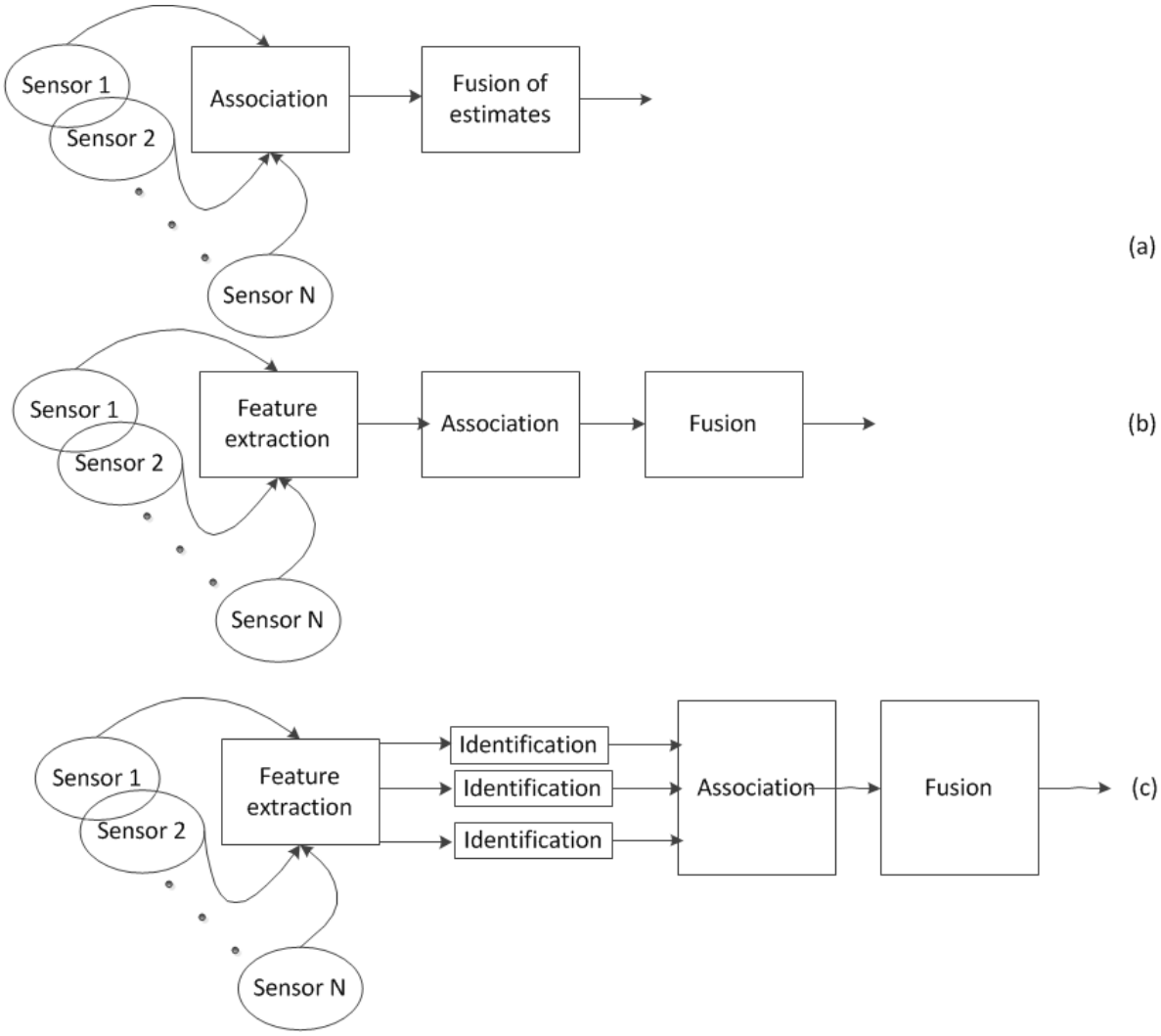

Figure 5.9: Different levels of data fusion

5.11 Simulation and Results

The simulation study is divided into two parts viz., monopulse at receivers & transmitter and distributed MIMO performance. For the purpose of simulating the monopulse characteristic we have assumed a uniform linear array (ULA). The number of element assumed is 160 with a spacing between them as half wavelength (Typical size of many surveillance radars).

The number of elements assumed for simulation is just for representative purpose only. We have evaluated the monopulse curves for ULA with uniform illumination and with aperture weighting as well.

TH-1898_08610214

The fig. 5.10 shows the sum and difference pattern for ULA with uniform illumination at receive. The same pattern is shown fig. 5.11 for receive antenna with aperture weighting. As it is seen from the figure that with aperture weighting in receive, along with the widening of sum beam, the difference beam also got widened. It may also be noted that in case of uniform illumination, the nulls in difference pattern were coinciding with the alternate nulls of the sum beam. With aperture weighting the difference beam does not have nulls and got widened. The difference pattern also dominates over the sum beam outside the $3dB$ beamwidth, which may also be used to reject targets coming through sidelobes.

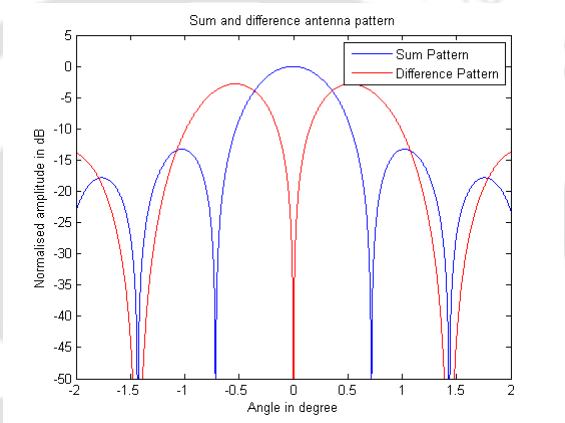

Figure 5.10: Sum and difference pattern without aperture weighting

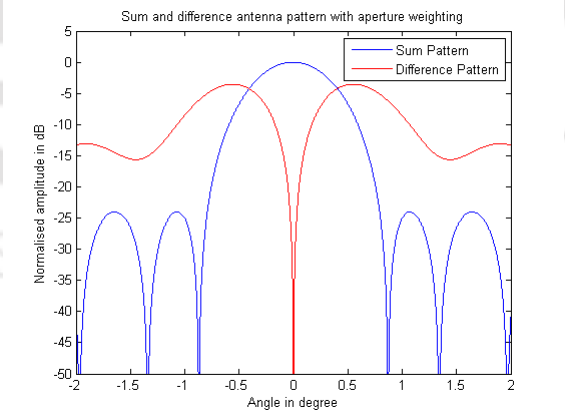

Figure 5.11: Sum and difference pattern with aperture weighting

From this patterns, the monopulse curve is generated which is also called as 'dbys' curves. The monopulse curve for receive antenna with uniform illumination is shown in fig. 5.12 and the one with aperture weighting is shown in fig. 5.13. As shown in preceding section, it can be seen from the figure that the real part of 'dbys ratio' is zero. Within the 3dB beamwidth of the main beam, the ratio is

TH-1898_08610214

almost linear.

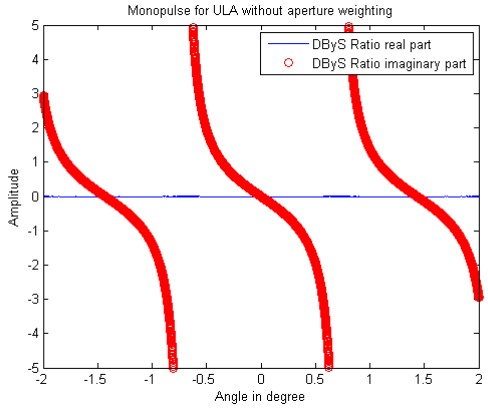

Figure 5.12: dbys curve without aperture weighting

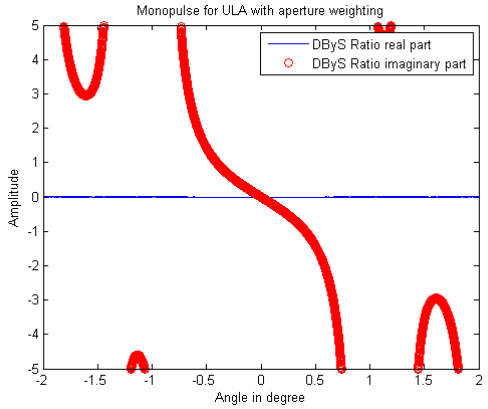

Figure 5.13: dbys curve with aperture weighting

Until this, the monopulse processing was done in receiver and it is used to ascertain the finer estimate of the target direction with respect to receive antenna. The monopulse in receive was simulated to show its equivalence with transmit monopulse. Fig. 5.14 show 'dbys curve' for transmit monopulse. As the transmit monopulse can be done only if the quadrants transmit orthogonal signals, the noise waveforms are used in the simulation as orthogonal waveforms.

It can be seen from the figure that the real part is not exactly zero at the points where the sum pattern go through the nulls. As the monopulse is used for refining the angle estimate within the main beam, this will not effect the angle measurement. Thus, this shows the efficacy of the transmit monopulse for refining angle measurement.

The efficacy of the fusion of the measurements and the resulting improvement in the estimation of location estimate of the target is simulated using the parameters in table 5.1.

TH-1898_08610214

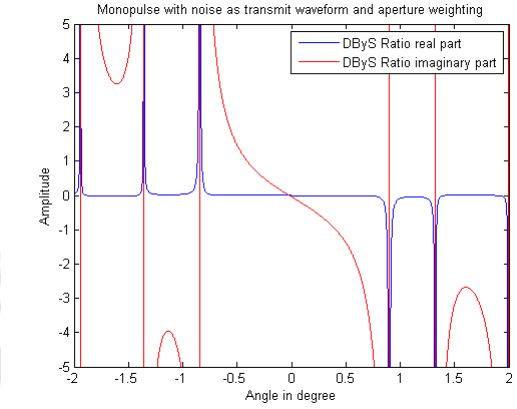

Figure 5.14: dbys curve with aperture weighting and noise waveforms

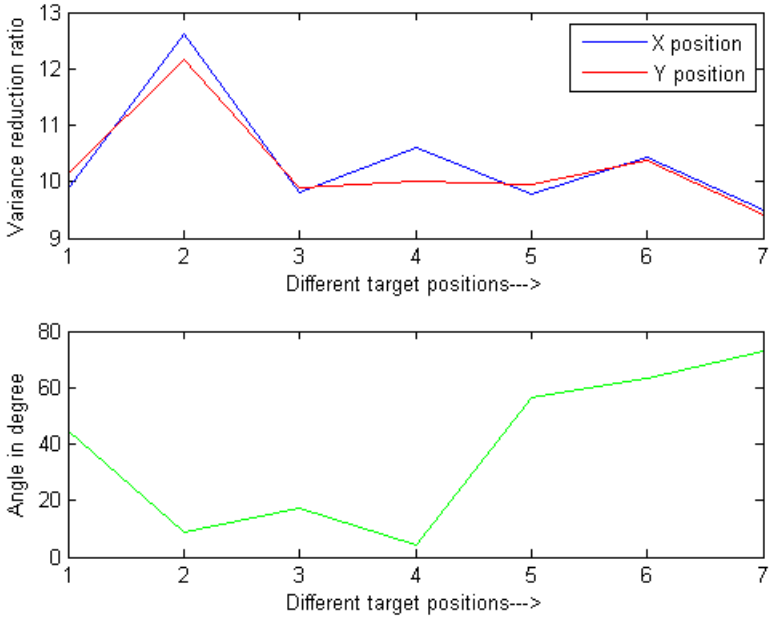

Figure 5.15: Distributed MIMO Performance with 12 receivers

TH-1898_08610214

Table 5.1: Simulation parameters for distributed MIMO

Parameters	Value
No of Rx	12, 6
No of Tx	1
No of targets	7
Avg distance of Rx from transmitter	100km
Avg distance of target from Tx	60km

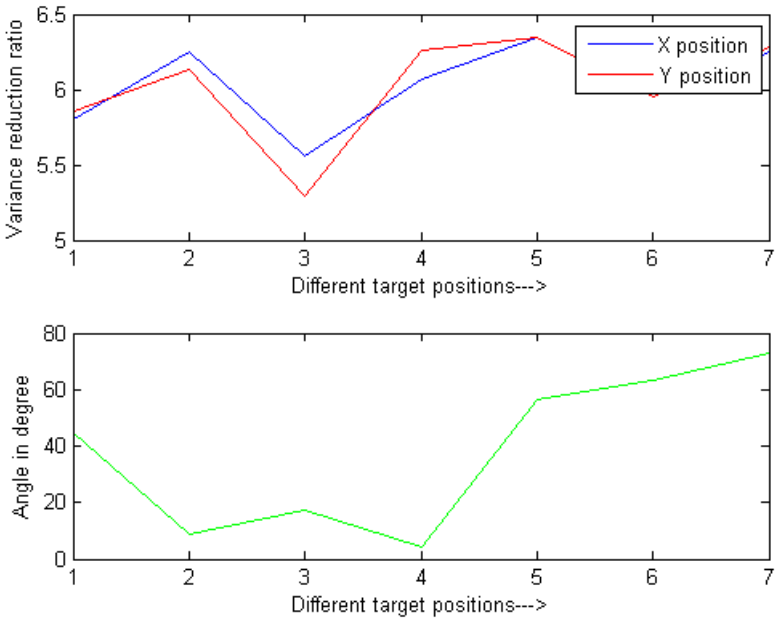

Figure 5.16: Distributed MIMO Performance with 6 receivers

To quantify the improvement, we have used the metric 'variance reduction ratio'. It brings out the reduction in variance of the single sensor measurement to the variance of fused measurement. It can be seen from the fig. 5.15 that the minimum variance reduction ratio is around 9.4 whereas the maximum variance reduction ratio is around 12.6. It is also to be brought out here that the antenna is assumed to be ULA and the receivers, transmitters and the targets are assumed to be in the same plane. The simulation was carried out for different locations of the targets, it shows that the variance reduction ratio depends on the location of the target. A comprehensive value for variance reduction ratio can be quoted for a given number of receivers and transmitters by averaging the variance reduction ratio, but this was not done to show the dependence of the same on location of the targets. The performance is also simulated with 6 receivers and the performance is shown in fig. 5.16.

TH-1898_08610214

5.12 Conclusion

A distributed MIMO configuration based on transmit monopulse to simplify the receiver is proposed. It is proposed to use '1pps' signal from GPS receiver and stable clock sources in transmitter and receivers to generate timing. It is also showed that the simplification of receiver along with wide beamwidth alleviates the problem of beam scan on scan and pulse chasing. In any case, if pulse chasing is used, it will require very slow stepping of antenna beam. Simulation is carried out for transmit monopulse with noise waveform as orthogonal waveforms. Further, the performance for distributed MIMO with different number of receivers was also simulated. The improvement in the performance as variance reduction ratio was brought out. The simulation was carried out assuming ULA as transmitter and receiver. The target, transmit antenna and receive antenna all are assumed to be in same plane. This brings out the performance improvement without any loss of generality. The simulation has been carried out for target at different angles with respect to the transmitter; it shows variation in the performance improvement achieved based on this angle.

TH-1898_08610214

6

High Range Resolution with Stepped FM in Subapertured MIMO Radar

Contents

TH-1898_08610214

6.1 Introduction

This chapter studies the use of MIMO radar for stepped frequency for higher range resolution. The use of stepped frequency across pulses for high resolution has been studied widely [55]. This configuration of high resolution radar has restriction for moving targets. The stepped frequency for high resolution radar depends on the varying phase differences produced by stepping of frequency for target at different ranges. For high resolution ranging with stepped frequency, it is assumed that all the phase shifts are produced because of stepping of frequency and the range of the target. For moving target, this technique experiences shortcomings as there will be additional phase changes because of the movement of the target. These phase changes are non separable from the changes produced by stepping of frequency. These additional phase changes distort the range profile of the target [56]. Secondly, if the pulse dimension is consumed for high resolution; doppler filtering can not be done on the return. Making a bunch of pulses for stepping of frequency and then repeating the same for carrying out doppler frequency reduces the unambiguous doppler space severely. In the proposed technique, the stepping of frequency is carried out across transmit subapertures. MIMO processing at receive allows separation of waveforms transmitted by different transmit subapertures. It also ensures that the doppler processing is not disturbed and the ambiguity function is also improved.

6.2 Brief Description

Radar detects the presence of target and estimates range, direction and optionally the doppler [57]. In the system under consideration, it is assumed that the antenna is directional and it covers the whole space under surveillance through electronic scanning. So, the estimated direction is look direction of the antenna and the estimate can be made finer if the radar uses monopulse. For estimating the range of the target, the roundtrip delay of the transmitted pulse is measured. For this purpose, a clock is run at the receiver triggered on the rising edge of the transmission of the pulse. This clock registers the time when the return from the target arrives at the receiver. As the range is marked at every clock cycles, the range takes discrete values (though centroiding process makes the range a continuous variable). The frequency of the clock, called as range clock, is equal to the inverse of the pulse width in case of unmodulated pulsed CW (Continuous wave) or inverse of compressed pulse width in case of modulated pulse used as transmit waveform.

In fig. 6.1 it is shown that the antenna is steered in a particular direction which provides the

TH-1898_08610214

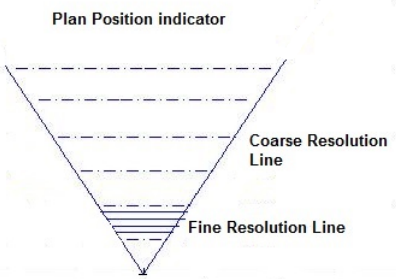

Figure 6.1: Scenario of high range resolution

direction of the target. The dotted lines are range circles (represented as straight lines) coinciding with the rising edge of the range clock. Thus, two targets between the space demarcated by two consecutive dotted range circles can not be distinguished. For obtaining finer range resolution, the space between the dotted arcs are to be further subdivided as shown in the same figure. The proposed technique of using stepped frequency across subapertures is used to obtain this further resolution. The use of transmit subaperturing in MIMO context in studied in [7]. The initial range estimate is called coarse resolution. Within a coarse range cell, there can be multiple targets. In case of multi-target scenario, all the targets may have same velocity or varying velocity. The performance of any technique for obtaining finer resolution should address this scenario. The first case may refer to an extended target where in the finer resolution is used to achieve high resolution profile of the target for the purpose of target classification. The second case may refer to targets flying closely spaced but with different velocity.

As the performance of any technique is required to be evaluated for both stationary and moving target, the ambiguity function [57] provides a good way of evaluating the same. It is known that the linear frequency modulated waveform (LFM) produces ambiguity as a line in delay-doppler space, where the slope depends on the chirp rate of LFM. The ambiguity function of the proposed waveform shall also be evaluated to ascertain its performance.

6.3 System Configuration

The configuration under study assumes collocated transmit and receive antennas. Let us consider an antenna array with N_s subapertures at transmit and single aperture at receive where the signal from

TH-1898_08610214

each element is accessible for beamforming. Stepped frequency is used as transmit waveform across transmit subapertures. At receiver, the signal is received by a single aperture that has combined contributions from all transmit subapertures. The received signal is digitised at each element and passed through filters to separate the contribution from each transmit subaperture. The baseband signal at each receive element is digitised at a rate dictated by the frequency content of each subaperture waveform. This signal from all receive elements are combined for a particular transmit subaperture to form a beam in particular direction. The beamformed output for each transmit subaperture is then passed through stepped frequency processing. This produces the finer range resolution. This resolves the target within a given coarse range cell. The movement of target also impacts the performance. Fig. 6.2 and fig. 6.3 shows the system configuration used in the current study.

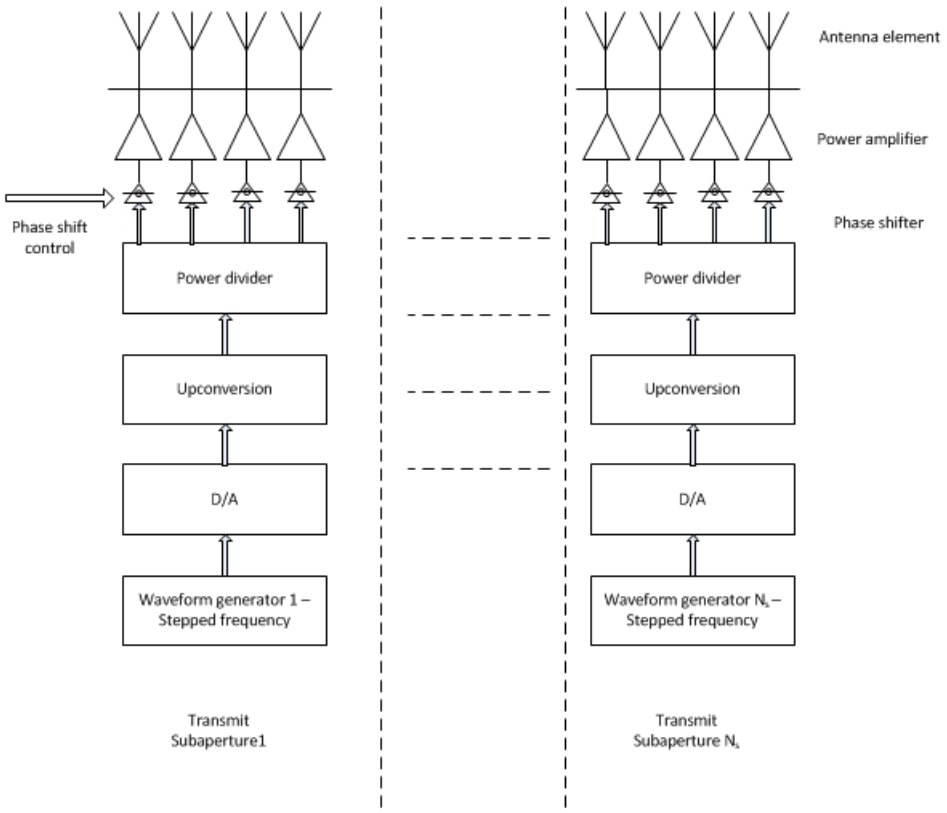

Figure 6.2: System configuration - Stepped frequency transmitter

6.4 Wideband Beamforming

Higher bandwidth ensures higher range resolution but at the same time it also requires that the beam remains focused at all frequencies. In the proposed configuration, the transmit beamforming

TH-1898_08610214

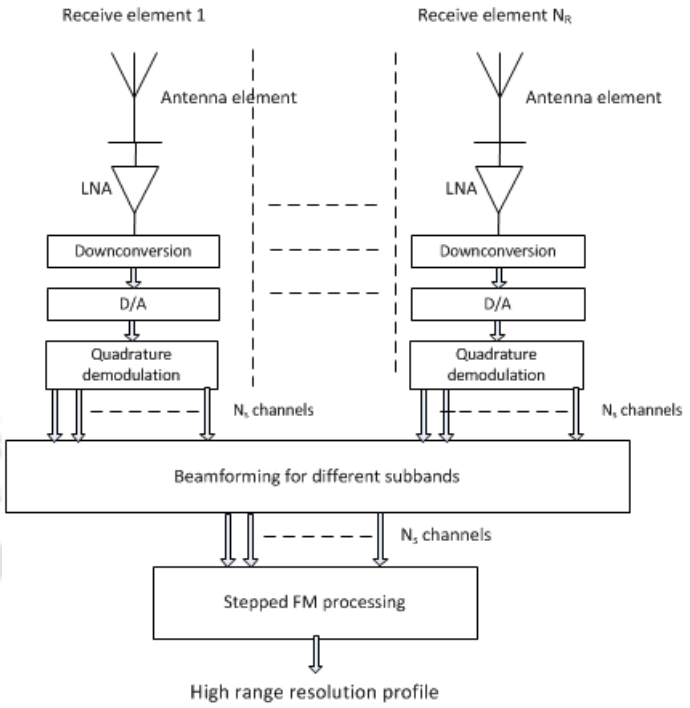

Figure 6.3: System configuration - Stepped frequency receiver

is done at subaperture level where the signals transmitted are narrowband. At receiver the signal is wideband, thus technique of wideband beamforming needs to be applied. The problem of wideband beamforming has been addressed widely in literature. For radars, there are additional constraints, e.g., taking care of doppler filtering, clutter mitigation etc. As the waveform is wideband, the doppler can not be approximated by a single value; the doppler value can at best be approximated by multiple single tone for different subbands in case subband beamforming is carried out. Subband beamforming entails decomposition of the fullband signal into many subbands followed by standalone processing which is followed by combining all the subbands into a single wideband signal again [58]. In [58] it is brought out that the individual subbands can be processed independently. In the context of radar, the clutter rejection filtering, doppler filtering is done on the subbands. Here, we propose to combine the contribution of all subapertures (subbands) from each doppler separately. As the movement of target produces dilation effect on the signal which generally is approximated by doppler shift in the frequency is invalid for wideband signal [58]. In wideband signal the signal can not be approximated by a shift in frequency because of movement of target, but each subbands (which in turn have narrow bandwidths) can be approximated to have doppler shift which is different from one subband to the other. Thus, the doppler filter shall be defined such that it has equal width corresponding to the

TH-1898_08610214

velocity. However, the width of the doppler filter in frequency domain will be unequal. The relation between the filter width of i^{th} and $(i+1)^{th}$ subband is given by

$$\Delta fd_{i+1} = \frac{f_{i+1}}{f_i} \Delta fd_i \tag{6.1}$$

The center frequency of the doppler filter in i^{th} and $(i+1)^{th}$ subband is given by

$$fd_{i+1} = \frac{f_{i+1}}{f_i} fd_i \tag{6.2}$$

where f_i is the center frequency of i^{th} frequency subband.

The scheme proposed to be used in the current study is shown in fig. 6.4:

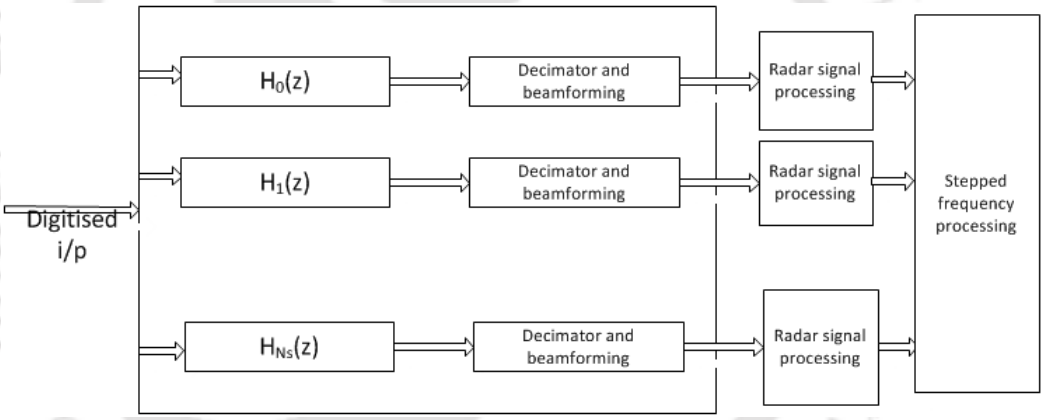

Figure 6.4: Wideband beamforming and stepped frequency processing

As shown in fig. 6.4, the digitised signal is divided into subbands followed by beamforming, radar signal processing and then the stepped frequency processing for obtaining finer range resolution.

6.5 Analysis

The configuration of the system assumes N_s subapertures in transmit. Full aperture in receive (N elements) is used for beamforming. The elements in receive are digitised to form beam in certain direction. Though the signal transmitted by each subaperture is narrowband, the signal received by the receive array is wideband.

Let the signal from i^{th} transmitter be $x_i(t)$. The waveform from each transmitter is considered to

TH-1898_08610214

be pulsed CW.

$$x_i(t) = B_i \,\mathrm{Re}\, e^{(2\pi f_i t)} \quad 0 < t < T \tag{6.3}$$

where

$$f_i = f_0 + i\Delta f$$

$$B_i = \text{Amplitude for } i^{th} \text{ subaperture}$$

Then the signal received by the j^{th} element of receive array from a target at a range of r_0 and moving with a velocity v is given by

$$y_j(t) = \sum_{i=1}^{N_s} e^{\phi_{ij}} \gamma_i x_i(\sigma t - \tau) \tag{6.4}$$

where

$$\begin{aligned} \sigma &= \frac{c-v}{c+v} \\ \tau &= \frac{2r_0}{c+v} \\ e^{\phi_{ij}} &= \frac{-2\pi f_i j d sin\theta}{c} \end{aligned} \tag{6.5}$$

Here c denotes velocity of light, θ denotes the look direction, d distance between two elements of receive array and γ_i is a complex multiplicative factor to take into account the attenuation because of spreading of the microwave energy, the phase change owing to the path length and the complex backscattering coefficient of the target. The signal $y_j(t)$ which has contribution from all transmit subapertures is downconverted using f_i; $\forall i$. Thus the receiver attached to each receive element will have N_s channels of signal after downconversion. The downconverted signal is filtered to obtain the subband corresponding to the frequency of transmit subaperture. Hence, the phrase 'contribution from each subaperture' will be interchangeably used with the term 'subband' hereafter. Let the signal be downconverted using f_i from j^{th} receive element be denoted as $y_{ij}(t)$. The downconverted signal will be complex baseband signal.

$$y_{ij}(t) = B_i e^{\phi_{ij}} \gamma_i e^{(j\psi_i)} \tag{6.6}$$

TH-1898_08610214

where

$$\psi_i = 2\pi f_i t(\sigma - 1) - \tau 2\pi f_i \tag{6.7}$$

The signal from individual receiver attached to each receiving element is digitised to produce $y_{ij}[n]$. The receive beamforming is done on $y_{ij}[n]$ by combining contribution from all receiving elements for each subband separately. Let the beamformed output for i^{th} subband be given by

$$y_i^b[n] = \sum_{i=1}^{N} y_{ij}[n] w_j \tag{6.8}$$

where w_n are weights for beamforming and depends on the look angle, distance between receive elements (d) and the frequency f_i.

Now

$$y_i^b[n] = B_i \gamma_i A_i exp(j\psi_i) \tag{6.9}$$

As B_i can be made to be B $\forall i$, γ_i does not vary significantly over different i and A_i is known for a given direction; hence they can be clubbed to a single variable C. Hence

$$y_i^b[n] = C exp(j\psi_i) \tag{6.10}$$

The phase difference between two consecutive subbands is given by

$$\Delta\psi = -2\pi\Delta f(\frac{2vt}{c+v}) - 2\pi\Delta f\tau \tag{6.11}$$

$$\Delta\psi = -2\pi\Delta f(\frac{2vt}{c+v}) - 2\pi\Delta f\frac{2r_0}{c+v} \tag{6.12}$$

The first term in above equation has non zero value only in case of moving target. Let us analyse the phase difference between subbands for stationary target. Thus for a stationary target

$$\Delta\psi_s = -2\pi\Delta f\frac{2r_0}{c+v} \tag{6.13}$$

Let r_0 be written as $r_0 = r + \Delta r$; where r is obtained by delay measurement of the pulse return and Δr is to be measured for finer range resolution.

TH-1898_08610214

$$\Delta\psi_s = -2\pi\Delta f\frac{2r}{c+v} - 2\pi\Delta f\frac{2\Delta r}{c+v} \tag{6.14}$$

As the coarse range is registered with the rising edge of the range clock; r in eq. 6.14 can be written as $r = mR_{res}$, where R_{res} is the coarse range resolution and m is an arbitrary integer. As $v << c$, the equation reduces to

$$\Delta\psi_s = -2\pi\Delta f\frac{2mR_{res}}{c} - 2\pi\Delta f\frac{2\Delta r}{c} \tag{6.15}$$

We know $\frac{2R_{res}}{c}$ is equal to the reciprocal of bandwidth of the transmitted waveform from transmit subaperture. Moreover, if we assume the frequency stepping (Δf) from one subaperture to the other as equal to the bandwidth, then

$$\Delta\psi_s = -2\pi m - 2\pi\Delta f\frac{2\Delta r}{c} \tag{6.16}$$

It is seen that the phase difference between two subbands for stationary target has two terms; the first term produces integral multiple of 2π which has no impact on complex exponential function, so let us analyse the second term.

The second term produces a phase shift which is proportional to the negative of finer range Δr of the target. Thus the finer range resolution can be obtained by passing the received signal vector $Y^b[n]$ through IDFT (Inverse discrete Fourier transform); where $Y^b[n]$ is given by

$$Y^b[n] = [y_1^b[n]\ y_2^b[n] \dots y_{N_s}^b[n]]^T \tag{6.17}$$

Each coarse range samples (for each value of n) is passed through the IDFT processing block. As the finer resolution is measured using the phase which can give unambiguous measurement only in interval $[0, 2\pi]$, hence $\Delta\psi_s$ shall not cross a value of 2π within a coarse range resolution cell. Thus, $\Delta\psi_s$ corresponding to largest Δr (denoted by Δr_{max}) shall not exceed 2π. Then Δr_{max} is given by

$$\Delta r_{max} = \frac{c}{2\Delta f} \tag{6.18}$$

which is also equal to the coarse range resolution. This means that the whole range between coarse range resolution can be resolved by this technique of finer resolution. As the resolution is obtained by

TH-1898_08610214

passing the range samples from all subbands through IDFT block; the fine range resolution is given by

$$\Delta r_{res} = \frac{\Delta r_{max}}{N_s} \tag{6.19}$$

The above analysis is carried out with the assumption of stationery target. Moving target will disturb the term $\Delta\psi$ which will produce ambiguity. The impact of moving target on range resolution for stepped frequency across pulses are brought out in [56]. The ambiguity function for the proposed technique is discussed in the next section.

6.6 Ambiguity Function

The ambiguity function is a tool for ascertaining the quality of the waveform [57]. The ambiguity for narrowband and wideband waveform is studied in [59] and [60] and the error introduced by using standard narrowband ambiguity for wideband signal is also brought out there in [60]. The narrowband ambiguity function is given by

$$NAF_x(f_d, \tau) = \int_{-\infty}^{\infty} \widetilde{s}(t)\widetilde{s}^*(t-\tau)e^{-j2\pi f_d t}dt \tag{6.20}$$

In cases where the effective bandwidth of the signal is higher, the wideband ambiguity as given below needs to be used

$$WAF_x(f_d, \tau) = \sqrt{\sigma}\int_{-\infty}^{\infty} x(t)x^*(\sigma t - \tau)dt \tag{6.21}$$

where $x(t)$ is the analytical signal.

The above equation provides a direct method to evaluate the ambiguity function of the waveform. The same can be evaluated using the exact processing performed to obtain the finer range resolution. Looking back at eq.6.12, the ambiguity function can be evaluated by having a target at a location r_0 and introducing velocity from minimum to maximum value and plotting the signal output in delay-velocity (range-velocity) plane. For an ideal ambiguity, the range remains invariant to change in velocity. Let us analyse the eq. 6.12 to understand the effect of the first term on ambiguity.

In this equation, it can be seen that the range localisation gets effected by the velocity and range

TH-1898_08610214

of the target. The parameter t in the equation can vary from 0 to PRT (Pulse repetition time). Thus, it is clear that the ambiguity depends on the range also in addition to the velocity. As brought out in sec. 6.5, a value of $\frac{2\pi}{N_s}$ for $\Delta\psi$ produces a finer resolution of Δr_{res} for stationary target. Thus the following condition needs to be satisfied for the first term of eq. 6.12, so that the movement of target does not distort the range profile significantly.

$$\frac{4vt\pi\Delta f}{c+v} << \frac{2\pi}{N_s} \tag{6.22}$$

6.7 Simulation and Results

The simulation studies are carried out to demonstrate the finer range resolution obtained using stepped frequency across transmit subapertures. The simulation brings out the following scenarios.

- Single stationary target
- Single moving target
- Multiple stationary targets
- Multiple moving targets with same velocity
- Multiple moving targets with different velocities
- Ambiguity function for same system parameters for target at 75km and 300km

The last scenario brings out the ambiguity function for target at different ranges to show the dependence on the same. It sums up the effect observed in scenario no. 2 and 5. The simulations are run for a coarse resolution of 60 meter and the bandwidth for each transmit subaperture is taken as 2.5MHz. The number of subapertures at transmit is taken to be 16. Thus, the achievable finer range resolution is 4.9 meter considering hamming window in performing the IFFT (Inverse fast Fourier transform). The value of different parameters are tabulated in table 6.1.

Fig. 6.5 shows a single target. X-axis shows the finer range for one coarse range cell (which varies from 0 to 60 meter). It can be seen that the 3dB main lobe width matches with the resolution value worked out analytically. The amplitude is normalised to maximum value. Fig. 6.6 brings out the single target while in motion (for two cases : 600m/s, 1200m/s) superimposed on the finer range profile while the target was stationary. It can be seen that the range of the target has moved. The

TH-1898_08610214

Table 6.1: Various simulation parameters - Stepped frequency

Scenario No	No. of targets	Range-km (Finer range - mtr)	Velocities - m/s
1	1	200(11.25)	0
2	1	200(11.25)	600, 1200
3	3	200(3.75, 14.53, 30)	0
4	3	200(3.75, 14.53, 30)	600, 600, 600
5	3	200(3.75, 14.53, 30)	800, -600, 600

portion of the plot showing the movement is zoomed and put in the inset. It can be seen that the amount of movement of range has doubled when the velocity is doubled which shows agreement with the analysis carried out in sec. 6.5. Now let us turn our attention to multitarget scenario, we

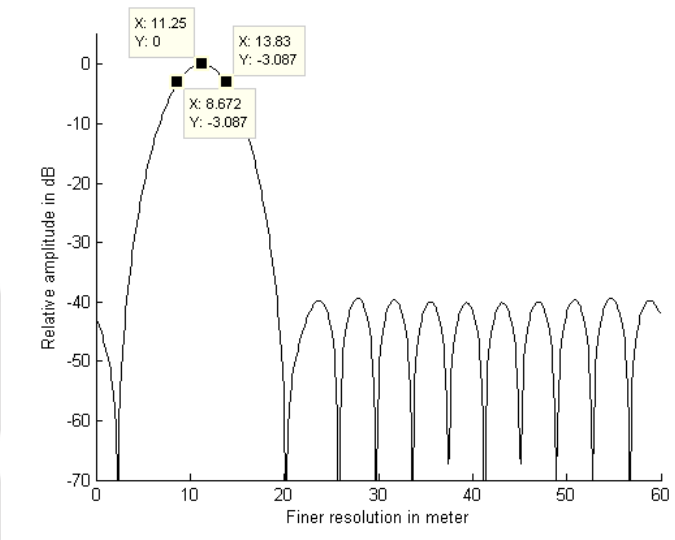

Figure 6.5: Range profile - Stationary single target

have simulated three targets; the second and third target has a relative amplitude of -10 and -17dB respectively with respect to the first target. The finer range profile is shown in fig. 6.7. Three targets are clearly visible in the figure. The relative amplitudes of all the targets are also marked. Fig. 6.8 brings out the range profile for same targets while all of them are moving with same velocity. We can clearly see from the inset of the figure that all the targets have moved in range by almost same amount. Thus the relative position of all the targets did not get disturbed. Fig. 6.9 now shows the case when targets are moving at different velocities. The profile in inset shows that the range has moved differently for different targets. Thus it clearly brings out the dependency of the range profile on the velocity of the target. But in all cases the shift in range localisation is very less compared to

TH-1898_08610214

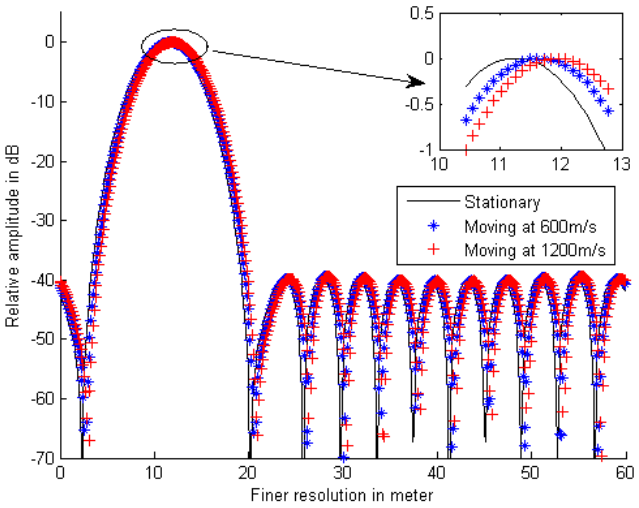

Figure 6.6: Range profile - moving single target

the finer resolution provided. Thus its effect is minimal. Here it shall be mentioned that in [56], the restriction on difference of velocities between the targets were brought out. It was seen clearly that a small difference of the order of 3m/s had totally spoilt the range profile of the target. The proposed technique has demonstrated its robustness against this aspect.

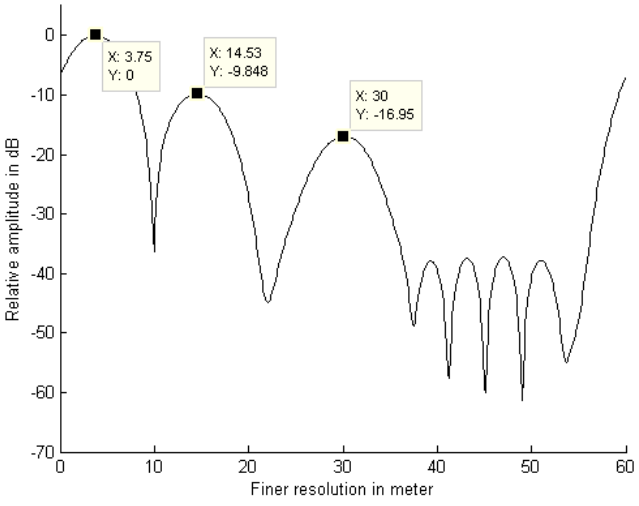

Figure 6.7: Range profile-multiple stationary targets

Now let us look at the ambiguity function for the said configuration. It was brought out that the ambiguity function is dependent on the range of the target. We have simulated the ambiguity function for target at 300km and at 75km. It can be clearly seen from the fig. 6.10 and fig. 6.11 that the

TH-1898_08610214

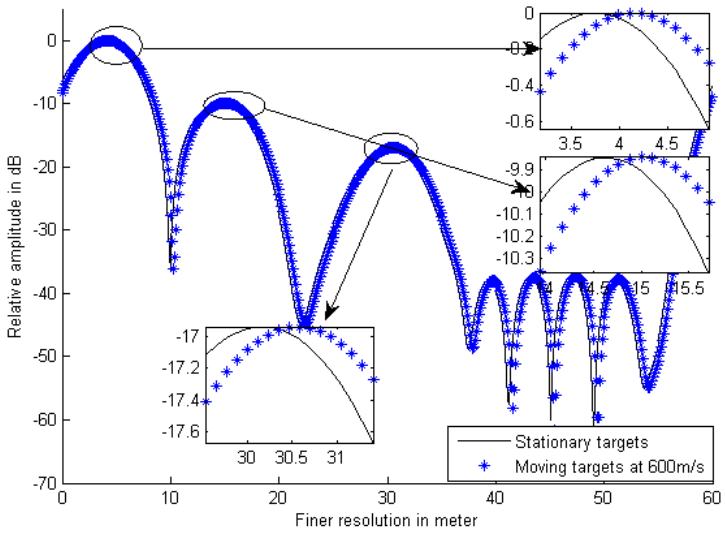

Figure 6.8: Range profile-Multiple moving targets with same velocity

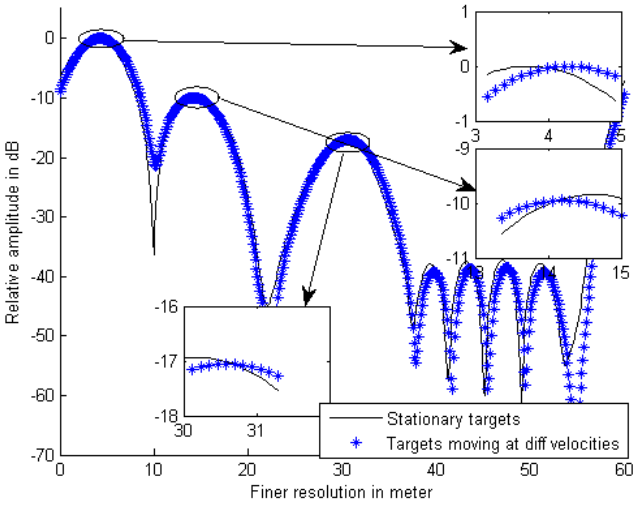

Figure 6.9: Range profile-Multiple moving targets with different velocity

TH-1898_08610214

ambiguity is more pronounced for higher range.

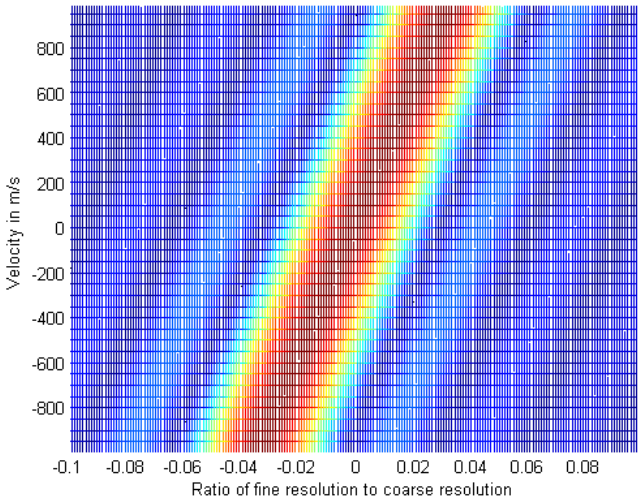

Figure 6.10: Ambiguity function for target at range of 300km

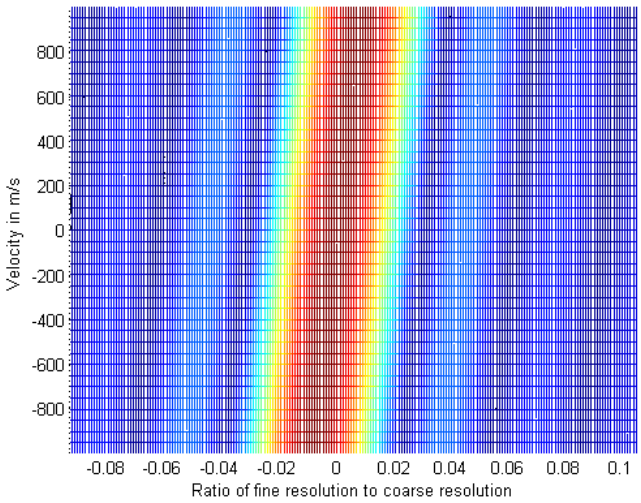

Figure 6.11: Ambiguity function for target at range of 75km

6.8 Conclusion

MIMO radar with stepped frequency across subapertures has shown to provide higher range resolution in the same lines of stepped frequency across pulses. Though it works in the similar lines of stepped frequency across pulses, it has additional benefits as brought out in this chapter. Major challenge in any radar is to mitigate clutter and the same is done using frequency domain processing

TH-1898_08610214

along slow time. The use of stepped frequency across subapertures enables the doppler processing. The use of stepped frequency across subapertures did not affect the normal doppler processing employed in radar as the frequency is not stepped along pulses which is used for slow time sampling for frequency domain processing or analysis. Also, the method of using stepped frequency across subapertures provides partial mitigation of effect of target velocity on finer range resolution. As time span over which the stepped frequency processing is carried out is much smaller than that of stepped frequency across pulses, the impact of velocity on phase of the signal is minimal. In addition to these, we have also studied the ambiguity function of the proposed technique. In conclusion, the proposed technique provides a superior method for obtaining finer range resolution with an additional cost of beamforming at element level.

TH-1898_08610214

7

Orthogonal Waveform for MIMO Radar Using Frequency Hopping Sequence

Contents

TH-1898_08610214

7.1 Introduction

Study of MIMO radar system assumes that there is availability of waveforms satisfying various criteria. For many years, conventional radars transmit and receive the same waveforms and process it in same way. Recently, several MIMO radar concepts and applications based on waveform orthogonality assumption have been proposed [61]. The issue of waveform design needs to be addressed including its practical application. Waveforms used in MIMO radar need to be orthogonal in transmit and receive. Additionally, they should also preferably have constant envelope. Orthogonality at receive means that the waveforms are orthogonal at all delays. In literature, various orthogonal waveforms are proposed based on polyphase sequence [22] [23] and also based on varying chirps (chirp rate, up-down chirps). In MIMO radar, more number of antennas will give more degrees of freedom but there should be enough orthogonal waveforms to support the number of antennas. Thus, it is required to generate large number of orthogonal waveforms. MIMO radar can also transmit correlated or partially correlated waveforms. The existing design methods for correlated waveforms often assume some prior knowledge for the target response and use the knowledge to optimize the waveforms, but generally no prior knowledge is available for actual MIMO radars [24]. Thus, we concentrate on the issue of design of orthogonal waveforms. The study of orthogonal waveforms for netted radar based on polyphase sequence is studied in [22] and [23]. Frequency-hopping (FH) signals are good candidates for the radar waveforms because they are easily generated and have constant modulus. In the traditional SIMO (Single input multiple output) radar, Costas codes [62] have been introduced to reduce the side lobe in the radar ambiguity function. The waveform based on FH sequence is studied in [63] [64]. The main performance metric for these waveforms are very low aperiodic auto-correlation sidelobe level and very low aperiodic cross-correlation. We propose to use the hyperbolic frequency hop sequences as orthogonal waveforms for MIMO radar. Generally auto and cross-hit array is used for analysis of FH sequence [65] [66]. We have used the actual signal for study of the auto and cross-correlation function of the waveform. We proposed the phase randomised FH sequence for improvement of cross-correlation function and the SLL of auto-correlation function.

The hyperbolic FH sequence provides a large number of orthogonal FH sequences equal to $(p-1)$; where p is a prime number which is decided based on the number of time slots required for the radar waveform, also called subpulses in the radar parlance. Generally, p will be a large number and shall be good enough to produce the required number of orthogonal waveforms as long as the number

TH-1898_08610214

of orthogonal waveforms is around or below 100. The hyperbolic FH sequences give entries having maximum value of 2 in auto and cross hit array; but the evaluation of same using the actual signal provides the precise values of auto and cross-correlation functions. The proposed signal using phase randomised FH sequence is studied in this thesis and evaluated against the waveform without phase randomisation. The doppler tolerance is also studied using MIMO ambiguity function.

7.2 System Configuration

MIMO radar under consideration uses orthogonal waveforms at the transmitter at element level or at subarray level [7]. The same signals are extracted at the receiver after passing through matched filter. A fully orthogonal waveform between transmitting elements will ensure that the contribution of each of the transmitting element can be extracted without any disturbance from the other. As this is not possible to be achieved in practice; it is desirable to have very low cross-correlation between the waveforms. From the standpoint of range resolution the waveform also should posses impulse like auto-correlation function.

The above requirements on the auto and cross-correlation function can be mathematically expressed as follows [63].

1) Minimize the signals auto-correlation function, everywhere except for the 0 time shift in which the normalized auto-correlation function has value one, and

$$A_u(\tau) = \int_{-\infty}^{\infty} u(t)u^*(t-\tau)dt \tag{7.1}$$

2) Minimize the cross-correlation function,

$$A_{(u_1,u_2)}(\tau) = \int_{-\infty}^{\infty} u_1(t)u_2^*(t-\tau)dt \tag{7.2}$$

of any two signals in the system, for every time shift. For radar, an additional doppler shift in the frequency of return signal also will be there; the evaluation of correlation has to consider this effect as well. This will modify the auto and cross-correlation functions to auto and cross-ambiguity function as follows:

TH-1898_08610214

$$A_u(\tau,\omega) = \int_{-\infty}^{\infty} u(t)u^*(t-\tau)e^{j\omega t}dt \tag{7.3}$$

$$A_{(u_1,u_2)}(\tau,\omega) = \int_{-\infty}^{\infty} u_1(t)u_2^*(t-\tau)e^{j\omega t}dt \tag{7.4}$$

In addition to these, the waveform shall be of constant envelope. The same can be written as

$$|u_i(t)| = C \tag{7.5}$$

where C is constant.

Here, we discuss the existing methods for generation of orthogonal signals. It is known that the up and down chirp signals are orthogonal. The following figure shows two chirp signals; one is up-chirp and other is down-chirp signal. The imaginary part of the signal is shown in fig. 7.1; real part is not shown as they will be same for up and down chirp. The auto-correlation and and cross-correlation output is shown in fig. 7.2. It can be clearly seen that they are nearly orthogonal at all delay.

7.3 Orthogonal Waveform Design Based on Existing Techniques

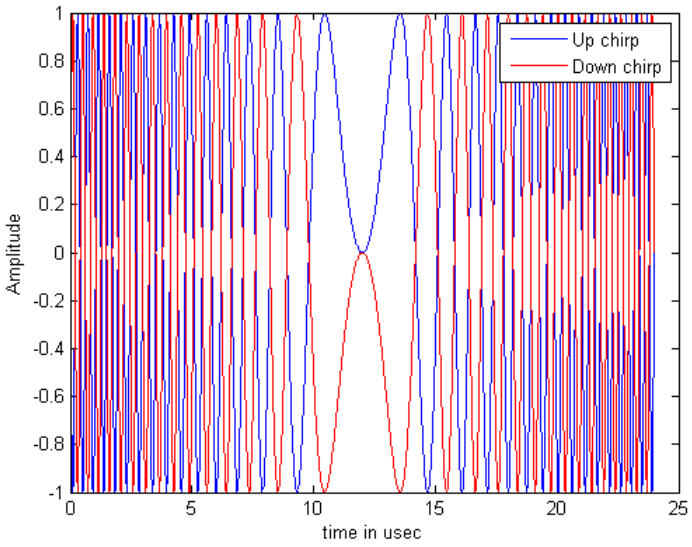

Figure 7.1: Baseband up and downchirp signal

It is also important to evaluate the ambiguity function of chirp signal. Fig 7.3 shows the ambiguity function of chirp signal.

TH-1898_08610214

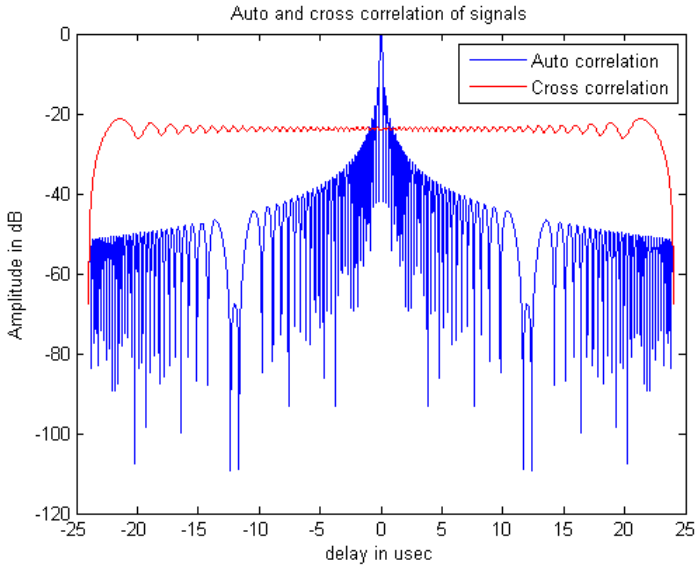

Figure 7.2: Auto and cross-correlation of up and down chirp

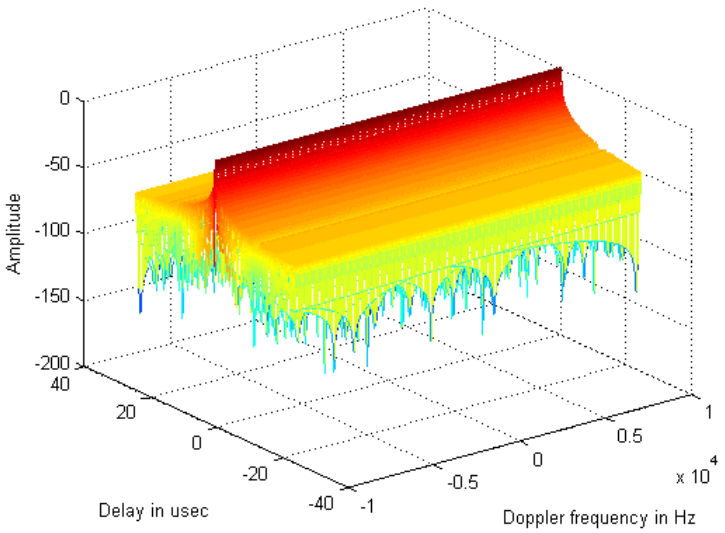

Figure 7.3: Ambiguity function of chirp signal

TH-1898_08610214

But this method of producing orthogonal signals has the disadvantage that they can produce only two orthogonal signals. In [24], it is proposed to design multiple orthogonal waveforms based on frequency and chirp rate diversity. The brief outline of the same is brought out here for brevity and later comparison.

In the paper [24], three waveforms using chirp rate and frequency diversity was simulated and performance was brought out. It was reported in the literature that the for a bandwidth of 200MHz and 8μsec signal duration, the pairwise cross-correlation value was 34.95dB below auto-correlation peak [24]. With lower bandwidth (bandwidth reduced to half), the cross-correlation got degraded to 32.48dB. The values of side lobe level quoted there was for pairwise cross-correlation values. In case of MIMO radar, the MIMO ambiguity function needs to be evaluated to ascertain the performance. As it is seen that the waveforms are never fully orthogonal so there will be cross-correlation of any given waveform with other, in cases when there are many orthogonal waveforms transmitted the cross-correlation with all signals will add up in some sense to degrade the overall ambiguity of the system.

7.4 Frequency Hopping Sequence

In modern radar and communication systems, FH techniques have become very popular. The hopping sequences are used to specify which frequency will be used for transmission at any given point of time. Compared with other sequences whose alphabet size is small e.g., two (bi-phase modulation) or four (quadrature phase modulation), FH sequence have much larger alphabet size which is available to number of frequencies [64].

Fig. 7.4 shows the the frequency hop signal of length T and N time slots.

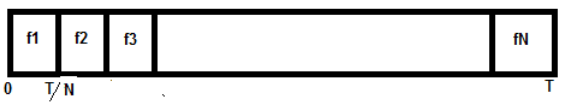

Figure 7.4: Frequency hop signal of length T

The signal is given by

$$u(t) = \Sigma_{k=1}^{N} p(t - kT/N) cos[2\pi(f_0 + f_k)t] + \theta_k \tag{7.6}$$

TH-1898_08610214

where

$$p(t) = \begin{cases} 1, & \text{if } t \leq T/N \\ 0, & \text{otherwise} \end{cases}$$

and f_0 is the carrier frequency, θ_k is the phase shift for each timeslots, f_k is the frequency for k^{th} time slot, T is the length of frequency hop signal and N is the number of time slots.

Let us consider that there are N_2 possible frequencies and there are N_1 number of time slots. Then the FH sequence can also be denoted as a matrix of 1 and 0 of dimension $N_2 \times N_1$. Let this be denoted by A_N. A superscript r is used to indicate the waveform index. Thus if there are L number of transmitters which require orthogonal waveforms, r will vary from 1 to L.

In radar or sonar systems, it is well known that the range of a target from the observer is proportional to the round trip delay time or time shift and the velocity of the target approaching or receding from the observer is proportional to the doppler or frequency shift. Because of the two dimensional nature of the shift operation, it is useful and natural to present the FH sequence by matrix having 1 and 0 as entries. An entry of 1 in (i, j) location of the matrix indicates that at j^{th} time slot frequency alphabet f_i is used for construction of the waveform. Let this matrix be denoted as A. In the receiver, the user ascertains the shift in time and frequency by comparing all possible shifts of a replica of the transmitted signal.

There are many FH sets proposed in literature [64]. The quality of FH sets are analysed using auto and cross hit array. This basically indicates the number of slots where the frequency of waveforms coincides for different shifts. Costas array is commonly used for very good auto-correlation. In spite of the fact that Costas array has very good impulsive auto-ambiguity properties, they generally have rather poor cross-ambiguity properties when sets of Costas array signals are considered. In fact its proved that Costas array can not have ideal one hit cross-ambiguity. On the other hand, linear congruence sequences have ideal one hit cross-ambiguity but have poor auto-ambiguity functions [67]. FH sequences based on cubic congruence have at most two hits in auto-ambiguity and at most three hits in cross-ambiguity functions [68]. The best known FH sequence is hyperbolic FH sequence [63].

7.5 Proposed Orthogonal Waveform

The proposed orthogonal waveform is based on hyperbolic FH sequence.

Let $A_N^r = \{a_{i,j}^r\}$

TH-1898_08610214

where A_N^r denotes the matrix with $'1'$ and $'0'$ entry. The row indicates the frequency alphabets and the column indicates the time slots. An entry of $'1'$ at a particular position indicates that at that time slot the frequency corresponding to that row is used to construct the waveform. The superscript is for different waveforms.

Hyperbolic FH sequence is generated following the below method [64]:

$$a_{i-1,j-1}^{r-1} = \begin{cases} 1, & \text{if } i = rj^{-1}(mod\ p) \\ 0, & \text{otherwise} \end{cases}$$

where $1 \leq r, i, j \leq p-1$. The length of the FH sequence is $N = p-1$. For any given prime p, one can generate a set of $M = p-1$ FH sequences. This matrix can also be written as a vector with entries as the index to frequency alphabet rather than $'1'$ and $'0'$. The entries will decide the frequency to be used in a particular timeslot.

Let us consider the following example for $p = 5$. With this value of p, four orthogonal sequences can be made with the length of each as 4 time slots or subpulses. The FH sequence is given below :

$a^{(0)} = \{(0\,2\,1\,3)\}$

$a^{(1)} = \{(1\,0\,3\,2)\}$

$a^{(2)} = \{(2\,3\,0\,1)\}$

$a^{(3)} = \{(3\,1\,2\,0)\}$

These entries indicate the index of the frequency alphabets at baseband which will be translated using a carrier. This is generally calculated as follows:

$f_i = i * BW/N - BW/2$

TH-1898_08610214

Table 7.1: Various simulation parameters for FH waveforms

Parameters	Values
Bandwidth	20MHz
p	257
L	25
Doppler span	$\pm$10kHz

With these values of frequencies, the signal can be generated by using eq. 7.6. We consider two cases:

Case I: where the value of θ_k is zero.

Case II: where the value of θ_k is uniformly distributed between 0 and 2π (Proposed phase randomised FH sequence).

Though it is important to investigate the auto-correlation of each sequence and cross-correlation of each possible pair; in case of MIMO, the total signal at the output of MIMO processing need to be evaluated to ascertain the performance.

The signal at the output of MIMO processing is given by:

$$S(\tau) = \sum_{i=1}^{L}\sum_{j=1}^{L}[\int_{-\infty}^{\infty} u_i(t)u_j^*(t-\tau)dt] \tag{7.7}$$

For return signal with doppler the eq. 7.7 will be modified to

$$S(\tau,\omega) = \sum_{i=1}^{L}\sum_{j=1}^{L}[\int_{-\infty}^{\infty} u_i(t)u_j^*(t-\tau)e^{j\omega t}dt] \tag{7.8}$$

This is also called as MIMO ambiguity function. The expression inside the double summation of eq. 7.7 shall be evaluated pairwise to ascertain the cross-correlation of each pairs and then the summed up value should be evaluated to quantify the total effect of residual cross-correlation of the signals.

7.6 Simulation and Results

The simulation is carried out for both the cases with the parameters as in table 7.1. The fig. 7.5 shows the auto and cross-correlation of the signal for Case I. Fig. 7.6 shows the signal at the output of MIMO processing at zero doppler where the results have the contribution of all the auto and cross-correlation for the same case. It is seen that the SLL is around 29.5dB. Further simulation is carried

TH-1898_08610214

out for the proposed phase randomised FH sequence. The fig. 7.7 shows the auto and cross-correlation of the signal for Case II. Fig. 7.8 shows the signal at the output of MIMO processing for second case. It can be seen that the SLL at the output of MIMO processing has improved by approximately 5dB for the proposed phase randomised FH sequence. Fig. 7.9 shows the ambiguity function for the proposed waveform for a doppler span of ±10kHz. It can be seen that there is no significant degradation in the sidelobe level. It can be seen from fig. 7.10 that there is gain loss of 3dB at 9 kHz doppler.

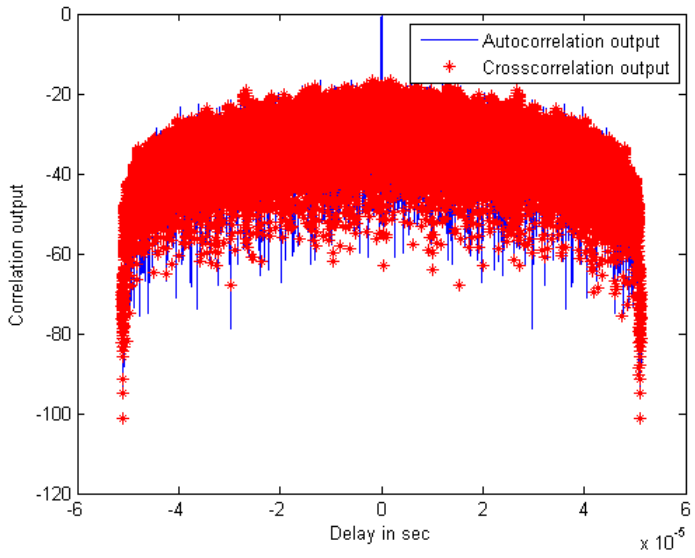

Figure 7.5: Correlation output of FH signals

It can also be seen that the sidelobe performance of this is much better than the polyphase sequences which is studied in literature [22]. It was shown there that for a sequence of length 40 the cross-correlation sidelobe was around 17dB which is expected to be better for longer length sequence by $\sqrt{N}$. Thus for a sequence of length 257, following the above said relation the SLL will improve by only 4dB making the SLL as 21dB; which is much inferior to the one proposed here. The performance achieved here is also compared with [24]. The cross-correlation was around 35dB for 200MHz bandwidth which got reduced by 2.5dB for 100MHz bandwidth. Thus, it can be reasonably assumed that the value will degrade further for a bandwidth of 20MHz which is the bandwidth assumed for our simulation. Moreover, we have evaluated cross-ambiguity for MIMO rather than pairwise ambiguity function which is a stricter evaluation criteria. This shows that the proposed technique has yielded better results than recently proposed orthogonal waveform design.

TH-1898_08610214

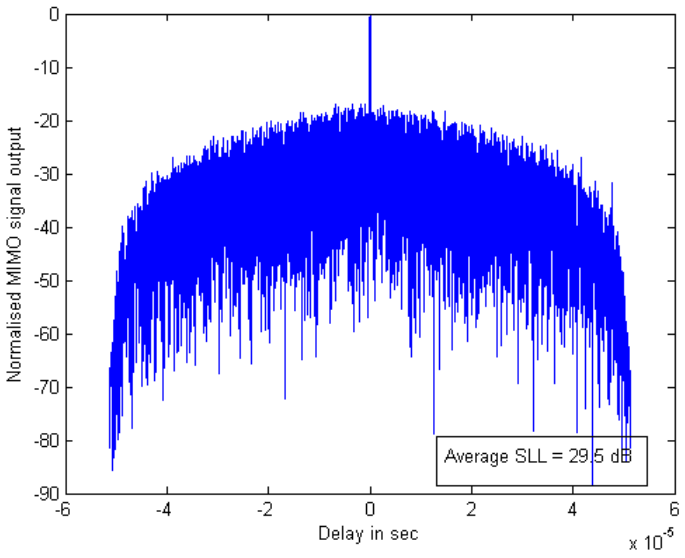

Figure 7.6: Output after MIMO processing of FH signals

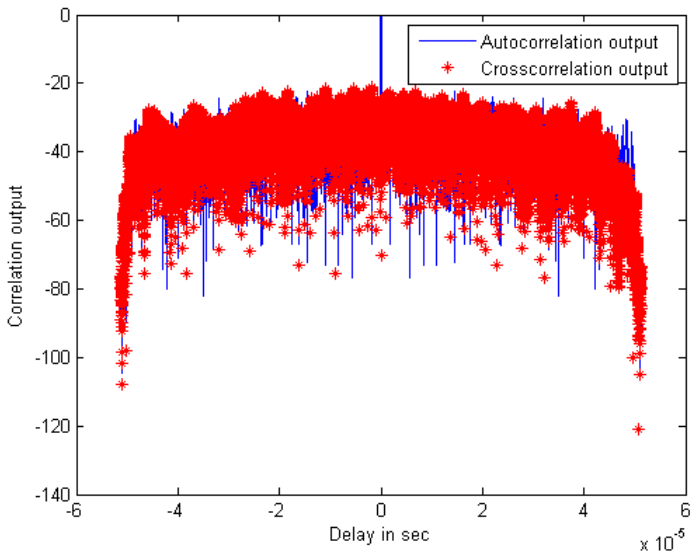

Figure 7.7: Correlation output of the modified FH signals

TH-1898_08610214

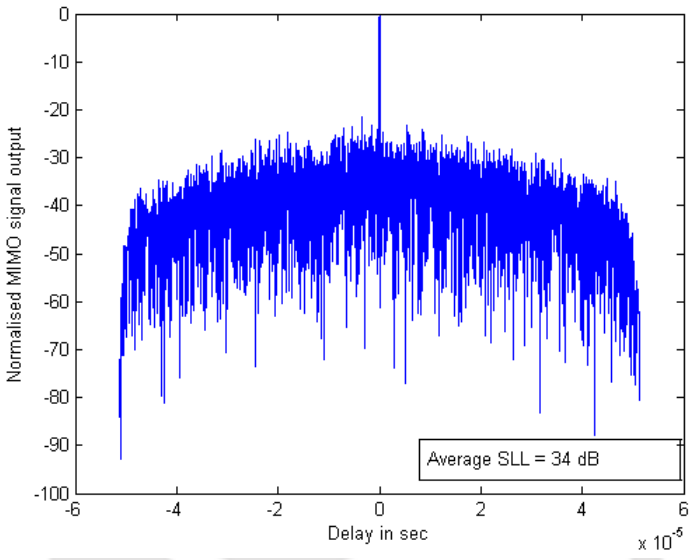

Figure 7.8: Output after MIMO processing of modified FH signals

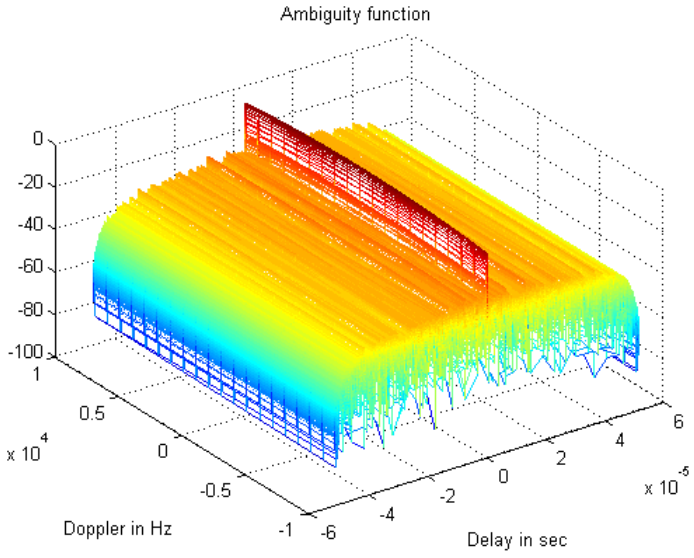

Figure 7.9: MIMO ambiguity function for modified FH signals

TH-1898_08610214

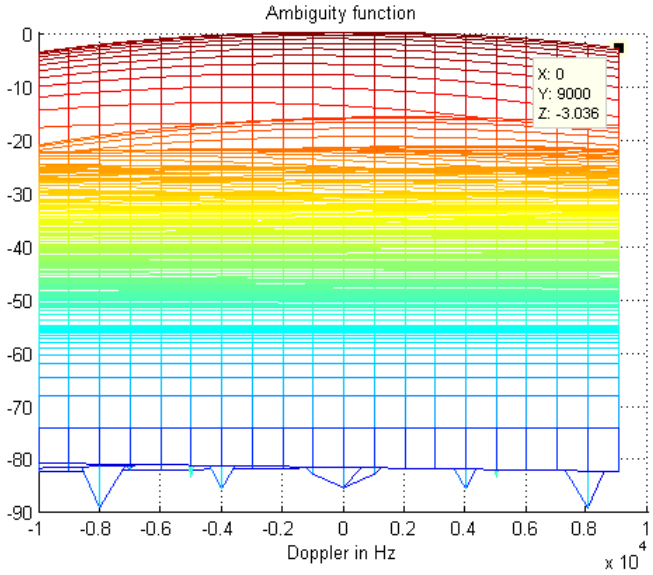

Figure 7.10: MIMO ambiguity function for modified FH signals - Gain loss

7.7 Conclusion

A method for design of orthogonal waveforms for MIMO radar with phase randomised FH sequence is proposed. The proposed method of waveform generation is based on hyperbolic FH sequence and it provides a large number of orthogonal waveforms for use in MIMO radar. It is also shown that it performs better than the FH sequence without phase randomisation. The sidelobe levels are much lower than the waveform designed based on polyphase sequence. Compared to the orthogonal waveforms designed based on chirp rate and frequency diversity as reported in literature, the proposed waveforms yield superior results. It is also shown that there is no significant degradation in sidelobe level with increase in doppler. A loss of around 3dB is encountered at a doppler frequency of 9kHz.

TH-1898_08610214

8

Conclusions and Future Work

भारतीय प्रौद्योगिकी संस्थान गुवाहाटी • Indian Institute of Technology Guwahati •

Contents

TH-1898_08610214

8.1 Conclusion

The work carried out in this thesis is to understand and analyse various facets of MIMO radar and propose new solutions and ideas to exploit the benefits of MIMO radar. The areas studied include collocated and distributed MIMO. Briefly the studies and results are summarised below:

- Comparative study of MIMO radar with phased array radar:

  The performance of collocated MIMO radar has been studied and compared with that of phased array. It has been brought out that the large virtual array produced by MIMO radar for monostatic fully filled array suffers from huge penalty. It is also brought out that to have a comparable sidelobe level in virtual array, the benefit of high resolution needs to be compromised. These penalties are in addition to the penalty in SNR. It is also brought out that improvement provided by virtual array becomes significant only for sparse monostatic array. But in all these cases the SNR penalty remains and the same can not be compensated by longer ToT because of range migration. Thus we need to use subapertured transmit MIMO radar to alleviate this problem.

- Sparse monostatic planar array:

  A configuration of planar array to produce very large virtual array has been proposed. Also a metric to ascertain the efficiency of any sparse monostatic array to produce large virtual array is introduced. We compared the efficiency with the sparse ULA proposed in literature and showed that the efficiency of the proposed sparse planar array is as same as that of ULA.

- Stepped frequency across transmit subapertures:

  The use of stepped frequency across transmit subapertures for enhancing the range resolution is proposed and benefits of this technique has also been brought out. The ambiguity function for the proposed technique has been evaluated and demonstrated the dependance of it on range of the target.

- Resource manager for MIMO radar:

  Resource manager plays a vital role in any multi-function radar. In MIMO there are additional degrees of freedom which can be used. A primitive resource manager is proposed and its benefits are demonstrated. It is also brought out that the benefit becomes only evident for special beams of radar.

TH-1898_08610214

- Distributed MIMO with transmit monopulse:

  This thesis has proposed transmit monopulse for MIMO radar. The principle of transmit monopulse has been brought out and system requirement for the same is elucidated. A distributed MIMO based on this concepts has been proposed. It has been shown that the distributed MIMO produces superior results as compared to monostatic system. The variation of the performance with respect to the target's angular location is also brought out.

- Design of orthogonal waveform:

  In most of the designs, MIMO radar relies on transmission of orthogonal waveforms from its multiple transmitters. It is of paramount importance to study this aspect of MIMO radar. The use of frequency hopping sequence for design of orthogonal waveform is proposed. It has also been shown that the modification of these frequency sequence produces superior performance than the one proposed in recent literature.

8.2 Further work

There are several ways the work presented in thesis can be extended and further investigated. Some of them are enumerated below:

(i) The performance comparison done in the present study was for basic parameters of the virtual array. The system level performance parameters of different configuration can be carried out as further work which will be closer to the actual deployable system.

(ii) The design of resource manager for MIMO radar in the current thesis work was to mainly demonstrate the advantage of using transmit subapertures to schedule multiple tasks simultaneously with some defined optimality. In the current work it is assumed that the waveforms used across subapertures are orthogonal. In further work, the possibility of using correlated waveforms to produce a continuum of beamwidth from very narrow beamwidth to a very wide beamwidth can be investigated, which can be used based on the requirement of keeping the target within the beamwidth based on revisit time and target dynamics. Additional parameters like timeliness of scheduling of tasks and more realistic scenario generators can be used to evaluate the performance of MIMO resource manager.

(iii) Future work on distributed MIMO may include the evaluation of detection performance. The

TH-1898_08610214

study may also be carried out for the scenarios when the transmitter is fixed and all the receivers are mobile which seems to be more realistic deployment scenarios in todays context.

TH-1898_08610214

A

Appendix

Contents

TH-1898_08610214

A.1 Derivation of Signal to Noise Ratio for MIMO Virtual Array without Phase Repetitions

Let us denote the number of antennas in the real array as N. Let the power transmitted by the full array is P.

Each antenna transmits a signal with amplitude proportional to $\sqrt{\frac{P}{N}}$; each of them transmits an orthogonal waveform. On receive, at each antenna, the contribution of each transmitter is extracted by matched filtering.

Let us assume that the energy of matched filter is normalised to unity. The number of signals extracted at receiver is N^2 as each receiver extracts N signals. Referring to chapter 3, the extracted signals are weighted by a value equal to the inverse of number of repetitions, thus for N length real array, the signal components after weighting will be $2N-1$. Thus, the total power at the output of beamformer will be given by

$$P_{total} = \left(k(2N-1)\sqrt{\frac{P}{N}} \right)^2 \tag{A-1}$$

where k is constant of proportionality.

Let the noise variance at each receiver be given by σ^2 before matched filtering. The noise samples are considered white Gaussian and independent. After matched filtering, the number of noise samples that needs to be combined in the beamformer is N^2. It can be seen from table 3.1 and table 3.2 that the samples are multiplied by weights to nullify the phase repetitions. Considering that, and collecting all the terms having same weights together; the following expression can be written for noise sample at the output of beamformer. Let us denote the noise sample as n_{total}.

$$\begin{aligned} n_{total} = n(i,j) + \frac{1}{2}\sum_{No.\ of\ terms=2} n(i,j) + \frac{1}{3}\sum_{No.\ of\ terms=3} n(i,j) + \ldots + \frac{1}{N-1}\sum_{No.\ of\ terms=N-1} n(i,j) \\ + \frac{1}{N}\sum_{No.\ of\ terms=N} n(i,j) + \frac{1}{N-1}\sum_{No.\ of\ terms=N-1} n(i,j) + \ldots + \frac{1}{2}\sum_{No.\ of\ terms=2} n(i,j) + n(i,j) \end{aligned} \tag{A-2}$$

The term $n(i,j)$ indicates noise sample at the output of j^{th} receiver corresponding to i^{th} transmitter. As we are interested only in variance of n_{total}, the exactly value of (i,j) for terms within the

TH-1898_08610214

summations are not important, only the number of terms shall be sufficient to ascertain the variance of n_{total}.

$$var(n_{total}) = 2\sigma^2\left(1 + \frac{1}{2} + \frac{1}{3} + \ldots + \frac{1}{N-1}\right) + \frac{\sigma^2}{N} \tag{A-3}$$

To evaluate the variance of n_{total}, the following property of independent Gaussian random variable is used.

(i) $var(Ln(i,j)) = L^2\sigma^2$ where $var(n(i,j)) = \sigma^2$

(ii) $\sum_{No\ of\ terms\ =K} n(i,j) = K\sigma^2$

For moderately large value of N, within a reasonable approximation the partial sum of harmonic series can be written as $ln(N)$, where N is the number of terms in the partial sum of harmonic series.

Thus

$$var(n_{total}) \approx 2\sigma^2 ln(N-1) + \frac{\sigma^2}{N} \tag{A-4}$$

where ln is natural logarithm

Thus the SNR is given by

$$SNR|_{MIMOWOPR} \approx \frac{k^2P(2N-1)^2}{\sigma^2(2Nln(N-1)+1)} \tag{A-5}$$

For comparison of SNR of MIMO without phase repetitions with other configurations, the SNR may be normalised with respet to $\frac{k^2p}{\sigma^2}$. Thus, the above expression can be rewritten as

$$SNR|_{MIMOWOPR} \approx \frac{(2N-1)^2}{(2Nln(N-1)+1)} \tag{A-6}$$

TH-1898_08610214

Bibliography

[1] J. Li and P. Stoica, *MIMO Radar signal Processing*. John Wiley Sons, Inc., Hoboken, New jersey, 2009.

[2] D. J. Rabideau and P. Parker, "Ubiquitous MIMO multifunction digital array radar," in *37th Asilomar conference on Signals, Systems Computers, 1057-1064 Nov, vol.1*, 2003.

[3] C.-Y. Chen, "Signal processing algorithms for MIMO radar," Ph.D. dissertation, California Institute of Technology, California, Jun 2009.

[4] N. Lehmann, "Some contributions on MIMO radar," Ph.D. dissertation, New Jersy Institute of Technology, Jan 2007.

[5] E. Fishler, A. Haimovich, R. Blum, D. Chizhik, L. Cimini, and R. Valenzuela, "MIMO radar: an idea whose time has come," in *Proceedings of the IEEE Radar Conference (IEEE Cat. No.04CH37509)*, April 2004, pp. 71–78.

[6] D. Tse and P. Viswanath, *Fundamentals of wireless communication*. Cambridge university press, Cambridge, 2005.

[7] H. Li and B. Himed, "Transmit subaperturing for MIMO radars with co-located antennas," in *8th European Conference on Synthetic Aperture Radar*, June 2010, pp. 1–4.

[8] V. S. Chernyak, "On the concept of MIMO radar," in *IEEE Radar Conference*, May 2010, pp. 327–332.

[9] V. Chernyak, *Fundamentals of Multisite Radar Systems; Multistatic Radars and Multiradar Systems*. Gordon and Breach Science Publishers, 1998.

[10] W. Zhu and J. Tang, "Robust design of transmit waveform and receive filter for colocated MIMO radar," *IEEE Signal Processing Letters*, vol. 22, no. 11, pp. 2112–2116, Nov 2015.

[11] H. Sun, C. Gao, and K. C. The, "Performance evaluation of practical MIMO radar waveforms," in *IEEE Radar Conference*, May 2016, pp. 1–6.

[12] C. Y. Chen and P. P. Vaidyanathan, "Properties of the MIMO radar ambiguity function," in *IEEE International Conference on Acoustics, Speech and Signal Processing*, March 2008, pp. 2309–2312.

[13] E. Brookner, "MIMO radar demystified and where it makes sense to use," in *IEEE International Symposium on Phased Array Systems and Technology*, Oct 2013, pp. 399–407.

[14] D. W. Bliss and K. W. Forsythe, "Multiple-input multiple-output (MIMO) radar and imaging: degrees of freedom and resolution," in *The 37th Asilomar Conference on Signals, Systems Computers, 2003*, vol. 1, pp. 54–59.

[15] J. Li, P. Stoica, L. Xu, and W. Roberts, "On parameter identifiability of MIMO radar," *IEEE Signal Processing Letters*, vol. 14, no. 12, pp. 968–971, Dec 2007.

[16] K. W. Forsythe, D. W. Bliss, and G. S. Fawcett, "Multiple-input multiple-output (MIMO) radar: performance issues," in *Conf. Record of the Thirty-Eighth Asilomar Conference on Signals, Systems and Computers,*, vol. 1, 2004, pp. 310–315 Vol.1.

[17] Y. Yang and R. S. Blum, "MIMO radar waveform design based on mutual information and minimum mean-square error estimation," *IEEE Trans. on Aerospace and Electronic Systems*, vol. 43, no. 1, pp. 330–343, January 2007.

TH-1898_08610214

[18] J. Li, P. Stoica, and X. Zheng, "Signal synthesis and receiver design for MIMO radar imaging," *IEEE Trans. on Signal Processing*, vol. 56, no. 8, pp. 3959–3968, Aug 2008.

[19] P. Stoica, J. Li, and Y. Xie, "On probing signal design for MIMO radar," *IEEE Trans.on Signal Processing*, vol. 55, no. 8, pp. 4151–4161, Aug 2007.

[20] K. W. Forsythe and D. W. Bliss, "Waveform correlation and optimization issues for MIMO radar," in *Conference Record of the Thirty-Ninth Asilomar Conference on Signals, Systems and Computers*, October 2005, pp. 1306–1310.

[21] D. R. Fuhrmann and G. S. Antonio, "Transmit beamforming for MIMO radar systems using partial signal correlation," in *38th Asilomar Conference on Signals, Systems and Computers,*, vol. 1, Nov 2004, pp. 295–299 Vol.1.

[22] H. A. Khan, Y. Zhang, C. Ji, C. J. Stevens, D. J. Edwards, and D. O'Brien, "Optimizing polyphase sequences for orthogonal netted radar," *IEEE Signal Processing Letters*, vol. 13, no. 10, pp. 589–592, Oct 2006.

[23] H. Deng, "Polyphase code design for orthogonal netted radar systems," *IEEE Trans. on Signal Processing*, vol. 52, no. 11, pp. 3126–3135, Nov 2004.

[24] W. Q. Wang, "Large time-bandwidth product MIMO radar waveform design based on chirp rate diversity," *IEEE Sensors Journal*, vol. 15, no. 2, pp. 1027–1034, Feb 2015.

[25] M. G. M. Hussain, "MIMO beamforming using quasi-orthogonal ultrawideband-impulse waveforms," in *IEEE Radar Conference*, Oct 2015, pp. 76–81.

[26] U. Majumder, M. R. Bell, and M. Rangaswamy, "Design and analysis of radar waveforms achieving transmit and receive orthogonality," *IEEE Trans. on Aerospace and Electronic Systems*, vol. 52, no. 3, pp. 1056–1066, June 2016.

[27] A. A. Gorji and R. S. Adve, "Waveform optimization for random-phase radar signals with PAPR constraints," in *International Radar Conference*, Oct 2014, pp. 1–5.

[28] G. S. Antonio, D. R. Fuhrmann, and F. C. Robey, "MIMO radar ambiguity functions," *IEEE Journal of Selected Topics in Signal Processing*, vol. 1, no. 1, pp. 167–177, June 2007.

[29] M. Radmard, M. M. Chitgarha, M. N. Majd, and M. M. Nayebi, "Ambiguity function of MIMO radar with widely separated antennas," in *15th International Radar Symposium (IRS)*, June 2014, pp. 1–5.

[30] A. Guruswamy and R. Blum, "Ambiguity optimization for frequency-hopping waveforms in MIMO radars with arbitrary antenna separations," *IEEE Signal Processing Letters*, vol. 23, no. 9, pp. 1231–1235, Sept 2016.

[31] E. Fishler, A. Haimovich, R. S. Blum, L. J. Cimini, D. Chizhik, and R. A. Valenzuela, "Spatial diversity in radars-models and detection performance," *IEEE Trans. on Signal Processing*, vol. 54, no. 3, pp. 823–838, March 2006.

[32] P. F. Sammartino, C. J. Baker, and H. D. Griffiths, "Target model effects on MIMO radar performance," in *IEEE International Conference on Acoustics Speech and Signal Processing Proceedings*, vol. 5, May 2006.

[33] S. Gogineni and A. Nehorai, "Monopulse MIMO radar for target tracking," *IEEE Trans. on Aerospace and Electronic Systems*, vol. 47, no. 1, pp. 755–768, Jan. 2011.

[34] M. Xie, W. Yi, T. Kirubajaran, and L. Kong, "Receive-beam allocation for multiple target tracking with distributed MIMO radar systems," in *IEEE Radar Conference (RadarConf)'2016, May*, pp. 1–6.

[35] F. Daum and J. Huang, "MIMO radar: Snake oil or good idea?" in *42nd Asilomar Conference on Signals, Systems and Computers'2008*, Oct, pp. 183–187.

[36] V. Chernyak, "Multisite radar systems composed of MIMO radars," *IEEE Aerospace and Electronic Systems Magazine*, vol. 29, no. 12, pp. 28–37, Dec 2014.

[37] E. Brookner, "Developments and breakthroughs in radars and phased-arrays," in *IEEE Radar Conference*, May 2016, pp. 1–6.

TH-1898_08610214

[38] O. Biallawons, J. Klare, and O. Saalmann, "Technical realization of the MIMO radar MIRA-CLE ka," in *European Radar Conference*, Oct 2013, pp. 21–24.

[39] F. Gini and M. Rangaswami, *Knowledge-based radar detection, tracking, and classification.* John Wiley Sons, Inc., USA, 2008.

[40] S. L. C. Miranda, C. J. Baker, K. Woodbridge, and H. D. Griffiths, "Comparison of scheduling algorithms for multifunction radar," *IET Radar, Sonar Navigation*, vol. 1, no. 6, pp. 414–424, Dec 2007.

[41] J. Butler, "Tracking and control in multifunction radar," Ph.D. dissertation, University College London, Aug 1998.

[42] L. Jie, "Resource management in MIMO radar," in *International Conference on Internet Computing and Information Services*, Sept 2011, pp. 604–606.

[43] W. Wiesbeck, L. Sit, M. Younis, T. Rommel, G. Krieger, and A. Moreira, "Radar 2020: The future of radar systems," in *IEEE International Geoscience and Remote Sensing Symposium (IGARSS)*, July 2015, pp. 188–191.

[44] F. E. Nathanson, J. P. Reilly, , and M. N. Cohen, *Radar Design Principles: Signal Processing and the Environment.* McGraw-Hill, Inc, 1990.

[45] J. J. Zhang and A. Papandreou-Suppappola, "MIMO radar with frequency diversity," in *International Waveform Diversity and Design Conference*, Feb 2009, pp. 208–212.

[46] D. K. Barton, *Modern radar system analysis.* Artech House, 1988.

[47] P. Wang, H. Li, and B. Himed, "Moving target detection using distributed mimo radar in clutter with nonhomogeneous power," *IEEE Transactions on Signal Processing*, vol. 59, no. 10, pp. 4809–4820, Oct 2011.

[48] Q. Hu, H. Su, S. Zhou, Z. Liu, and J. Liu, "Target detection in distributed mimo radar with registration errors," *IEEE Transactions on Aerospace and Electronic Systems*, vol. 52, no. 1, pp. 438–450, February 2016.

[49] M. Skolnik, *Radar Handbook.* McGraw-Hill, 1990.

[50] M. Weib, "Synchronisation of bistatic radar systems," in *IGARSS' 2004,Sept*, 2004, pp. 1750–1753 vol.3.

[51] W. Rowe, J. Karlsson, and J. Li, "Error analysis of mimo monopulse for tracking radar," in *2013 14th International Radar Symposium (IRS)*, vol. 1, June 2013, pp. 71–76.

[52] S. Sherman, *Monopulse Principles and Techniques.* Artech House, Inc., Dedham, MA,, 1984.

[53] C. H. Park and J. H. Chang, "Closed-form localization for distributed mimo radar systems using time delay measurements," *IEEE Transactions on Wireless Communications*, vol. 15, no. 2, pp. 1480–1490, Feb 2016.

[54] D. L. Hall and J. Llinas, *Handbook of multisensor data fusion.* CRC Press, New York, 2001.

[55] D. R. Wehner, *High resolution radar.* Artech House, Norwood, Mass, USA, 1997.

[56] Q. Zhang and Y.-Q. Jin, "Aspects of radar imaging using frequency-stepped chirp signals," *EURASIP J. Appl. Signal Process.*, vol. 2006, pp. 43–43, Jan. 2006. [Online]. Available: http://dx.doi.org/10.1155/ASP/2006/85823

[57] M. Skolnik, *Introduction to Radar Systems*, ser. Electrical engineering series. McGraw-Hill, 2001.

[58] W. Liu and S. Weiss, *Wideband Beamforming Concepts and Techniques.* John Wiley and Sons, Ltd, Publication, UK, 2010.

[59] G. Kaiser, "Physical wavelets and radar: a variational approach to remote sensing," *IEEE Antennas and Propagation Magazine*, vol. 38, no. 1, pp. 15–24, Feb 1996.

[60] M. Ruggiano and P. v. Genderen, "Wideband ambiguity function and optimized coded radar signals," in *European Radar Conference*, Oct 2007, pp. 142–145.

TH-1898_08610214

[61] W. Q. Wang, "MIMO SAR imaging: Potential and challenges," *IEEE Aerospace and Electronic Systems Magazine*, vol. 28, no. 8, pp. 18–23, Aug 2013.

[62] J. P. Costas, "A study of a class of detection waveforms having nearly ideal range doppler ambiguity properties," *Proceedings of the IEEE*, vol. 72, no. 8, pp. 996–1009, Aug 1984.

[63] S. V. Maric and E. L. Titlebaum, "A class of frequency hop codes with nearly ideal characteristics for use in multiple-access spread-spectrum communications and radar and sonar systems," *IEEE Trans. on Communications*, vol. 40, no. 9, pp. 1442–1447, Sep 1992.

[64] P. Fan and M. Darnell, *Sequence design for communication applications.* Research Studies Press, England, 1996.

[65] W. Chang and K. Scarbrough, "Costas arrays with small number of cross-coincidences," *IEEE Trans. on Aerospace and Electronic Systems*, vol. 25, no. 1, pp. 109–112, Jan 1989.

[66] S. V. Maric and E. L. Titlebaum, "Frequency hop multiple access codes based upon the theory of cubic congruences," *IEEE Trans. on Aerospace and Electronic Systems*, vol. 26, no. 6, pp. 1035–1039, Nov 1990.

[67] E. L. Titlebaum, "Time-frequency hop signals part i: Coding based upon the theory of linear congruences," *IEEE Trans. on Aerospace and Electronic Systems*, vol. AES-17, no. 4, pp. 490–493, July 1981.

[68] S. V. Maric and E. L. Titlebaum, "Frequency hop multiple access codes based upon the theory of cubic congruences," *IEEE Trans. on Aerospace and Electronic Systems*, vol. 26, no. 6, pp. 1035–1039, Nov 1990.

TH-1898_08610214